PUERTO RICO ENERGY CENTER

SUMMER INTERNSHIP 2015

CLEAN TECHNOLOGIES RESEARCH

Volumen 3

DE-NA0000672

August 21, 2015

2015 Summer Internship

Clean Technologies Research

Editors

Suheilie Rodríguez González

Sandra R. Pedraza Torres

Armando Soto

2015 Summer Internship

Clean Technologies Research

Preface

The 6th Summer Research Internship on clean technologies was a great success. This effort of Puerto Rico Energy Center (PREC) and Universidad del Turabo with the sponsorship of the Samuel P. Massie Chair Program of Excellence of the Department of Energy (DoE) is intended to provide students and researchers an opportunity do work on innovative research projects and get valuable research experience. During eight weeks, twenty one students and ten mentors (professors and graduate students) participated conducting research on new technologies and solutions for everyday energy issues.

These proceedings include, among others, current issues of interest in areas such as photodegradation process, aerodynamic, hydrogen production, nanotechnology. We are grateful to the PREC team, to the Innovation and Commercialization Office and to the staff of Universidad del Turabo Vice-chancellor's Office for their contribution to accomplish successfully this experience.

Dr. Roberto Lorán
Principal Investigator
Samuel P. Massie Chair
Program of Excellence-DoE

Dr. Amaury Malavé
Executive Director
PREC

August 21, 2015

2015 Summer Internship

Clean Technologies Research

Contents

Nutritional Stimulation of *Chlorella sp.* in Batch Culture prior Production of Biofuel*

Jonathan J. López-Carrasquillo[1], HS, and José R. Pérez-Jiménez[2], PhD
Universidad del Turabo, Gurabo, PR, USA, jlopez644@email.suagm.edu[1], ut_jperezjm@suagm.edu[2]

Abstract*– Algae can produce oils for biofuel without compromising food supplies. They are easily to grow by providing common atmosphere and illumination. However, yield can be increased and modeled by applying by selecting efficient alga strains and optimizing growth conditions. Wastewater is being considered as nutritional supplement to increase oil production in algae. Chlorella sp. is known to produce oils for biofuels. Our objective is to determine the nutritional regime that promotes Chlorella sp. growth. Chlorella sp. was cultivated in mineral media supplemented with wastewater from cheese production and pasta preparation. Optical density (600 nm) was measured three times a day during a week to triplicate growth in supplemented media. Media not supplemented was used as control. Each supplement, pasta residual water (PRW) and cheese serum (CS), stimulated the algae growth more than the basal medium (F2), at similar levels. F2+PRW provided a more consistent trend than the F2-CS. F2+CS persisted as heterogeneous solution based on flocks that may interfere with measurements and require additional biodegradation efforts in Chlorella sp. Future work will consider response in continuous culture to these substrate and the efficiency in oil production for biofuels.

Keywords-- Chlorella* sp., *nutritional regimes, algae

I. Introduction

Over the past decade, scientific studies have focused their research on the search for alternative cleaner energy sources. Because fuel based on carbon fossil have a high emission of CO_2 its have been one of the mayor problems in the 21st century. Researches have been focused on finding ecofriendly and cost efficient alternative to reduce the gas emissions that can affect the atmosphere. The high demand in the energy field has caused non-renewable resources in the future to reach a point of exhaustion where they should turn to other horizon that doesn't require fuel based on carbon fossil.

Microalgae have been identified as an alternative source that promises to be producing useful oil. These eukaryotic microorganisms use photosynthesis to convert sunlight, water and carbon dioxide to useful biomass. Furthermore, it was found that microalgae have potential for commercial production such as cosmetics, ethanol and biodegradable plastics [1]. The advantage of microalgae on other subjects of study is that they can be grown easier, do not require too much attention and they can use wastewater to obtain their nutrients to grow. For these reasons microalgae have a better productivity and growth rate than agricultural crops [2].

Past research had suggested that biodiesel based from microalgae oil is similar to the standard biodiesel that we common use and it is more stable [3]. Severe studies had identified that *Chlorella* is a good candidate for the production of biodiesel. However, further studies are needed to increase the lipid content without affecting the growth of biomass [4].

II. Methods

Algae Reactivation. *Chlorella* sp. was reactivated using an original stock culture from UTEX Culture Collection of Algae. General media consists of 3.79 L of distilled water and 1 ml of F2 (concentrated nutrient solution). The nutrient solution (F2) is composed of trace metals, vitamins, and nitrogen and phosphate compounds. Cultures were reactivated in tubes with 10 ml of media and 500 µl of algae. They were exposed to artificial light for about a week. Once we observed high turbidity, we transferred on 5 ml of media with diverse nutritional regimes.

Nutritional Regimes. In order to determine the nutritional regime that increases the algal growth, we prepared two alternative media to compare with the original (F2). These media were supplemented with a different carbon sources. Wastewater was collected from cheese preparation and pasta cooking. These supplements were sterilized by autoclave. The original F2 media was independently amended with 10% (v/v) of each nutritional supplement: pasta residual water (F2+PRW) and cheese serum (F2+CS). Triplicates for each media were examined. Active culture of *Chlorella sp*. (500 µl) was inoculated in each tube. Optical density (600 nm) was measured for a period of 8 days using a spectrophotometer. Optical density (600 nm) represents increment in protein production as the alga grows. One measurement was taken in the morning (~10:00 am), at noon (~1:00 pm), and in the afternoon (~4:00 pm) throughout each day. Data was plotted using Microsoft Excel.

III. Results and Discussion

Chlorella sp. demonstrated faster growth, based on the production of its characteristic pigment, among the eight algae strains activated. Microscopically, all algal strains were pure and preserved typical morphological features. Despite this collection consisted on unicellular strains, some of them can

* This work is partially supported by the Puerto Rico Institute for Microbial Ecology Research, Universidad del Turabo, Gurabo, PR.

form aggregates during their life cycle. *Chlorella* sp. was selected for nutritional experiments.

In other to determine the most stimulating substrate for growth, *Chlorella* sp. was cultivated in F2 mineral media (F2) and independently supplemented with 10% of cheese serum and 10% pasta residual water. Growth was assessed by optical density for seven days. Culture tubes allowed 40% space for atmosphere containing CO_2 (carbon source for photosynthesis) and were kept static under illumination with white light (source of energy).

F2 mineral medium is a source of nitrogen, phosphorous, and trace metals. *Chlorella* sp. grew on the medium with variability among replicates (Fig. 1). In general terms, the algae grew during the period. Atypical peaks may be due to transient aggregates. In an early stage of growth, algae showed potential formation of aggregates. Variability in growth rate may be due to physiological state of the inoculum. Thus, in the future inoculum must have a common concentration and unusual peaks must require microscopic examination of morphological state.

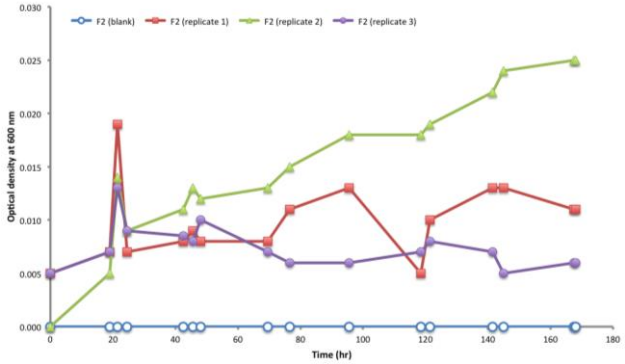

Fig. 1. Growth of *Chlorella* sp. in F2 medium

The typical growth media (F2) was supplemented wastewater (10% v/v) from food processing as additional carbon source. Pasta residual water (PWR) from cooking resulted in a homogeneous solution that mixed with F2 without evident separation of phases or aggregate formation. This medium (F2+PWR) showed a gradual growth of algae biomass. Among the three replicas (Fig. 2), *Chlorella* sp. follows a similar growth trend: adaptation (lag) phase in the first 20 hours, log phase slowly but consistent for about 70 hours, and later the growth became to stabilized. The medium F2+PWR conserved it homogeneity throughout all the experiment.

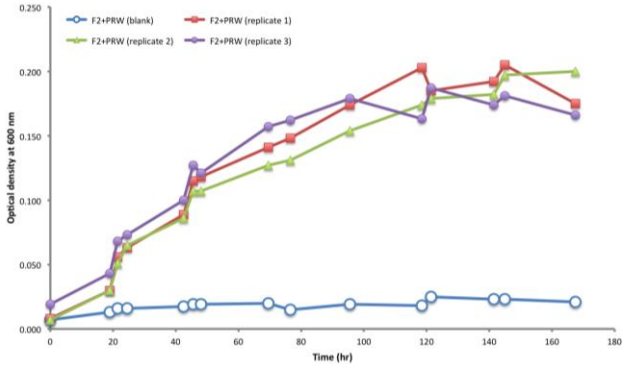

Fig. 2. Growth of *Chlorella* sp. in F2+PWR medium

F2 medium supplemented by cheese serum (CS) was a solution more heterogeneous. F2+CS exhibited flock prior inoculation that persisted over the course of the experiments. *Chlorella* sp. growth on F2+CS showed variations but there was a substantial biomass increase (Fig. 3). This increase can't be quantified at this time because the scale of absorbance needs to be calibrated in order to know the concentration of cells. The flocks interfere with optical density measurements that were minimized with a sterile control (used as blank). Also, flock may serve as nucleation center for the formation of aggregates with the algae. In the future, filtered media can be used to reduce interference of flocks. Also, microscopic examination must be coupled to optical density measurement to assess the formation of aggregates. This time, microscopic examination was excluded to prevent contamination of cultures.

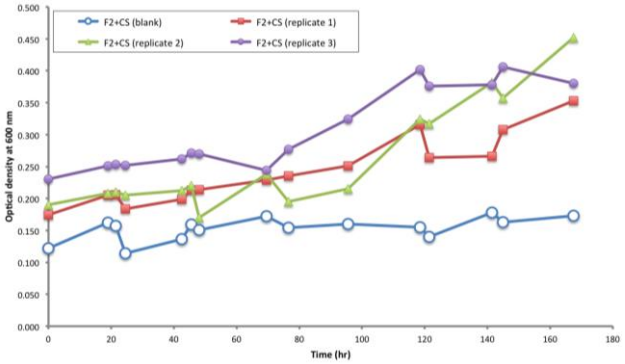

Fig. 3. Growth of *Chlorella* sp. in F2+CS medium

Ultimately, there was an increase of biomass in all three nutritional treatments (Fig. 4). *Chlorella* sp. experienced greater growth when the basal media was supplemented with food residual waters either from cheese production or pasta. For each supplemented, the arithmetic difference in optical density between the sterile controls and the active cultures in F2+CS (0.222) and F2+PRW (0.159) requires additional calibration to determine the most useful substrate. The qualitative difference is useful to plan future experiments.

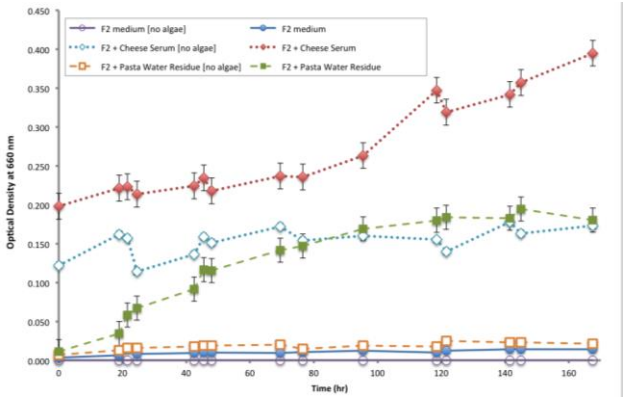

Fig. 4. Growth of *Chlorella* sp. under nutritional regimes

The biomass increase is more substantial when a homogeneous supplement is added (PRW). A heterogeneous supplement, as CS, seems to require additional biodegradation work on the algae. Once significant increased in algae cell number is obtained, we can put the algae in a starvation regime to stimulate production of oils. Dynamics of algae growth in batch culture guides the need to refine and control parameters to predict the algae growth. It can be achieved by continuous growth in a photobioreactor. Because we used batch culture, algae have to growth and work with the nutrients that we gave them. If we use a continue culture, we can add nutrients and neutralize wastes so they can have a more efficient growth in order to produce useful oils. These parameters can be used for a large-scale production in order to have a more significant production.

ACKNOWLEDGMENT

We are fully grateful to Puerto Rico Energy Center and Massie Chair for Excellence Program Grant #DE-NA000672 at the Universidad del Turabo for their opportunity to work on their 2015 Summer Internship, and the collaboration provided by Karin Millan and lab mates.

REFERENCES

[1] K. E. Apt, and P. W. Behrens. "Commercial developments in microalgal biotechnology". *Journal of Phycol*ogy. vol. 35, pp. 215-226. 1999.

[2] K. Gaurav, R. Srivastava, and R. Singh. "Exploring Biodiesel: Chemistry, Biochemistry and Microalgal source". *International Journal of Green Energy*. Vol. 10, no. 8, pp. 775-796, May 2013

[3] V. Rekha, R. Gurusamy, P. Santhanam, D. A. Shenbaga, and S. Ananth. 2012. "Culture and biofuel production efficiency of marine microalgae *Chlorella marina* and *Skeletonema costatum*". *International Journal of Geo-Marine Sciences* Vol. 41, no. 2, pp. 152-158, April 2012.

[4] R. Luque, and J. A. Melero. Advances in biodiesel production: processes and technologies. Woodhead Pub Ltd. Oxford; Philadelphia. 2011. 288 p.

SiO_2 as catalyst support for the production of synthetic diesel, as a possible source of clean energy

Juan C. Arango Lozano[1], Dayna M. Ortiz Rodríguez[2], Abniel Machín De Jesús[3], María D. Cotto Maldonado[4], Francisco Márquez Linares[5]
University of Turabo, Puerto Rico, jcarangolozano@hotmail.com[1], dortiz23@email.suagm.edu[2], machina1@suagm.edu[3], mcotto48@suagm.edu[4], fmarquez@suagm.edu[5].

Abstract*– There is an imperative necessity to find ways to obtain ecofriendly energy sources. Fossil fuels, the primary source of energy of the world, are known to cause serious environmental problems. The production of clean fuels is a challenge that must be taken very seriously. SiO_2 is mostly used as a support for the addition of catalytic metals to perform the Fischer and Tropsch method (FT) to synthetize clean diesel fuel. Here, an easy way to synthetize (via Stöber method) and characterize micro spheres of silica oxide. The effect of temperature during the synthesis was studied. It was found that at higher temperatures, the diameter of the sphere tend to decrease, indicating the formation of spheres with higher superficial areas. The characterization of the SiO_2 particles were performed using a Scanning Electron Microscopy with Energy Dispersive Spectroscopy (SEM-EDS), effectively the SEM analysis suggested the formation of SiO_2 micro spheres with a definite topography and EDS analysis confirmed the presence of Si and O in the synthetized compound.

Keywords: SiO_2 support, Stöber method, Fischer and Tropsch method, temperature.

I. Introduction

Nowadays we are facing the necessity to find new ways to produce clean fuels. This need becomes from the excessive use of this source as energy and the well-known adverse environment effects than these fuels represents. Actually the fossil fuels represent about the 70% of the world energy sources. This dependency has brought some important problems of contamination such as global warming and climate change, acid rain, alterations of the carbon cycle, among many others. [1].

Industries such as electric power and transportation are the biggest consumers of fossil fuels in the world, liberating to the atmosphere vast amounts of CO_2, NOx, SOx, lead (Pb), mercury (Hg), and many others. These pollutants are not only harmful to the environment but also to the human health, causing lung and heart diseases along with cancer [3].

Nitrogen and sulfur oxides have been of great interest to the scientific community the last century since they are mostly responsible for the acid rain. The acid rain is a mix of nitric and sulfuric acid. These acids are formed in the atmosphere when nitrogen and sulfur oxide, resulting from the incomplete combustion of fossil fuels, combines with water vapor and volatile hydrocarbons. The interaction with water creates the acid rain and the reaction with the hydrocarbons produces ozone, both harmful to human health. Acid rain can cause some serious environmental problems since most of the organisms are not adapted to abrupt changes in pH, dying in the process. While ozone can cause severe respiratory infections, especially in children and aged people [4].

The increase of price and demand of this fuels and the contamination generated by them, makes imperative the search of viable clean technologies looking for the production of clean fuels with high commercial value [2]. Contaminants produced by the combustion of fossil fuels exposed before represents the challenge to develop new clean fuels. Despite the fact than this fuels will still producing CO_2, the use of alternative energy sources is a field that have not gave cost-effective alternatives, for example we have the production of hydrogen as an alternative energy source, this is an option for a future, when the technology to develop this production will be good enough to consider it as convenient.

Since this source of energy presents issues specially transportation, such process will require energy and expensive equipment, which adds cost to the use of hydrogen. Right now is a non-profitable alternative [5].

One alternative that does not require new technology or the investment of a lot of money is the synthesis of clean diesel fuel thorough the Fischer-Tropsch method (FT). This method produces clean diesel starting from a mix of H_2 and CO obtained from renewable or not energy sources [6]. FT method was demonstrated initially in Germany in 1902 by Sabatier and Sendeners; in 1926 the technique was patented by Fischer and Tropsch using this catalytic technique for the conversion of gases into liquid clean hydrocarbons similar to petroleum [7].

This synthesis produces a mix of linear high weighted hydrocarbons with high purity. The fuel produced this way is clean since doesn't present aromatic compounds or heteroatoms like N or S, hence after combustion these fuels eliminates the production of NO_x and SO_x, as environment contaminants [2].

To develop the FT reaction is necessary the use of heterogeneous catalyzers. These catalyzers consist in high surface solids where there are deposited metallic particles like Co, Ru and Fe [2-8]. These high surface solids are known as supports, one of the most popular compounds used to achieve this end is SiO_2.

Silica oxide (SiO_2), is an important inorganic material, it has received tremendous research interest over the past decade

because of its applications in a vast array of technological fields. This paper introduces the most popular method to synthetize SiO_2 microspheres, the Stöber method. Which uses reactants that are not expensive, are easily available; and most important, it requires no organic additives (e.g. surfactants or polymers). Most important, this method allows synthesizing monodisperse spheres with desired diameter and sizing [9].

The Stöber method consists of hydrolysis and condensation of alcoholic tetra ethyl orthosilicates (TEOS) in the presence of aqueous ammonia. Generally, the synthesis procedure involves mixing the alcohol(s) and ammonia solutions followed by the addition of the TEOS under stirring [10].

The main objective of this research is to present an easy way to synthetize SiO_2 microspheres. Different synthesis temperatures were tested to study the correlation between temperature and size of the sphere. The characterization of the obtained products were performed thorough a scanning electron microscopy, equipped with an Energy Dispersive Spectrometer (SEM-EDS). The resulting support could be used for the deposition of catalytic metals to develop the Fischer and Tropsch FT method to produce liquid clean diesel fuels.

II. EXPERIMENTAL SECTION

Materials

The Materials for the production of the micro spheres of SiO_2 are Ethanol (Fischer Scientific, 98.3%); Tetra Ethyl Ortho silicate (TEOS, 98%, ACROS Organics); Ammonium Hydroxide (ACROS Organics, 28-30%); deionized ultrafiltred water (D.I.U.F, Milli-Q).

Methods

Synthesis of SiO_2 micro spheres.

In a 125 ml Erlenmeyer flask occurs the reaction between ethanol, ammonium hydroxide and deionized water. This solution is vigorously and maintained at the desirable temperature.

When the solution reaches the temperature begins the addition of the silica source, TEOS; this addition has to be slowly. TEOS addition produces a white precipitated, which are expected to be the formed SiO_2 micro spheres, the product has to be under constant agitation and constant heat for one hour.

The syntheses of the microspheres at 30 and 40 °C occurs in a 200 ml round bottom flask, in a preheated heating mantle at 30 °C or 40 °C, the reactive solution ($EtOH+NH_4OH+$ DI H_2O) is placed. For both temperatures, for stirring, a mixer adapted to a drill was used, holded to an iron support. The mixer was placed into an appropriate height into the flask; this method was improved to maintain the reaction under constant agitation.

When the reactive solution reaches the desired temperature, the silica source TEOS is added slowly and after the precipitation if formed the solution is maintained under strong stirring for one hour.

The temperature has to be always constant in every step of the synthesis.

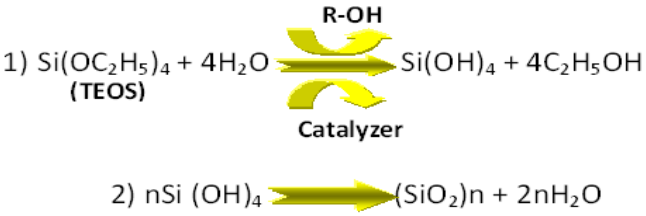

Fig. 1 Chemical process for the formation of SiO_2.

In figure 1 is described the reaction process for the formation of the SiO_2 support, the first stage of the reaction describes the controlled hydrolysis of the precursor (TEOS), this part of the reaction occurs in D.I.U.F water, which is the reactant that determines the final yield of the product. The addition of TEOS gives the formation of a white precipitate. The presence of ethanol in defined proportions and a catalyzer, in this case ammonium hydroxide (NH_3OH), are the determinant facts to obtain the expected amorphous SiO_2 supports [15]. In the second stage occurs a condensation process to get the desired micrometric particles of SiO_2 [11, 12].

After each synthesis the separation process is through centrifugation at 6,000 revolutions per minute (rpm) for 10 minutes. The synthetized product was washed 4 times with deionized water (D.I.U.F) and one last time with ethanol.

The product is transferred to a flask and dried in an oven at 60 °C.

The characterization of the obtained compound is performed using Scanning Electron Microscopy equipped with an Energy Dispersive Spectrometer SEM-EDS, model JEOL JSM 6010-LA.

III. RESULTS AND DISCUSSION

A. Scanning Electron Microscopy (SEM).

Using the Stöber method, were synthetized samples of SiO_2 support at different temperatures, which will serve as catalyst carrier, these samples were characterized by scanning electron microscope (SEM-EDS). The images were obtained using SEM-EDS, model JEOL JSM-6010LA.

Morphology of SiO_2 micro particles was observed whether they were spherical or not, and the degree of dispersion and size of it. The correlation between the average diameter of the spheres and the temperature at which they were synthesized was determined.

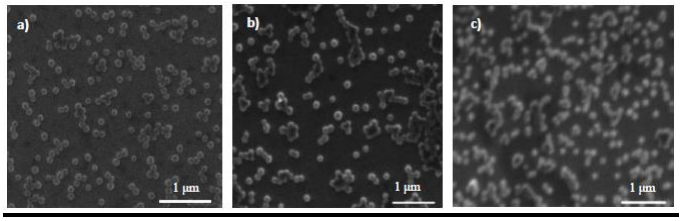

Fig.2 (a) Image of the SiO_2 support at 20.0 °C, X 22,000 ; (b) Image of the SiO_2 support at 30.0 °C, X 22,000; (c) Image of the SiO_2 support at 40.0 °C, X 22,000.

Figure 2 shows the images of SiO_2 synthetized supports. In all images are observed the formation of the desired microspheres with definition in the three determined temperatures in which the syntheses were developed.

Also were determined the average size of the micro spheres using the SEM, the three images presented at figure 2 are at the same magnification to show the difference in size.

Figure 2 a) shows the support at 20.0 °C, the image shows a good dispersion of the micro particles and a very defined and homogeneous formation of SiO_2 microspheres. In the synthetized support at 20.0 °C was determined an average particle size of 0.07µm.

In figures b) and c) are presented the images of the support synthetized at 30.0 °C and 40.0 °C respectively; in this cases, appears also the formation of the desired micro spheres, but appears small agglomerations of the formed micro particles induced possibly because of the formation of the product during the Stöber reaction, which independent of the precursor occurs in four stages; hydrolysis, condensation and polymerization of monomers to form the particles, growing of the particles and the agglomeration of the particles followed by the formation of SiO_2 webs and the subsequent formation of silica gel support[13-14].

In the synthetized support at 30.0 °C (figure 2b) was determined an average particle size between 0.06 µm.
Similarly in the support at 40.0 °C (figure 3b), the determined size was between 0.05 µm.

These results suggest a relation between the temperature and the particle size. Where at the highest temperature used for this experiment, appear the smallest micro spheres. Thus the micro sphere size goes downward with the increase of the temperature.

The size and the specific area of the synthetized support could be affected by the temperature. The temperature accelerates the induction period; thus, in the nucleation stage gives the formation of a high number of particles decreasing the size of the particle in contrast with the formation at lower temperatures [13-14].

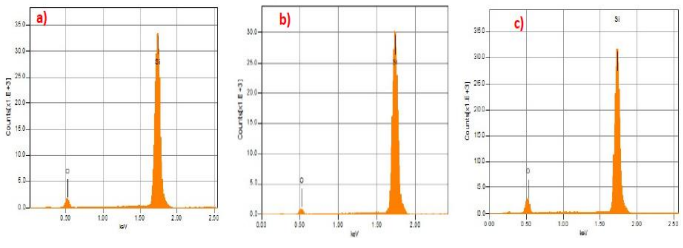

Fig. 2 EDS spectrum for the SiO_2 support. a) support at 20.0 °C, b) support at 30.0 °C, and c) support at 40.0 °C.

B. Energy Dispersive Spectrometer (EDS)

Using EDS could be determined the presence of elements in the analyzed samples, figure 3 shows the EDS spectrum for the three analyzed samples. Figure a) shows the EDS spectrum for the sample synthetized at 20.0 °C, it confirms the presence of Si and O in the synthetized material. Similarly the spectrums b) and c) are respectively for the 30.0 °C and 40.0 °C SiO_2 samples confirming the presence of Si and O in both of them.

IV. CONCLUSION

The result from this research demonstrates that the modification of the temperature, following the Stöber method allows to synthetize SiO_2 microspheres at different sizes.
At highest temperatures can be obtained smaller microspheres, which means a highest superficial area and a better support for metals deposition used as catalysts, the main objective of this research. Change of temperature affects the nucleation process during the particles formation according to the cited literature, which allows the formation of different particle sizes.

ACKNOWLEDGEMENTS

The authors gratefully acknowledge the financial support provided by the Department of Energy through the Massie Chair of Excellence Project Grant# DE-NA0000672 at the University of Turabo. Also, the collaboration of Abraham Garcia, Master student of the Natural Sciences and Technology; Ian Gutierrez, Engineer of the Puerto Rico Energy Center (PREC) for the help in the SEM-EDS study.

REFERENCES

Lenntech, fossil fuels: characteristics origin, applications and effects of fossil fuels. Recovered from. http://www.lenntech.es/efectoinvernadero/combustibles-fosiles.htm

S Rojas, M Ojeda, T Herranz, F. Pérez., J. Gonzalez. "Production of liquid synthetic fuels", *chemistry and environment*, vol 1, pp 69-75, 2011.

C. Amarales., "El transporte y la contaminación atmosférica que este provoca", *Revista trasporte, desarrollo y medio ambiente*, vol 31, NO 1, 2011.

L. Paz. Et al, "Tabloide cambio climático", parte 1 y 2, editorial academia, La Habana Cuba

C. Liao, C. Huang., J. Wu, "Hydrogen production from semiconductor based photocatalysis via water splitting", *Catalysis*, Vol 2, pp 490-516, October 2012.

J. Fierro, P. Terreros, M. Granados, M. Ojeda, F. Pérez, "La síntesis de hidrocarburos Fischer Tropsch. Retos y perspectivas.", *Real Sociedad Española De Química*, Vol 2, pp 107-114, June 2013.

G. Briceño, "Aerogelesde carbón como soportes catalíticos para la síntesis Fischer-Tropsch, *Tesis Doctoral*, Universidad Nacional De Colombia, 2014.

C. Costa, A. Leite, E. Sousa, F. Galembeck, "Size effects on the microchemistry and plasticity of stöber Silica particles: A study using EFTEM, FESEM and AFM-SEPM microscopes", *Langmuir*, vol 17, pp 189-194, October 2000.

K. Yao, H. Zeng, "Simultaneous chemical modifications and structural transformation of stöber silica spheres integration of nanocatalysts", *Chemistry of Materials, Vol 24, pp 140-148, November 2011.*

V. Valtchev, L. Tosheva, "Porous nanosized particles: Preparation, properties and applications", *Chemical Reviews, Vol 113*, pp 6745-6748, may 2013.

F. Marquez, R. Roque, "Synthesis and characterization of large specific Surface area nanostructured amorphous silica materials", *Journal of nanoscience and nanotechnology*, Vol 6, No 4, January 2006.

[12] F. Marquez, R. Roque, "Synthesis and characterization of silica sphere-packing mesoporous materials", surface *and interface analysis, Vol* 37, No 4, April 2005.

[13]M. Echeverri, L. Giraldo, B. López, "síntesis y funcionalización de nano partículas con morfología específica", *Scientia et technica,* Vol 13, No 36, September 2007.

[14] I. Flórez, E. Zarazúa, E. Cuellar, L Garza, L. Torres, P Valdez, K. Sovolev," Effect of nano-SiO_2 on properties of cement based materials", *First conference on advanced construction materials,* 2006.

[15] W. Stöber, A. Fink, E. Bohn, "Controlled growth of monodisperse silica spheres in the micron size range", *Journal of Colloid and Interface Science,* Vol 26, pp 62-69, 1968.

Microbial Conversion of Xylose for the Production of Biofuel

Casandra Santiago-Nieves, AD Biopharmaceutical Technology[1], Karin Millán, Masters Environmental Analysis[2], and José R Pérez-Jimenéz, Doctorate Environmental Microbiology[3]
[1]Universidad del Turabo, Puerto Rico, csantiago232@email.suagm.edu[1], karinmillan1302@gmail.com[2]
[2]Rutgers the State University, United States, ut_jperezjm@suagm.com[3]

Abstract*– For many years a main concern for society has been the carbon footprint that is being left behind for the future generations and the deterioration of the planet in doing so. In attempt to improve, many scientists have worked on alternative energy sources that release little to no carbon fuels in order to lessen or eliminate the use of products that release carbon fuel. With less carbon being exposed, that means environmental protection, better products from plantations and healthier human beings and animals (pets and other animals that would be for later consumption). An alternative that scientists use is microorganisms as it has been proven for many years that the microorganisms are an organic matter that naturally help in many ways. One example is in fermentation as they have helped in elaboration of food, organic gases, energy and ethanol. For such reason the investigation performed was to isolate bacteria that ferment xylose. In order to do so, testing was done by growth, isolation and purification in general culture mediums and xylose culture mediums. The results obtained were that many of the samples obtained degrade xylose. From the results, it can be concluded that the study site has bacteria that are xylose-fermentating microorganisms that can be further studied to create biofuel as an alternative energy source and fuel.

I. Introduction

Xylose is a pentose sugar that "comprises about one-third of the total carbohydrate sugars in lignocellulosic biomass" [1]. Xylose is degraded through fermentation and the "major metabolic pathways for xylose fermentation are similar in bacteria, yeasts and fungi with the notable exceptions of significant differences in transport, regulation, co-factor requirements and the products of pyruvate fermentation" [1]. Also, "xylose is one of the most abundant polysaccharides in nature" and "because of its heterogeneity its hydrolysis requires the action of a complex system of enzymes" [3]. For such reason, in order to produce large quantity of ethanol from lignocellulosic materials requires the understanding and conversion of xylose.

Studies have been conducted to understand xylose fermentation to ethanol by yeast, fungi and bacteria. "Microorganisms that rapidly ferment xylose at high yields are essential to the development of cost-effective, large-scale xylose to the ethanol processes" [1]. Because of the bacteria's low rate production of ethanol and higher rates by yeast, studies with bacteria have decreased. Studies are being focused on wild-type, but some are finding better results through recombination. Some of the "recombinant bacterial and yeast genera incapable of direct high-yield xylose fermentation in their native genotype are being used as hosts in genetic engineering research aimed at developing improved xylose-fermentating microorganisms" (McMillan 1993).

TABLE I/II
DIRECT FERMENTATION OF XYLOSE TO ETHANOL*

Yeast (Genera)	
Wild-Type	Recombinant
Brettanomyces	Sacchatomyces
Candida	Schiozsaccharomyces
Clavispora	
Kluyverinyces	
Pachysolen	
Pichia	
Schizosaccaromyces	

Bacteria(Genera)	
Wild-Type	Recombinant
Aerobacter	Erwinia
Aeromonas	Escherichia
Bacillus	Klebsiella
Bacteroides	
Clostridium	
Erwinia	
Klebsiella	
Thermoanaerobacter	

*Suggested microorganisms of McMillan 1993 [1].

II. Methodology

However, during the investigational study the goal was to isolate xylose-fermentating microorganisms. Of said microorganisms, the bacteria would be the area of interest for further testing. After the microorganisms were isolated, the next project would be to understand and identify the xylose-fermentating microorganisms. If microorganisms were identified to degrade xylose, then the long time goal would be to identify the bacteria in order to create biofuel. The objectives were to collect samples, activation of the wild type microbe and the testing for degradation of xylose. The objectives were elaborated through numerous activities that are explained throughout the paper, including the procedures and results.

The first step to the study is the collection of a sample from the study site at the Experimental Station of the Universidad de Puerto Rico in Gurabo. The study site is a plantation of tobacco, ornamental plants and cover plants. The area of interest for this study is of the soil of the cover plants. Then, activation of the native microbe in a saline solution of 85% is required in order to have growth in test tubes for future testing. In test tubes, nine (9) milliliters were added with one (1) milliliter of the native microbe. After growth in the testing tubes were confirmed (through turbidity), testing growth was done in general culture medium through pour plate and spread plate methods as they were the next tests performed. Before beginning the test, general culture medium was prepared and in order to prepare the medium, the container's recipe was followed. The medium that was used was the Tryptic Soy Agar (TSA) with the recipe of 40 grams per one (1) liter. For two Erlenmeyer flasks of 300 milliliters of distilled water, twelve (12) grams of TSA were used for each flask.

The inoculation was done with 1000 microliters, 500 microliters and 200 microliters of the native microbe. The pour plate test was performed by inoculating the previous amounts in Petri dishes. After the TSA medium was sterilized through the autoclave and had cooled down, the culture was inverted in the Petri dishes. Then, with the culture still liquid the Petri dish was moved in a manner that the inoculation would spread within the TSA. After the culture solidified the Petri dishes were incubated for 24-48 hours at 24 degrees Celsius and 30 degrees Celsius awaiting the observation of separated colonies. In the spread plate testing, the TSA culture medium was prepared, sterilized in the autoclave, cooled and inverted into the Petri dishes. After the culture had solidified, then the sample was inoculated with the amounts previously mentioned. When inoculated, the Petri dish was moved slightly so that the native microbe could spread throughout the culture medium.

Once there was growth in the general culture, the next goal was to isolate and purify the microorganisms. Isolation testing was performed through streaking in general culture in order to have pure colonies. After pure colonies were obtained, purification was practiced through one streak in general culture. Isolation and purification testing was incubated at 30 degrees Celsius for 48 hours. Once the purification testing was a success, preservation of the microorganisms was performed. In order to prepare for the preservation, another general culture medium titled Tryptic Soy Broth was prepared from its recipe of 30 grams of culture for every one (1) liter of distilled water. For two Erlenmeyer flask of 300 milliliters of distilled water, nine (9) grams of culture was used. Each microorganism was inoculated in Tryptic Soy Broth that was autoclaved into tubes in order to obtain growth of that one microorganism. With the growth of the microorganisms, the preservation was done in 1.5 microliters Ependolf tubes sterilized with 500 microliters of Tryptic Soy Broth with Glycerol (to prevent crystallization in the freezer where it would be preserved) and 500 microliters of the microorganism.

After growth testing was done with general culture mediums, testing in xylose medium was done to observe the tendency for degrading xylose. Although xylose medium is a broth (liquid), the medium was modified to work with the xylose in Petri plates. The recipe for xylose is 20 grams for every one (1) liter of distilled water for tubes. In Petri dishes, the modification was done with adding one (1) gram of yeast extract for every one (1) liter of distilled water and 5 grams of agar for solidification to the 20 grams of one (1) liter of distilled water. Phenol red was also added to the mixture as a pH indicator; if there was fermentation then the culture medium would change colors from red to yellow. The modification was done because working with Petri dishes gives faster results, a better idea of growth and the quantity of colonies. When inverting the culture into Petri plates if a thicker medium is inverted, then there is less oxygen on top of the medium and the microorganism has to find its nutrients within the culture. Therefore, if there is growth within the medium then that microorganism ferments xylose.

The testing was done with the culture modification and pour plate with 200 microliters of the native microbe. After the xylose medium was sterilized through the autoclave and had cooled down, the culture was inverted in the Petri dishes. Then, with the culture still liquid the Petri dish was moved in a manner that the inoculation would spread within the xylose. After the culture solidified the Petri dishes were incubated for 48 hours at 30 degrees Celsius awaiting the observation of separated colonies. Then in the xylose medium the same steps were taken to isolate, purify and preserve as was done with the general medium. Other testing for xylose fermentation was done by inoculation of microorganisms in fermentation testing tubes through Durham Tube test. To prepare the Durham Tube test, a smaller Durham tube is placed with the opening facing down into a larger tube of 15 milliliters. Then the tube is filled with sterilized xylose medium in its broth form with ten (10) milliliters and the inoculation of the microorganisms. Incubation was for three (3) weeks at 37 degrees Celsius.

Additional testing was done for further information of the xylose-fermentating microorganisms. The tests were of Indole Acetic Acid (IAA), ammonia (NH_3), osmotic stress and Gram Stains. For the IAA test the procedure was to inoculate the xylose-fermentating microorganisms as a deep agar test and incubate at 37 degrees Celsius for 48 hours. After the incubation period, initial observations were made and if there was a black precipitation that would be positive for the production of hydrogen sulfide(H_2S). Then, three (3) drops of the reactive Kovac were added and if there was a superficial color change of reddish it would be positive for IAA and if the change was brown then it would be negative for the production of IAA. The test for the production of ammonia was done by inoculating the microbe into the ammonia solution and incubating the tubes at 30 degrees Celsius for 72 hours. At the

time of incubation, 500 microliters of the reactant Nessler was added and at a maximum wait time of ten (10) minutes observations were made. If there was a color change of green to the solution, then the microbe is negative for producing ammonia. If the color change was of orange-brown, then the microbe inoculated positively produces ammonia. The osmotic test is performed by inoculating the microorganisms in an osmotic solution of ten percent (10%) and incubating at 30 degrees Celsius for 24 hours. At the incubation time, the tubes were observed and if there was turbidity (bacterial growth) then there was a positive result and can tolerate osmotic stress at 10%. In order to realize a Gram Stain a smear on a laminate slide with the bacteria has to be done to then add the first color dye that is Crystal Violet for 30 seconds. Then, wash the slide with distilled water and carefully remove the excess water to then add Gram Iodine for 60 seconds. Next, clean the slide with Gram Alcohol (a mixture of acetone and ethanol that should not be done more than five (5) seconds) and remove it gently and swiftly. Lastly, add the safranin dye as a counter stain for 30 seconds, remove with distilled water, dry with bibulous paper and observe. With the Gram Staining the physical and chemical type of wall and its morphology can be observed as if it is tinted purplish/blue then it is Gram positive and has a thicker wall whereas if it stains reddish then it is Gram negative and its wall is thin and does not absorb the Crystal Violet dye.

III. Results

The first table reflects the results of the Gram stains. The laminates were inoculated with three (3) to four (4) microorganisms per laminate slide. The bacteria inoculated from the same treatment resulted to be categorized the same, as in the stain being positive or negative and the morphology of the bacteria.

TABLE III
GRAM STAINING RESULTS

Laminate	Gram Stain	Morphology
1	Negative	Bacillus
2	Positive	Cocco
3	Positive	Cocco
4	Positive	Cocco
5	Positive	Cocco
6	Positive	Cocco
7 I	Positive	Cocco
7 II	Positive	Cocco
7 III	Positive	Cocco
-Yellow	Positive	Cocco

The results of the general mediums are a result that there is bacterial growth in the study site. These also reflect that the bacteria have some unique features. In the first table of results, depicts the growth, medium color change or encapsulation and purification growth. The inoculation code change from general inoculate to purification growth inoculate because after the growth of all the microbes, the ones that were further studied were the bacteria colonies that grew most and in most interest.

TABLE IV
GENERAL CULTURE MEDIUM RESULTS

Inoculate General	Colony	Color	Inoculate General	Pure Growth
1R1	yes	Cream (C)	1R1 rose	-
1R2	Yes	C	1R1 white	+/little
1R3	Yes	C/Yellow (Y)	1R2 I	+
1R4	Yes	C/Y	1R2 II	+
2R1	Yes	Medium Blue	1R2 redo	+
2R2	Yes	White (W)/ C	1R4	-
2R3	Yes	C	2R2	+/pink
2R4	Yes	C	2R2 II	+/pink
3R1	Yes	W/C	2R3	+
3R2	Yes	W/Y	3R1	+
3R3	Yes	W	4R1 Blue I	+/blue
3R4	Yes	Y/ C/W	4R1 Blue II	+/blue
4R1	Yes	W/ C	4R1 Blue III	+/blue
4R2	Yes	W/ different patterns (DP)	4R2	+/encapsulated
4R3	Yes	W	4R3	+/Green (G)/Y
4R4	Yes	W	5R1	+/G
5R1	Yes	W	5R2 I	+/G
5R2	Yes	W	5R2 II	+/G
5R3	Yes	W	5R2 III	+/G
5R4	Yes	W/C	5R3	-
6R1	Yes	C/W	6R1	+
6R2	Yes	W/Y/ Medium blue	6R1 II	+
6R3	No	no	7R1	-/fungi
6R4	Yes	W/ DP	7R2	+
7R1	Yes	Black/W/C	7R2 II	+
7R2	Yes	W	7R4 I	+/Y/Pink
7R3	Yes	W	7R4 II	+/Pink
7R4	Yes	White/ C	7R4 III	+/Pink

The xylose culture medium results and the xylose tube results are in the following table. The "+" sign means positive for fermentation and the "-" means negative and the microbe inoculated does not ferment xylose. These results depict the

growth, color change or encapsulation, growth in its purest form and the fermentation difference in tubes.

TABLE V
XYLOSE CULTURE MEDIUM RESULTS

Inoculate Xylose	Plate	Inoculate Xylose	Tubes
1R1 rose	+	1R1 rose	-
1R1 white	+/little	1R1 white	-
1R2 I	+/red	1R2 I	-
1R2 II	+	1R2 II	+
2R3	+	2R3	+
3R1	+	3R1 White Region	-
	N/A	3R1 Pink Region	-
4R2	+/encapsulated	4R2 Pink Region	+
	N/A	4R2 White Region	+
4R3	+/orange	4R3	-
5R1	+/yellow	5R1	+/little
5R2 I	+/yellow	5R2 I	-
5R2 II	+/red	5R2 II	-
5R2 III	+/red	5R2 III	-
5R3	-		N/A
6R1	+	6R1 White Region	+/ less than pink
6R1 II	+	6R1 Pink Region	+/ more than white
7R1	+/little		N/A
7R2	+	7R2 Pink Region	+/same as white
	N/A	7R2 White Region	+/same as pink
7R2 II	+/yellow	7R2 II	+
7R4 I	+	7R4 White Region	+/more than pink
	N/A	7R4 Pink Region	+/less than white
7R4 II	+/orange		N/A
7R4 III	+		N/A

The following table includes the results of the reactant tests that were done of indole acetic acid, ammonia and the osmotic stress. The "+" is positive for growth in the osmotic stress test that was confirmed through turbidity. The "+" and "-" negative are positive and negative respectively for growth in the ammonia tests and "fast precipitation" is a unique observation made when the reactant was added to the test. The "-"in the indole acetic acid test is negative for growth and reaction, where as "+H_2S" is positively reacting and producing hydrogen sulfide.

TABLE VI
ADDITIONAL TESTING RESULTS

Inoculate	Osmotic Stress 10%	Ammonia	Indole Acetic Acid
-yellow	+	+	-
1R1 white	+	+	+ H_2S
1R1 pink II	+/little	-	-
1R2 II	+	-	-
1R2 I	+/little	-	-
2R2 II	+	-	-
2R2 Pink Region	+	-	-
2R2 White Region	+	-	-
2R3	+	-	-
3R1 White Region	+	-	-
3R1 Pink Region	+	-	-
3R4 Yellow	+	+	-
4R1	+	+/ fast precipitation	-
4R2	+	+	-
4R3	+/little	-	-
5R1	+	+/ fast precipitation	-
5R2 I	+	-	-
5R2 II	+	-	-
5R2 III	+/little	-	-
6R1	+	+/fast precipitation	-
6R1 II	+	+/fast	+ H_2S
7R2	+	-	-
7R2 II	+	+/ fast precipitation	-
7R4 I	+	+	-
7R4 II	+	+	-
7R4 III	+	+	-

The pie graph in Appendix I include the interpretation of the table where the colors of the colonies are grouped in a numerical manner. The chart in Appendix II depicts the difference in fermentation between the positively and negatively growth in plate versus tube. In the Appendix III, it reflects the results of the production of ammonia by the purified microorganisms and in Appendix IV it has the results from the osmotic stress test of ten percent. From the results it can be summarized that from the study site of the Experimental Station of the Universidad de Puerto Rico in Gurabo, P.R. and the soil of cover plants there are bacteria that are xylose-fermentating microorganisms. Twenty-six of twenty-eight inoculations are positive for degrading xylose in the Petri plates. Of the positive Petri dishes and the positive

tube fermentations, eight (8) plus their color colonies of a total of twelve (12) bacteria are xylose-fermentating. The results from the additional testing with the positively fermentating bacteria, depict that five (5) of the Gram positive bacteria also produce ammonia, two (2) produce hydrogen sulfide and a total of eight (8) can withstand ten percent (10%) osmotic stress. Lastly of the results, most of the fermentation testing was done with a modified recipe of the culture medium previously mentioned except for the tube fermentation.

IV. Future Work

After finding the positive xylose-fermentating microorganisms, future work goals are to extract DNA and do a PCR to identify the gene to degrade xylose. After successfully finding the gene, digestions will be performed to find the diversities of communities that are found within the study site that ferment xylose. Benefits from finding the xylanase, or the enzyme that degrades xylose are for the paper industry. This is so because when "found free of cellulase, the xylanase are used for the whitening of the pulp in the fabrication of paper including its recycling" [3]. Also, according to Loera (2002) this would help avoid or lessen that amount of toxins used for the previous processes without diminishing its quality.

Another benefit according to Loera 2002, is in conjunction with other hemicellulase the xylanase permits the ability to obtain the oligosaccharides of xylose (product of agriculture waste) for the use of food additive, coloring and with the conjunction of cellulase the modification of bakery dough and diets are also beneficiated. Precipitation testing will be performed as well.

Acknowledgment

We are fully grateful to Puerto Rico Energy Center and Massie Chair for Excellence Program Grant #DE-NA000672 at the Universidad del Turabo. The author is thankful to Dr. José R Pérez-Jimenéz for his support, the laboratory facilities and the opportunity to work under his guidance; Karin Millán for being the mentor of the pilot project, planning the structure of testing, help in the redaction and help with testing. I also thank Yomarie Bernier and Kenya Álamo for providing protocols and the reactant tests; Jonathan López for his assistance his molecular testing. Thankful for the funding by National Science Foundation's AMP and Puerto Rico Electric Company

References

McMillan, J.D. "Xylose Fermentation to Ethanol: A Review" unpublished 1993. January

Van Maris, Antonius J.A, et al. "Development of efficient xylose fermentation in saccharomyces cerevisiae:xylose isomerase as a key component" Springer-Verlag Berlin Heidelberg. 2007. April

Loera Corral, Octavio. "Las xilanasas microbianas y sus aplicaciones". vol. 7 no.2 2002

Appendix I

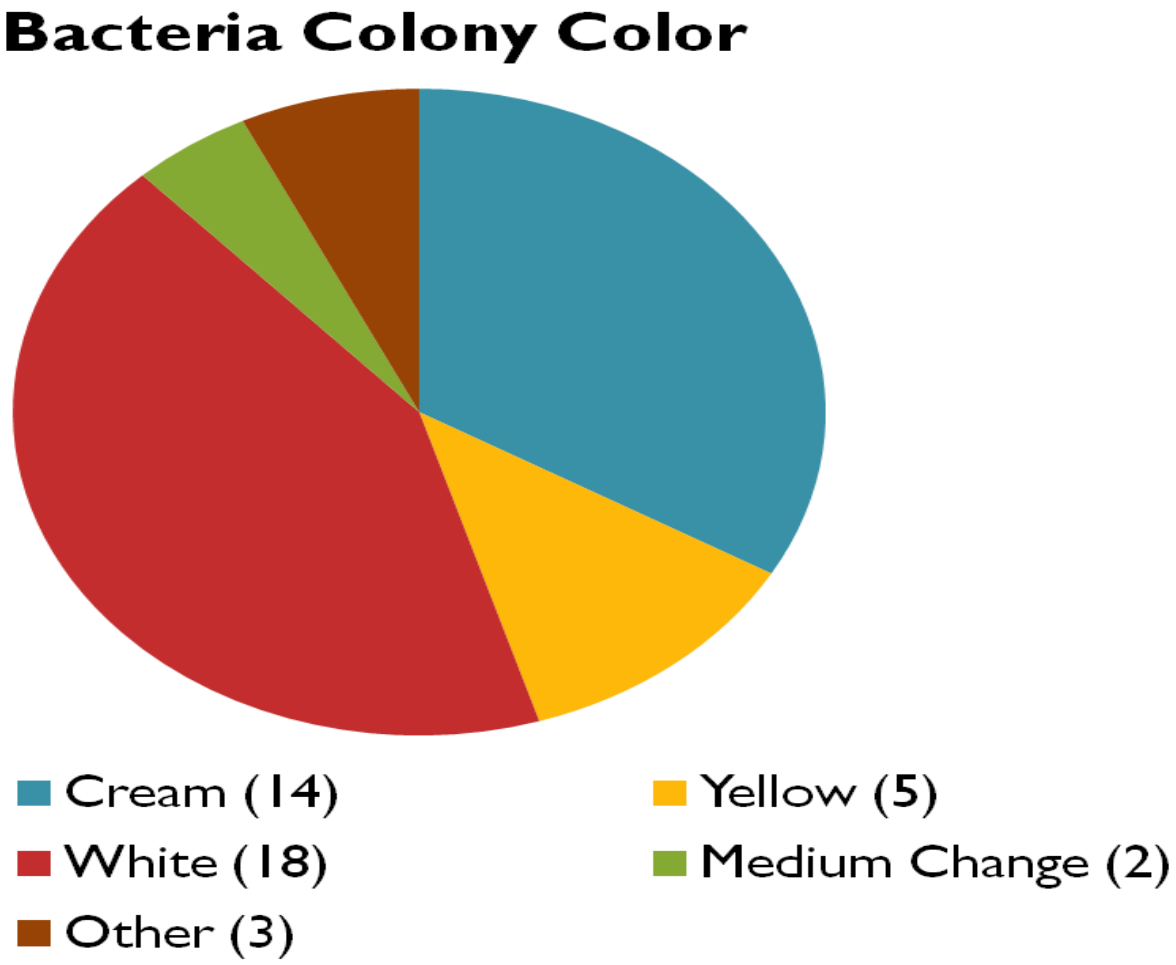
Bacteria Colony Color
Cream (14)
Yellow (5)
White (18)
Medium Change (2)
Other (3)

Appendix II

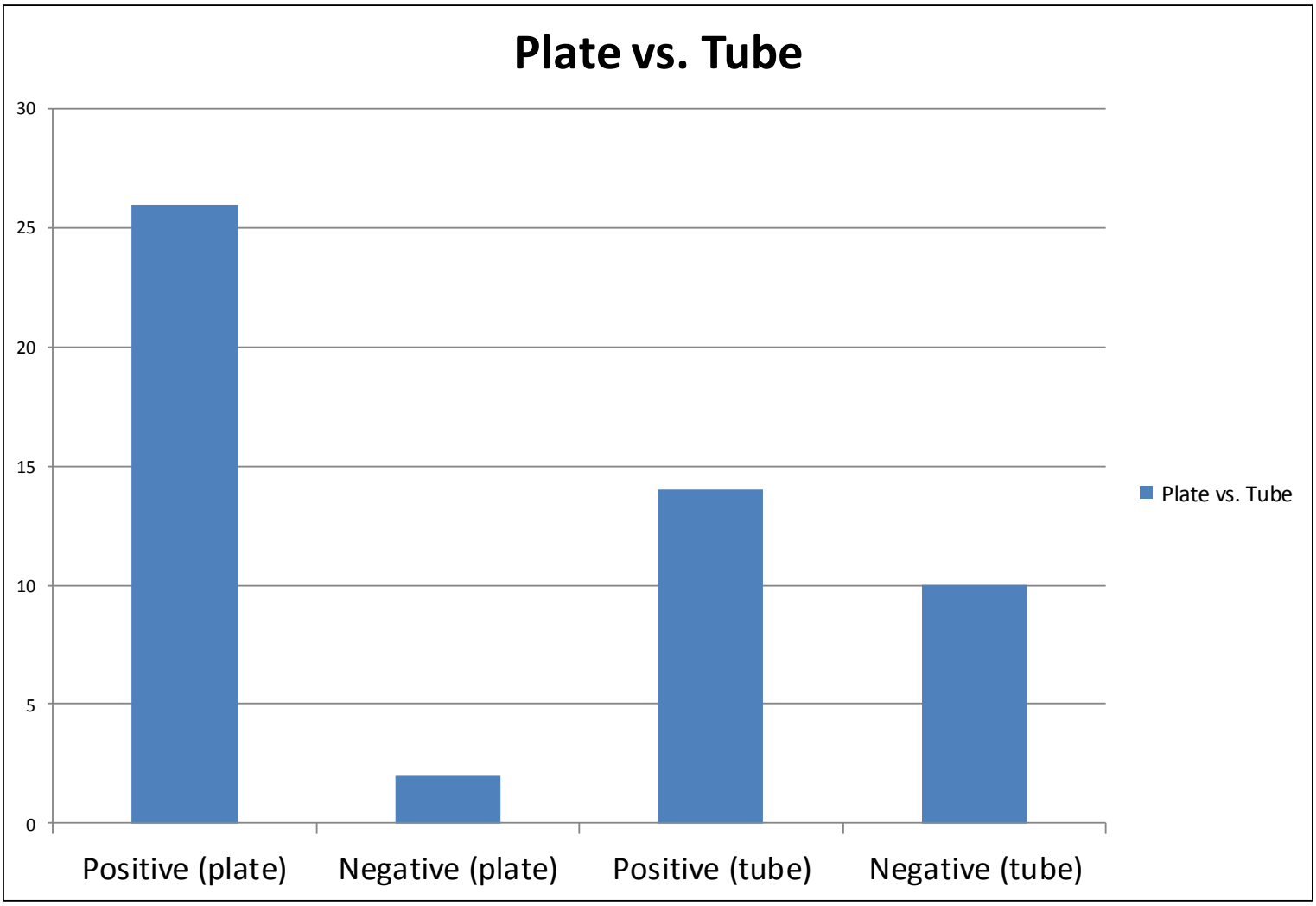
Plate vs. Tube
30
25
20
15
10
5
0
Positive (plate)
Negative (plate)
Positive (tube)
Negative (tube)
Plate vs. Tube

Appendix III

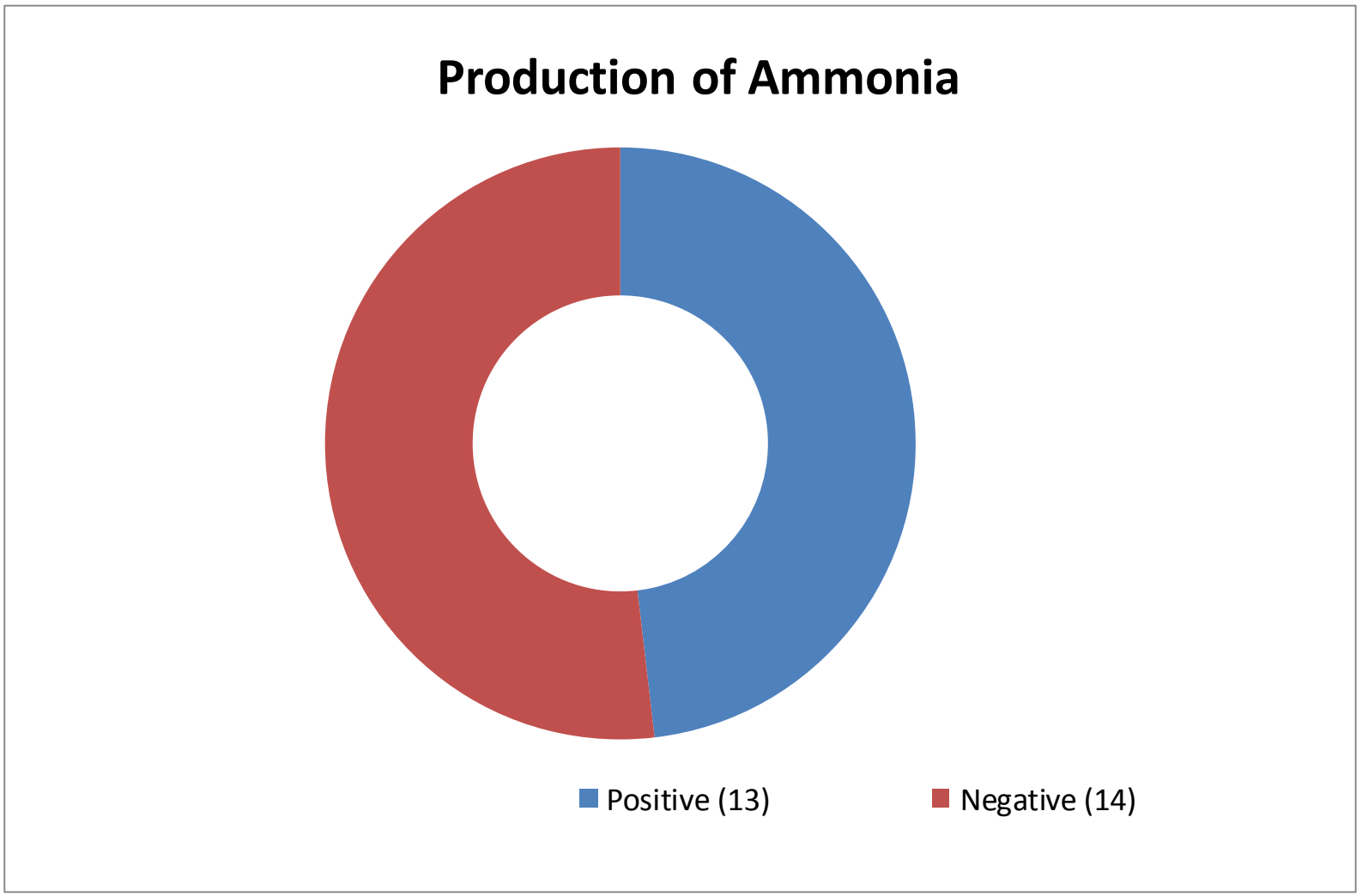

Appendix IV

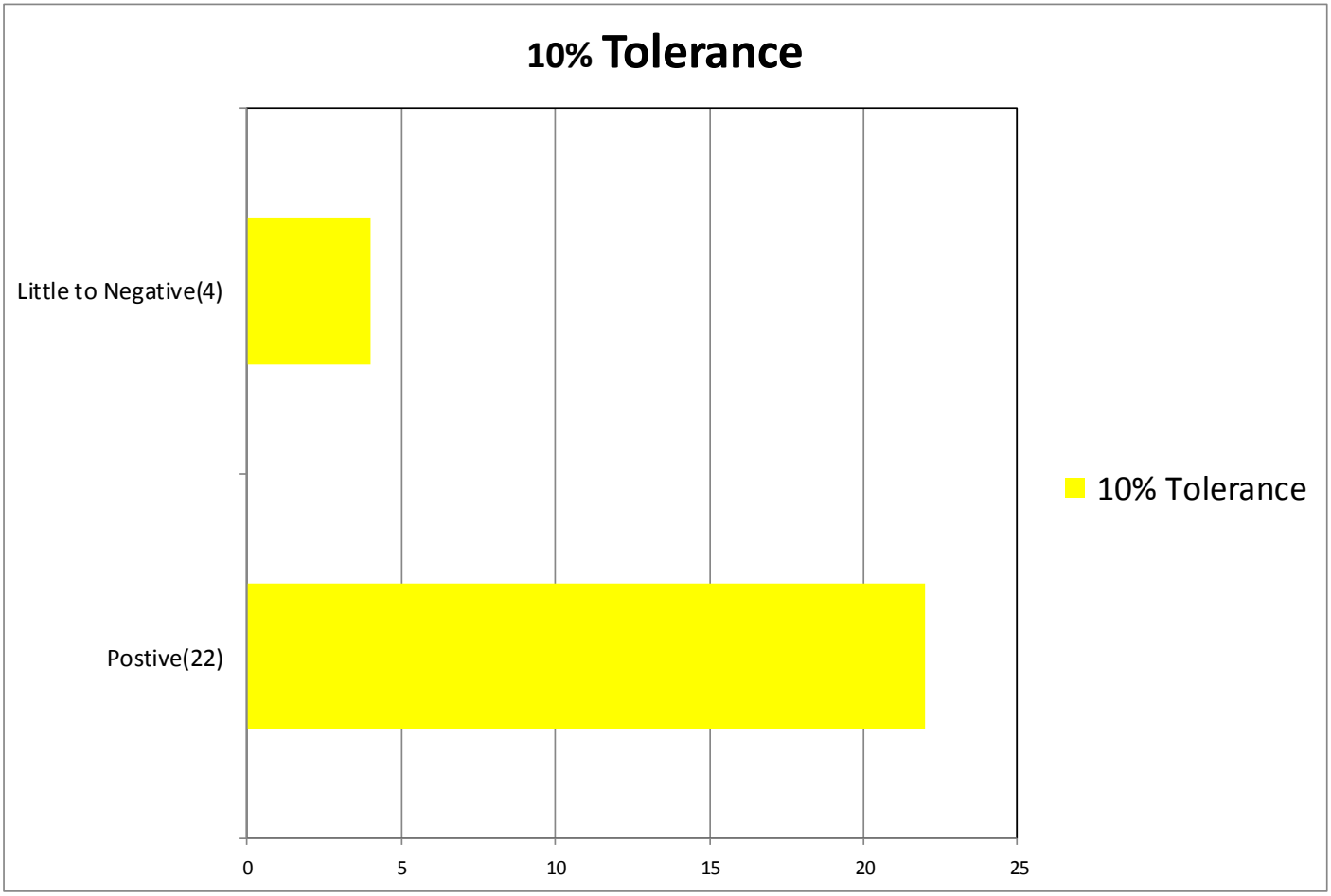
10% Tolerance
Little to Negative(4)
Postive(22)
0
5
10
15
20
25
10% Tolerance

Degradation of Propranolol by Photocatalysis using TiO_2

Jorge I. Valentín[1], Luis G. Gonzalez[2], and Francisco Marquéz[3],
mr1valentine@hotmail.com[1], gonzalez_hernandez@yahoo.com[2] and fmarquez@suagm.edu[3]
Scholl of Natural Science and Technology, Department of Chemistry and Physics,
Universidad del Turabo, P.O. Box 3030, Gurabo, P.R,

Abstract*– Pharmaceutical products are reaching environmental media over the world. The effects on the biota are unknowns, basically because the drugs synergism varies per organism. Several researchers demonstrated adverse effects over different organism. The photo-degradation activity of the synthesized titanium oxide nanostructure (rutile) and the titanium oxide for industrial use (anatase) was determined by measuring degradation of propranolol in the aqueous solution with a concentration of 0.7 g L^{-1}. The reaction was conducted in MFA polymer tubular reactor. The system was tested with variation of reactor diameter, usage of solar collector and titanium oxide morphology. The system with and without the solar collector was demonstrated be efficent, proving a better results by using the solar collector also prove rutile as titanium oxide phase. All results were analyzed by UV-vis spectroscopymeter. The photocatalytic activity in the MFA (perfluoro methyl alkoxy) pipe was observed in the ranges of 400 nm to 200 nm.

Keywords—Nano-structures, Titanium Dioxide, photo-degradation, propranolol, AOPs

I. Introduction

A lot of medicines products are produced worldwide to treat health disease. As a consequence of high demand of these pharmaceuticals products, large water bodies are contaminated. Pharmaceutical products have been detected in water bodies like rivers, seas, lakes, and groundwater and in wastewater treatment plants. For many pharmaceutical substances is hard to get a complete degradation. By this reason some portions are leaving in the environmental by the management of wastewater [2]. The effects on environmental ecosystem are unknown and their biochemical mechanisms are not well defined. For most pharmaceuticals, we are a long way from having the answers we require, and hence it is not possible to conduct meaningful environmental risk assessments for most pharmaceuticals in use today [12]. But possibly the greatest damage will be reflected in aquatic organisms, which are part of the food of our food chain, like fish, shellfish or any aquatic animal or plant of this environment.

Propranolol is a beta-blocker used as a cardiovascular Active Pharmaceutical Ingredient (API) for treatment of angina, hypertension and cardiac arrhythmia. Also is an optional medicine pain relieved of migraine (according drugs.com). Over 70 million of Americans have high blood pressure and are potential user of this drug [4]. Indeed, one of three Americans has pre-hypertension. The high blood pressure cost to the American Nation approximately $46 billion each year, and some part of this money is used to the production of medicine or treatment. The American adult population with diagnosed heart disease is 26.6 million [5]. The propranolol is a selected as water soluble API with toxicity in some aquatic species. The exposition of mussels, fish or other aquatic organism to propranolol has been investigated in the literature [11]. These adverse effects demonstrated a decrease in strengths of byssus, reduced the abundance byssus thread, decreased reproduction and others [3]. But this can turn more severe. The scientific community is in broad agreement with the possibility that adverse effects may arise from the uncontrolled presence of pharmaceuticals in the environment, not only for human health, but also for aquatic organisms. At the present time, regulations are in effect or planned in countries such as the United States and Canada. Chemicals released into the environment may have endocrine-disrupting effects in living organisms [9].

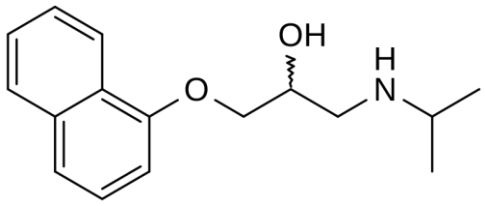

Figure. 1. Molecular structure of Propranolol, nomenclature $C_{16}H_{21}NO_2$

The titanium oxide is an n-type semiconductor and a typical photocatalyst. At present the TiO_2 is used for industrial areas (like purification), solar cells, sensors and cosmetics. Additionally to these applications, TiO_2 is a great catalytic. The main advantages of TiO_2 are its high chemical stability when exposed to acidic and basic compounds, its nontoxicity, it's relatively low cost and it's highly oxidizing power, which makes it a competitive candidate for many photocatalytic applications [10]. TiO_2 is almost used in two crystalline forms, anatase and rutile (for example nano wires). The photocatalysis effect consists when the irradiation energy (light or solar source) interacts with the catalys. The UV light excites the electrons from the valence band to the conduction band of TiO_2, leaving holes in the valence band. These electrons and holes can initiate redox reactions with the molecular species adsorbed on the surface of the catalyst, found in their border areas. Some of these electron-hole pairs disappear by

recombination on bulk TiO_2, while other electrons and holes diffuse to the surface of the TiO_2 catalysts to react with molecules, which led to photocatalytic reactions such as hydrogenolysis and the formation of oxygen-containing organic compounds [8]. The semiconductor catalyst only needs a photon of light to generate these holes. Electrons are liberated of the conduction band, producing radicals of the oxygen molecule in aqueous solution. In this phase oxidizing species, either bound hydroxyl radical (•OH) or free holes, which attack contaminants, are generated producing a progressive breaking of molecules yielding CO_2, H_2O and dilute inorganic acids[7]. H_2O_2 (peroxide) can be used a source of oxygen on TiO_2 photocatalyst

Advance oxidation process (AOPs) a great alternative for degrading pharmaceuticals products, but need a highly reactive hydroxyl radical (•OH). The energy required for translate the electron from the valence band to the conduction band is greater than 3.2 eV (electron volts).

The surface area of the catalys is important to this research, because the morphologies with high surface area will produce more degradation. According to previous research, the TiO_2 in the anatase phase has a surface area of ca. 56 m^2 g^{-1} [13] and the TiO_2 as nanowires in rutile phase can be synthesized with surface areas of 480 m^2 g^{-1} [1], in this way rutile is expected to produce higher degradation of propranolol.

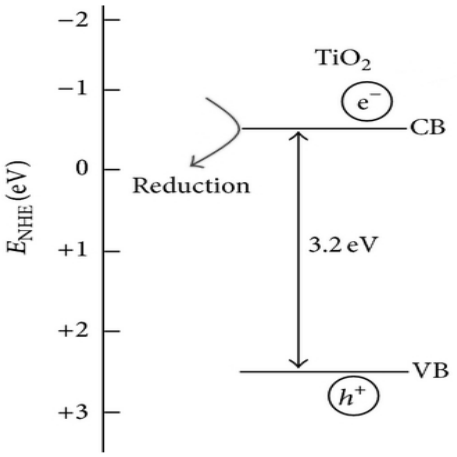

Figure 2. Energetic diagram of the catalytic process.

As mentioned above the light is the energy source. An energy of at least 3.2 eV is required for the electron jump occurs from the valence band to the conduction band (see Figure 2).

The MFA is a very clear polymer of terafluoroethylene and perfluoromethyl vinyl that only absorbs 40% of the UV light in the wavelength range of 300-500 nm. The MFA provide a durable, feasible and marketing alternative for photocatalyst reaction in reactor. An MFA will be put in the focus of a parabolic solar collector. The incidence of the light on the reaction can be increased with the use of solar collector panels. Solar collector panels with parabolic shape can efficiently concentrate the light in the focus. The concentration of light radiation will be focussed onto the center of the MFA pipe by the parabolic solar collector, according to the parabolic theory. And the focal point can be determinate by the equation of the Parabola:

$$x^2=4.p.y \qquad (1)$$

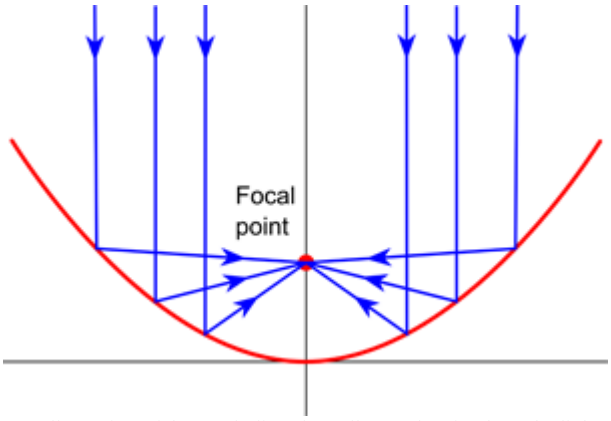

Figure 3. Illustration of the parabolic solar collector showing how the lights is directed to the focal poin (MFA pipe).

The complete application will be performed through an idealized system. This aqueous solution of propranolol will be exposed in the MFA to the solar collector at different periods of time. The effect of the diameter of the MFA pipe (from 0.0625 in to 0.1875 in) will be tested. Pipes with different diameter generate different residence times with the light source. The concentration of propranolol was measured by spectroscopy and compared with the catalytic process observed in presence or absence of the oxygen source (namely hydrogen peroxide) from to two original samples, one with peroxide and the other one without peroxide.

II. METHODOLOGY

A. Materials and Reagents

All solution were prepared using ultra-pure water (Milli-Q), with 18.2 $M\Omega cm^{-1}$ at 25 ºC. After reactions all aliquot was filtered with 0.45 µm syringe filters. The titanium oxide anatase was obtained from Acros Organics with a purity of 98% and the titanium oxide rutile (nanowires) was previously synthesized in the laboratory of Nanomaterials Research Group using Titanium tetracholide (Fluka, 99%) as precursor. The hydrochloric acid was obtained from Acros Organics (37% in water). The Propranolol HCl was acquiring from Acro Organics (99%). The Hydrogen Peroxide (55%) was adquired from Fisher Scientific. The lamps system includes a fluorescent spiral lamp with 3700 lumens and 55 watts. The peristaltic pump was fabricated with a capacity of 125 millimeter per minute. The perfluoro methyl alkoxy (MFA) was acquired from AltoFlo in two different diameters (1/16 inches and 3/16 inches). Two sources of oxygen are used (air and hydrogen peroxide). The solar collector was built of steels and aluminum. The catalytic process has been studied using Shimadzu 2401-PC Spectrophotometer. With the aim avoid

external irradiation sources; a black blanketed was placed over the solar collector.

B. *Solution Preparation*

A solution of 50 ppm of propranolol was prepared using 75 mL of ultra-pure water and 25 mL of propranolol at 200 ppm. The pH was adjusted to 6.0 with HCl. A first aliquot of 10 mL was extracted. Next 2.992 g of peroxide (XXX M) was added, and then a second aliquot of 10 mL was extracted. A 70 mL was introduced to the reactor system. Titanium oxide (0.049 g) was added to the reactor to maintain a concentration of 0.7 g L^{-1}.

The reactor container was placed on the center of a stirring board. Air was added to the reactor container as additional source of oxygen. A tube is positioned to extract the solution by a peristaltic pump to one side and another for returning the solution to the other side. The solution was stirred and pumped all time by a time of 6 hours. An aliquot was extracted at the finish run, to be analyzed with the two other sample by UV from Shimadzu 2401-PC Spectrophotometer.

A second set of run was repeated changing the MFA diameter to the system. Following the same steps mentioned previously.

III. Results

This research has a design of experiment of three treatment and two factors. Distributed by three different treatments, such as diameters, morphology and light variation implement through a solar panel. To obtain a system of variables 2x2x2 which gives equal to eight different run, repeat by three times to have a satisfying result. The recirculation flow of the solution was set to 90 mL min^{-1}. All under the same source of oxygen (i. e. air and hydrogen peroxide) and agitation pattern of their six hours of photo-degradation process. Also the same concentration of TiO_2 that was 0.07 g L^{-1} and pH the adjusted to 6.0.

A. *Data Runs*

Average of the all runs summarized in the eight parameters.

#	Treatment			Degradation (%)
	Morphologies	Diameter	Panel	
1	Anatase	D1	None	18.958
2	Rutile	D1	None	41.375
3	Anatase	D2	None	57.041
4	Rutile	D2	None	62.291
5	Anatase	D1	Panel	27.041
6	Rutile	D1	Panel	54.625
7	Anatase	D2	Panel	60.958
8	Rutile	D2	Panel	71.375

** D1=0.0625 in, D2=0.1875 in*

B. *Surface Area*

The surface area is an important part of this research. While more surface area is the molecule better will be the photo-degradation. Using two kind of crystalline form (rutile and anatase), the SEM can provides a scale difference view of both nano-structures. Larger surface areas can be obtained by decreasing the particle size of the photocatalyst when the particle has a single domain size [6]. The anatase surface area was 50 g m^{-2} and the rutile surface area was 350 g m^2

C. *Photocatalytic Degradation*

The charts 1 show how the degradation increases between the changes of variable. Using the two diameter of the MFA pipe, demonstrated that diameter of 0.1875 inches has better results than the diameter of 0.0625 inches. And the TiO_2 NWs have a better degradation than the use of anatase form. Because of this combination of the two variables we get the best result in this specific scenario. Can be appreciated that with (green line) the solar panel the degradation is better than without (blue line) the solar panel. As additional fact, the data with the solar panel has an increase of degradation of 10% more than without panel, by the same condition. This result brings a positive conclusion of our statement from the use of solar collector, making this parabola aluminium reflector an ideal application for future research or method to degradation system. Also the implement of the glass and the black blanked can improve the results. Each point of this chart was repeated three times to get a satisfactory result. The data shows that at all times the TiO_2 used in rutile morphology causes a large increase in degradation, demonstrating the slope formed on the chart

CHART I

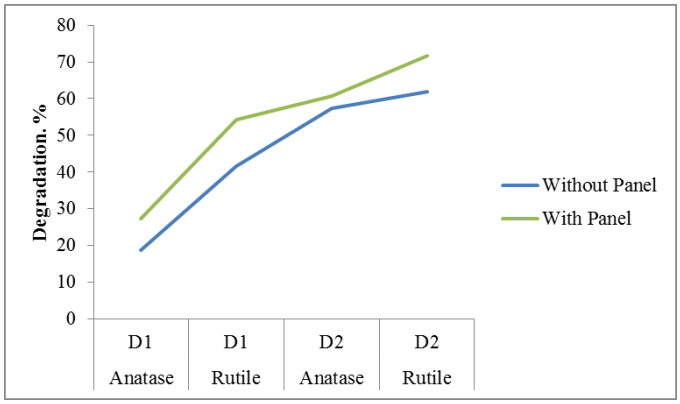

Chart 1. Compare Data With and Without Solar Panel

The chart 2 show how increase the degradation between crystalline morphologies of anatase and rutile. Taking as variable the diameter and the solar panel. The data, like the previously chart the best match for this scenario was using the variable of rutile morphology, with the solar collector and the bigger diameter of MFA pipe. Then again, in this setup the degradation of rutile form begins a 20% over the anatase, by the same condition. Also a highly impact in the change of two pipe diameter was prove. The slope ascending generated

between the small pipes to large pipe show that a residence time in the very clear polymer was an important factor to investigate. As well, the big difference between the first points of both morphologies can express mentioned above. A big negative factor for the industrial use of TiO_2 it was the large accumulation of waste in the walls of the pipe. Creating an obstacle to light, thus having a slower process of photo-degradation. Maybe this problem comes thru the physical characteristic differences between both titanium oxide morphologies. Nevertheless, the use of rutile morphology does not have any accumulation in the pipe walls, making a system eco-friendly, because no need continuously cleaning and greater results.

CHART II

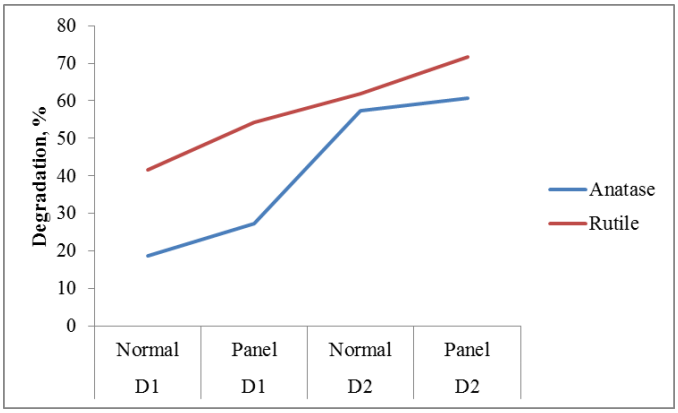

Chart 2. Compare Data of Anatase and Rutile

The chart 3 shows how the degradation increases between the changes of variable in diameter size. The data confirm that both diameters have better degradation, with the solar panel and the morphology of rutile. Also the diameter of 0.1875 inches shows better efficiency than the diameter of 0.0625 inches. In addition, the impact of the use of the diameter of 0.1875 inches is 40% over the other diameter. It is our hypothesis the difference that generated the two diameters is the residence time influenced by the volume of the pipe line. The flow rate in the system is an important factor. For the pipe of 0.1875 inches, the flow rate used for this research was to be approximately 90 mL min^{-1} (1.5 mL s^{-1}) to obtain a residence time of 3.84 seconds. The pipe of 0.0625 inches of diameter also has the same flow rate of 90 mL min^{-1}, but to be a diameter more closely the residence time decrease to 0.4324 seconds. Also the volumetric size of the 0.1875 inches diameter pipe was 5.88 mL whereas the pipe line of 0.0625 inches was 0.653 mL. This mean that by a flow rate of 90 mL min^{-1} the volume of 5.88 mL (0.1875 inches pipe) it passes through the MFA polymer 5,571 times. In comparison of the volume of 0.653 mL (0.0625 inches pipe) that it passes through the MFA polymer 50,168 times, too fast to have a good interaction with the light and generated a photo-degradation. In the case of diameter of 0.0625 the residence time is less than a second, is 0.4324 second in compare to the diameter of 0.1875 inches that was 3.84 seconds. Nine time more than the little diameter. These mean an important variable to study for future research. According to the theory of mass conservation this situation can be explained. Because, according to the theory of mass conservation the mass of fluid in a flow tube is constant. Where streamlines crowd together the flow speed increases, in other words if the cross sectional area are reduced, the velocity will increased.

CHART III

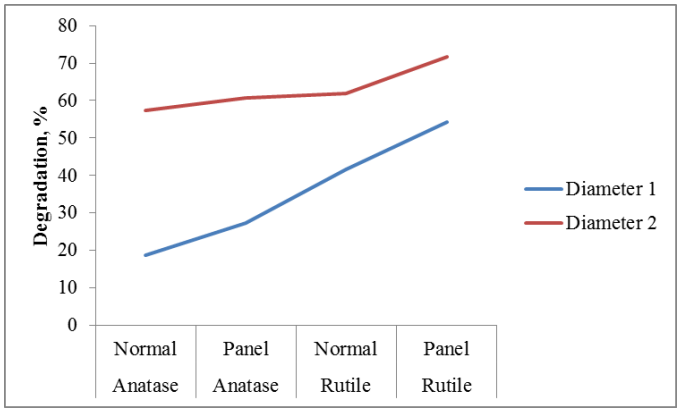

Chart 3. Compare Data of Both Diameter

D. Best Data Run

From 24 run, with three different treatments the best result was obtained using titanium oxide nanowires, the solar collector panel and the bigger diameter.

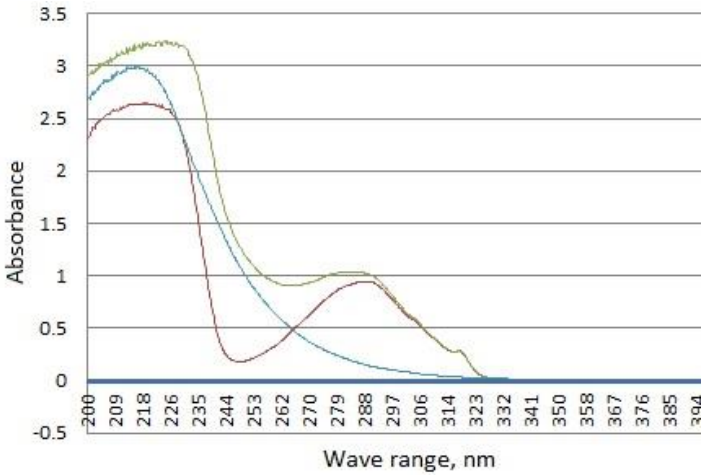

Chart 4. Spectrum degradation of Propranolol with the best match treatments.

E. Summarized Results

The diagram 1 summarized all the results. Each face represents a diverse parameter. The upper face represent the data of the diameter of 0.1875 inches, the lower face represent the data of diameter of 0.0625 inches, the left side face represent the data of anatase runs and the right side face

represent the rutile morphology data. The front face is the data without the solar panel and the back side is the data with the solar panel. With this view, in the top-right back show the best achievement of 71% propranolol reduction.

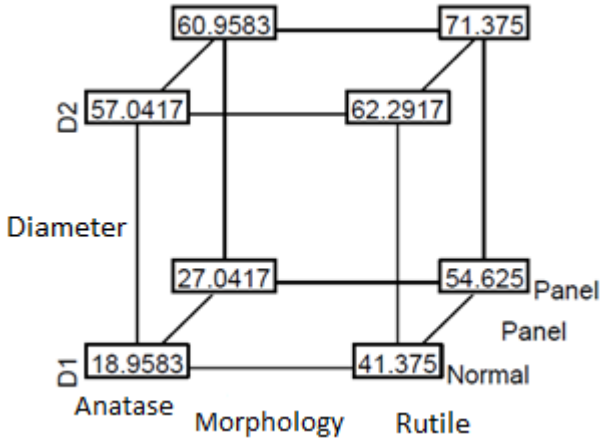

Diagram 1. Cube Plot data summarized

F. Statistical View

To make sure have collected great information, a statistical analysis was done. The chart show a good response predicted with a lower P-value of <0.0001. The data results show a good distribution and response.

P-VALUE

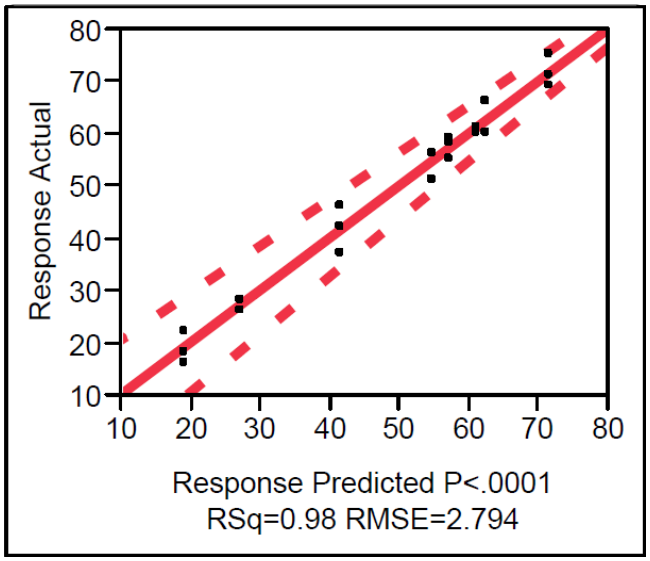

Chart 5.Response to response P-value.

IV. CONCLUSION

The solar collector was tested successfully in the application. TiO_2 NWs (rutile) form been demonstrated has best feasible nanostructure degradation with the complement of a solar collector and the use of a MFA polymer of a 3/16 inches diameter. In addition it was prove that titanium oxide nanowire has a better degradation on propranolol on all treatment level. In future research can be tested other diameter and flow rate influence.

ACKNOWLEDGMENT

We are fully grateful to Puerto Rico Energy Center and Massie Chair for Excellence Program Grant #DE-NA000672 at the Universidad del Turabo. The authors would like to thank to the Nanomaterial Research Group and the Laboratory ELC 206 for the use of their facilities.

REFERENCES

[1] Cotto-Maldonado M del C. 2012. Heterogeneous catalysis applied to advanced oxidation processes (AOPs) for degradation of organic pollutants [dissertation]. [Gurabo (PR)]: Turabo University.

[2] Cunningham V, Buzby M, Hutchinson T, Mastrocco F, Parke N, Roden N. 2006. Effects of Human Pharmaceuticals on Aquatic life: Next Steps. Environ Sci Technol. 1:3456 3462.

[3] Ericson, H., Kumblad, L., & Thorsén, G. (2010, August 1). Physiological effects of diclofenac, ibuprofen and propranolol on Baltic Sea blue mussels. Retrieved July 29, 2015.

[4] Heart Disease Fact Sheet. (2015, February 19). Retrieved July 21, 2015, from http://www.cdc.gov/dhdsp/data statistics/factsheets/fs heart_disease.htm

[5] High Blood Pressure Facts. (2015, February 19). Retrieved July 21, 2015, from http://www.cdc.gov/bloodpressure/facts.htm

[6] Jang-Dong HD, Seong-Kim K, Seung-Jin K. 2001. Effect of particle size and phase composition of titanium dioxide nanoparticles on the photocatalytic properties. J Nanoparticle Res. 3:141–147.

[7] Malato S, Blanco J, Vidal A, Richter C. 2002. Photocatalysis with solar energy at a pilot-plant scale: an overview. Appl Catal B Environ. 37:1–15.

[8] Masaku A, Masato T. 2003. The design and development of highly reactive titanium oxide photocatalysts operating under visible light irradiation. J Catal 216:505–516.

[9] Nikolaou A, Meric S, Fatta D, Rizzo L. 2007. Occurrence patterns of pharmaceuticals in water and wastewater environments. Anal Bioanal Chem. 387:1225–34.

[10] Ohama, Y., & Gemert, D. (2011). Principles of TiO2 Photocatalysis. In *Applications of Titanium Dioxide Photocatalysis to Construction Materials* (pp. 5-10). Dordrecht: Springer.

[11] Solé, M., & Shaw, J. (2010). Effects on feeding rate and biomarker responses of marine mussels experimentally exposed to propranolol and acetaminophen. Analytical and Bioanalytical Chemistry, 396, 649-656. July 29, 2015, http://dx.doi.org/10.1007/s00216-009-3182-1

[12] Sumpter JP. 2007. Environmental effects of human pharmaceuticals. Drug Inf J. 41:143.

[13] Velegraki T, Mantzavinos D. 2008. Conversion of benzoic acid during TiO2-mediated photocatalytic degradation in water. Chem Eng J. 140:15–21.

Cardiovascular Effects of *Crataegus oxyacantha* on Hypertensive Patients in Clínica S.A.N.O.S.

F. Valentín, MD.[1], B. Ramos, BS.[1], C. Meléndez, Undergraduate Student[2], Y. Rodríguez, Undergraduate Student[2]
[1]Universidad del Turabo, Gurabo, fvalentin8@suagm.edu, bruramos1@gmail.com
[2]Universidad del Turabo, Gurabo, carolis.melendez@upr.edu, yrodriguez312@suagm.edu

Abstract*– Naturopathic Medicine is a distinct primary health care profession, which develops an individual therapeutic plan according to their philosophy. This alternative medicine brings different ways to treat diseases including botanical medicine. Crataegus oxyacantha also known as Hawthorn, is a plant that in previous investigations have mentioned their properties to reduce blood pressure and lipids in blood. For this study we did a medical record review of two hundred patients in the Naturopathic Medicine Clinic of Turabo University in S.A.N.O.S. to verify the effectively of Crataegus oxyacantha as a treatment for hypertensive patients. Crataegus oxyacantha was only recommended like a treatment for hypertension in one patient. We analyze the possible causes why so few patients use this plant for cardiovascular diseases against other treatments.

***Keywords*—Crataegus oxyacantha, Hawthorn, Hypertension, Naturopathic Medicine, Botanical Medicine**

I. Introduction

Cardiovascular diseases remain the most prevalent cause of human mortality all over the world. According to the survey by Global Burden of Disease Study, 29.6% of all deaths worldwide were caused by cardiovascular diseases in 2010. It is estimated that the number of people die from cardiovascular problem that will increase in the next years. According to the Health Department of Puerto Rico for 2005, the leading cause of death in the island was heart disease.

The American Association of Naturopathic Physicians (AANP) defines Naturopathic Medicine (NM) as a distinct primary health care profession, emphasizing prevention, treatment, and optimal health through the use of therapeutic methods and substances that encourage individual inherent self-healing process. The practice of NM includes modern and traditional, scientific, and empirical methods. Also can be used alone as an alternative treatment or combined with allopathic medicines as complementary. This type of medicine is more cost effective at long terms but it needs more investigation here in Puerto Rico and all around the world to keep sustaining results and to acquire more knowledge of it.

Crataegus oxyacantha is a medicinal plant that has been used for a variety of functional cardiovascular disorders and has a protective effect against ischemia/reperfusion. The multiple cardiovascular protective effect are: (1) endothelial protective effect, (2) antiarrhythmic, (3) antioxidant, (4) positive inotropic, (5) anti-inflammatory, (6) reduction of smooth muscle cell migration and proliferation, (7) blood pressure-lowering, (8) lipid-lowering, (9) anti-cardiac remodeling, (10) antiplatelet aggregation, and (11) vasodilating [19]. Those benefits are due to the active constituents in hawthorn leaves, flowers and berries. The active constituents include two groups of polyphenolic compounds: flavonoids and oligomeric proanthocyanidins (OPCs) [20]. Recent research shows *Crataegus* extracts has a wide range of positive actions, low-risk and effective treatment for different heart conditions including hypertension, atherosclerosis, hypercholesterolemia and chronic heart failure. Pharmacologic activities attributed to the flavonoids and/or OPCs include: (1) angiotensin converting enzyme (ACE) inhibition; (2) type-III/IV phosphodiesterase inhibition; (3) Na^+/K^+ ATPase activity; (4) antioxidant activity; and (5) decreased production and release of histamine, prostaglandins, leukotrienes, and inhibition of neutrophil elastase [20]. Actually, the role of Hawtorn efficacy is still debatable, to any final conclusions about the standard of therapeutic doses.

Published data evaluating the efficacy, adverse effect, recommended doses of hawthorn are limited and inconclusive. Recent research used different dosage for the clinical trials, from 160 mg to 900 mg hawthorn extract per day in 2 or 3 divided doses. There is no standard dose in humans associated with hypotension and sedative effect, only large doses in animals. In between, the most common adverse effects reported were dizziness/vertigo and gastrointestinal intolerance [13]. Also published studies in humans assessing efficacy in short and long term for hypertension and hyperlipidemia need to be clarify. Self-treatment with this herb may delay the initiation of prescription medications but may be unsafely in patients with conventional treatment and needs to be evaluated by naturopathic physician before start the botanical therapy.

The aim of this study is to compare the scheme of traditional medicine and the cost of this medical services acquiring knowledge of what treatments have been used here in Puerto Rico for cardiovascular diseases. In between, the evaluation for hypertension (HTN) patients with the berry and flower of *Crataegus oxyacantha*, the improvements in clinical symptoms (such as fatigue, palpitations, and exercise dyspnea) lowering the blood pressure and resting pulse and the effects of *Crataegus oxyacantha* usage in cardiovascular disease prevention, lowering lipids (LDL, VLDL, triglycerides and total cholesterol). This study is the first step for further studies at molecular level of *Crataegus oxyacantha* since the mechanism of the plant are yet unknown and cardiovascular physiology. It is a long term goal to make pre-clinical trials

with *Crataegus oxyacantha* as a first step of investigation instead of medical record review (MRR) study finding then the ways of interactions with the plant (if there is any) and to provide the basis for specific drug design enhancing the mechanism of action in the cardiovascular system. The MRR was selected because it is the best method of answering the research question. Using the MRR we can access a useful data for the *Crataegus oxyacantha* interventions. *Crataegus oxyacantha* treatment will be very effective in reducing blood pressure. As well as it has a positive effect reducing lipids, cause of many heart problems.

II. METHODS

A. *Study design and setting*

A retrospective medical record review (MRR) study of two-hundred patients in the Naturopathic Medicine Clinic of Turabo University in Caguas, Puerto Rico was undertaken to investigate the prevalence of patient using *Crataegus oxyacantha* for hypertension and the herbal response for the symptoms relieve and decreasing hyperlipidemia. The MRR was selected because it is the best method of answering the research question. Using the MRR we can access a useful data for the Crataegus oxyacantha interventions. Patient-focused data can be found in paper-based medical records. In the MRR studies there is data that typically limits or excludes the case-identifying information, for that reason the reviewers provide the HIPS, RCR and IRB certifications to guarantee the privacy and safety of all information seen of the patients in this study. All medical records to be accessed for study were already in existence for the IRB submission. This study was review and approved by the Institutional Review Board of the Sistema Universitario Ana G. Méndez and its branch Universidad del Turabo.

B. *Data collection and analysis*

A 2-year period of registry files was reviewed and the information was recollected in the table of data collected for the patients accepted by the IRB. This table shows the following information for each visit to the Naturopathic Medicine Clinic of Turabo University: record number, vital signs, age, CBC abnormal results, lipid panel abnormal results, weight, height, initial diagnosis, final diagnosis, allopathic or conventional treatment and naturopathic intervention or treatment. In this table, we add gender, chief complaint of each visit made to the clinic and natural supplements or vitamins taken before the first visit. The source of the information in the MRR include: naturopathic physicians, primary naturopathic students and secondary naturopathic student notes also diagnostic test (e.g. electrocardiograms, radiographs, laboratory tests). As an instrument, for the data analysis, tables and graph we use the Minitab 17 computer program. This study does not need any informed consent because it is not a direct intervention with patients.

III. RESULTS

The first two-hundred records of the patients from 2012 to

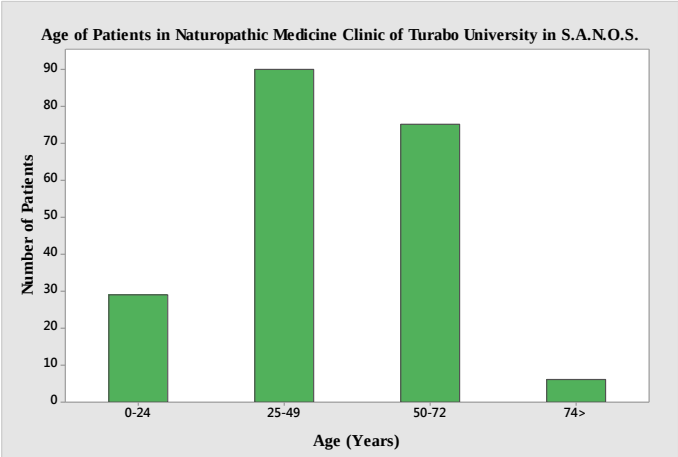

2015 in the Naturopathic Medicine Clinic of the Turabo University was cautiously examine one by one and sort them in different categories to examine the effects of *Crataegus oxyacantha*. In the Figure 1 we analyze the age of the patient

Fig. 1 Age of patients attending to the Clinic of Naturopathic Medicine of the University of Turabo in S.A.N.O.S.

dividing it into four categories (0-24, 25-49, 50-74, over 74). The age range that most visited the clinic was people between 25-49 years (46.5%) followed by patients between 50-74 years old (36.5%). The populations between 0-24 years (13.5%) and over 74 years (3.5%) had much lower participation in the clinic.

The Figure 2 shows the analysis and comparison between visits made by males and females to the Clinic of Naturopathic Medicine of University of Turabo in S.A.N.O.S. The result was that the clinic has more females' patients in the analysed data. Female patients was 149 (74.5%) and male patients 51 (25.5%). These amounts include men and women of any age and any chief complaint who visited the clinic. This chart doesn't include information about the number of visits made by each patient.

Patients go to the Naturopathic Medicine Clinic not just for cardiovascular diseases, a chief complaint is the first sentence written by a doctor saying the main purposed the patient visit to the Naturopathic Medicine Clinic. It is worthy to distinguish that the chief complaint is not taken only in the first visit of the patient; it has to be written every time the patient visits the clinic. The figure 3 represents the twenty most common chief complaints of the two-hundred patients in the Naturopathic

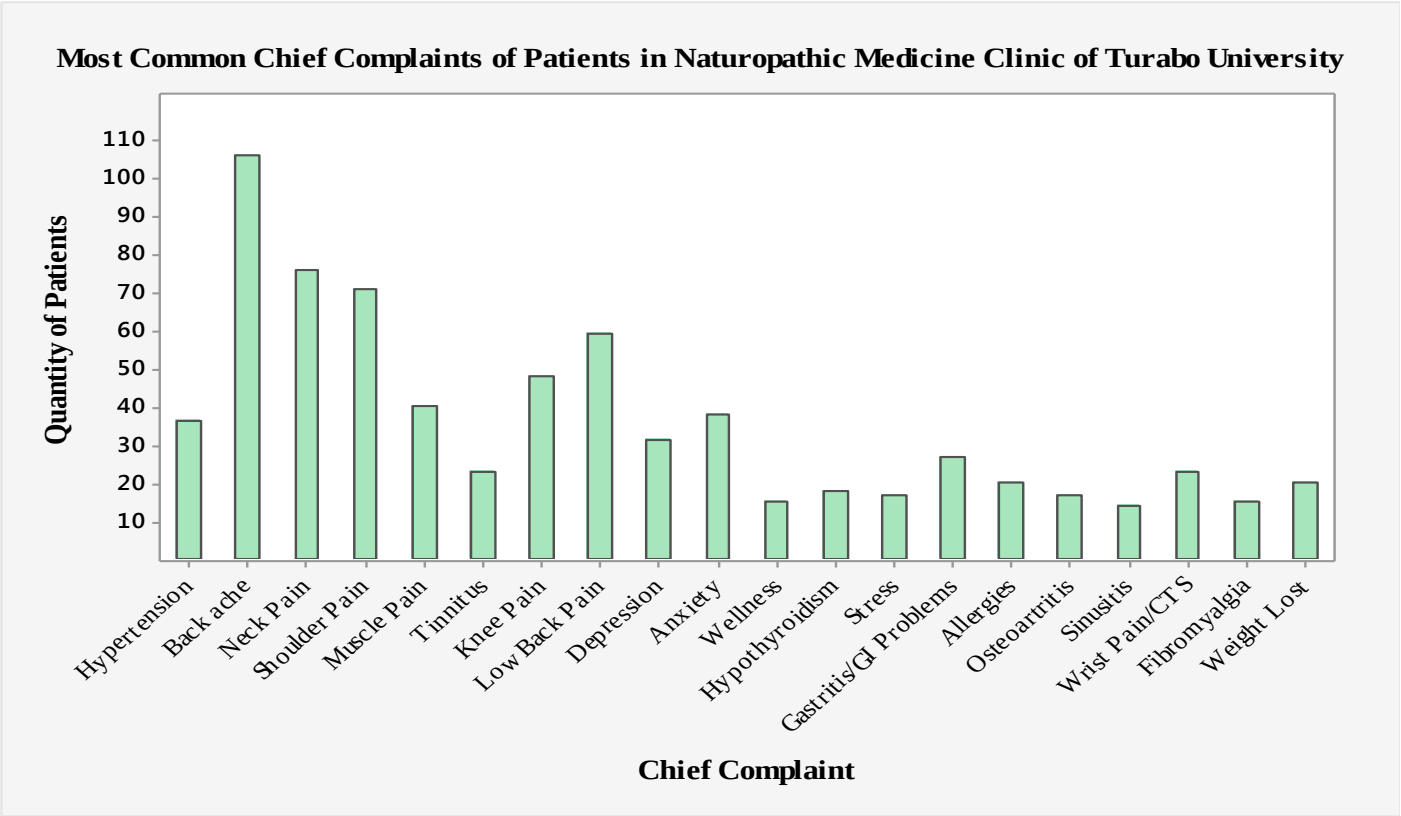

Fig. 3 Top 20 Most Common Chief Complaints attending to the Clinic of Naturopathic Medicine in S.A.N.O.S.

Medicine Clinic. There are 36 patients visits with a chief complaint of hypertension, a 106 with backache, 76 with neck pain, 71 with shoulder pain, 40 with muscular pain, 23 with tinnitus, 48 with knee pain, 59 with low back pain, 31 with depression, 38 with anxiety, 15 for wellness, 17 for osteoarthritis, 14 for sinusitis, 23 for wrist pain / carpal tunnel syndrome, 15 with fibromyalgia and 20 for weight lost.

Among the 200 records analysed 18 patients had diagnosis of hypertension, 7 of these reported are taking five or more medicines. This is considered polypharmacy conducts. Three polypharmacy people came to the clinic seeking treatment for hypertension. About 36 hypertensive patients visits, 58% of cases were accompanied by other health conditions. In the table 1 we summarize the most common health conditions that hypertensive patients had. The most common of these was the hypertriglyceridemia followed by the Diabetes Mellitus type 2.

In the figure 4 we analyse the number of visits made by patients. This graphic shows the number of views made by each of the 200 patients tested in the study. One can observe that 40% of patients visited the clinic only once. The 60% had two or more visits. Among the patients who visited the clinic several times 3 visits was the most common with 13.5% of

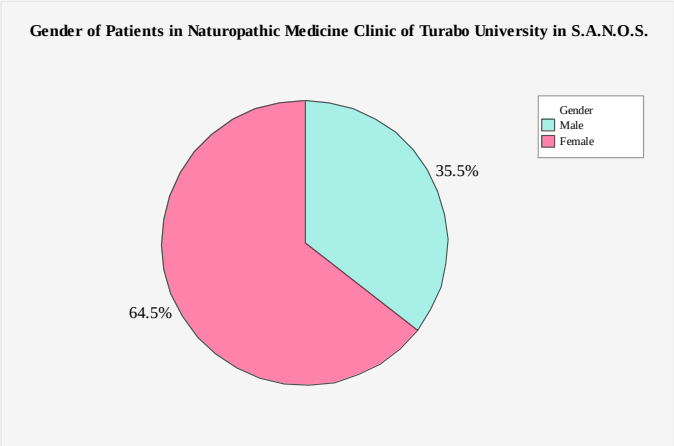

Fig. 2 Gender of Patients attending to the Clinic of Naturopathic Medicine of the University of Turabo in S.A.N.O.S.

visits. In the range of 1 to 5 visits there were 154 patients. The distribution was 80 patients visited the clinic once, 26 visited twice, 29 were treated three times, 9 patients received attention four times and 10 in five occasions.

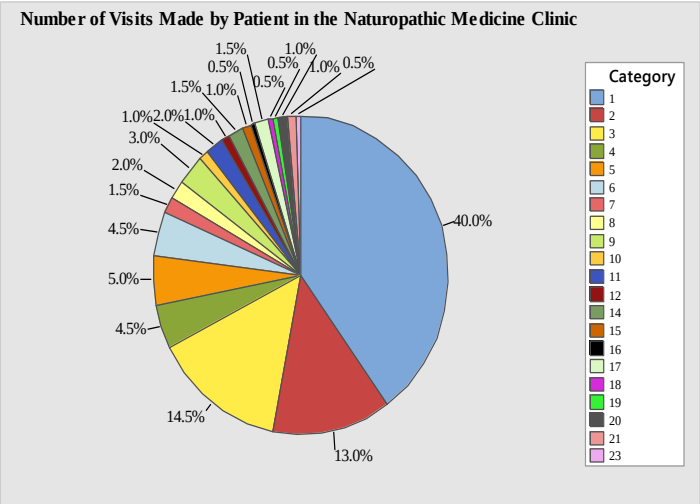

Fig. 4 Amounts of visits by patients attending to the Clinic of Naturopathic Medicine of the University of Turabo in S.A.N.O.S.

Conditions Associated with Hypertension	Number of Patients with Chief Complaint of Hypertension + Other Condition Associated
Hyperthyroidism	4
Diabetes Mellitus Type 2	4
Hypertriglyceridemia	11
MI recovery + DM	1
HTN + DM + Glaucoma	1

Table 2 Different treatments given or recommended to the patients in the Naturopathic Medicine Clinic of the University of Turabo in S.A.N.O.S.

Only 18 patients suffer from hypertension. We carefully examined the chief complaints and diagnosed of these patients and found that they were given a numerous of other treatments. The table 2 shows the treatments that were given or recommended to the patients instead of *Crataegus oxyacantha*.

Treatment	of patients with chief complaint/diagnosed HTN/HBP
Fish oil	9
Acupuncture	8
Diet Diary	8
Auricular Acupuncture	7
Nutritional Counselling	7
Paleo Mediterranean Diet	4
Vitamin C	4
CoQ10	4
Physical Medicine	4
Vitamin D3	3
Niacin	3
Increase Water Intake	3
Whey Protein	3
Milk Thistle	3
Pain X	2
Chromium Pico Linate	2
NAC	2
Gingko Biloba	2
Hydrotherapy	2
Homeopathy	1
Exercise	1
Vitamin E	1
Haworth	1

Table 1 Health conditions developed together with hypertension by patients that attend to Naturopathic Medicine Clinic of the University of Turabo in S.A.N.O.S.

IV. DISCUSSION

In the MRR in Naturopathic Medicine Clinic of the University of Turabo in S.A.N.O.S Corporation we observed that the main reason people visit the clinic was for pain management, especially backache. This may be due because pain management is one of the most concern of the people want naturopathic medicine alternative treatments. Besides the population most visited clinic was a young and middle-age adult, 25-49 years range, who is still in the workforce.

Only one patient was taking *Crataeugus oxyacantha* supplement to treat her HTN. This 71 years old female patient came to the clinic for generalized pain, nasal allergies, leg and hip pain and also other conditions like allergic rhinitis, diabetic retinopathy, obesity and multiple arthralgia's. Diabetic retinopathy suggested a long time poor controlled HTN, supporting a *Crataegus oxyacantha* treatment for prevention of cardiovascular disease complication. In the other hand, she also is a polypharmacy patient, consuming seven allopatic medicines. Three of these drugs are to treat HTN (Losartan 25mg, Metropolol 50mg, Terazosin 5mg). This is one of the reasons why so few patients were found taking Hawthorn. Another reason is the therapeutic order of NM. Prescribing a medication or supplement is not the main objective of the therapeutic approach. NM is to be as less invasive as possible. The first step is to know the lifestyle of the person and try to

balance or correct them. If after several interventions the chief complaint is not corrected the Naturopathic Doctors (ND) proceed to prescribe a medication or supplement.

Regarding the table 2, in these patients the most common treatment for hypertensive patients was fish oil; this is because essential fatty acids found in fish oil work in the prostaglandins mechanisms like an anti-inflammatory agent. Also other properties found like anti-atherosclerosis, promoting a rising in high density lipoprotein (HDL), known as "good cholesterol". The second most common treatment was acupuncture. Acupuncture facilitated a significant reduction in blood pressure promoting relaxation. Seven patients were recommended to do a diet diary which goes later with nutritional counselling. People with cardiovascular problems, especially hypertension need a diet with more low-fat protein sources, whole grains, and plenty of fruits and vegetables.

These results are explained for many reasons. The most three important are: naturopathic medicine philosophy, therapeutic order and naturopathic doctor approach. As a naturopathic doctor it is not an option to treat immediately with *Crataegus oxyacantha* skipping the therapeutic order, especially without follow there philosophic principles. These include: (1) The Healing Power of Nature (*Vis Medicatrix Naturae*): NM recognizes an inherent self-healing process in people that is ordered and intelligent. naturopathic physicians act to identify and remove obstacles to healing and recovery, and to facilitate and augment this inherent self-healing process. (2) Identify and Treat the Causes (*Tolle Causam*): The naturopathic physician seeks to identify and remove the underlying causes of illness rather than to merely eliminate or suppress symptoms. (3) First Do No Harm (*Primum Non Nocere*), naturopathic physicians follow three guidelines to avoid harming the patient: Utilize methods and medicinal substances which minimize the risk of harmful side effects, using the least force necessary to diagnose and treat; avoid when possible the harmful suppression of symptoms; and acknowledge, respect, and work with individuals' self-healing process. (4) Doctor as Teacher (*Docere*): Naturopathic physicians educate their patients and encourage self-responsibility for health. They also recognize and employ the therapeutic potential of the doctor-patient relationship. (5) Treat the Whole Person: Naturopathic physicians treat each patient by taking into account individual physical, mental, emotional, genetic, environmental, social, and other factors. Since total health also includes spiritual health, naturopathic physicians encourage individuals to pursue their personal spiritual development. (6) Prevention: Naturopathic physicians emphasize the prevention of disease by assessing risk factors, heredity and susceptibility to disease, and by making appropriate interventions in partnership with their patients to prevent illness [18].

Socio-economic status is another reason for our results. Often when natural treatments are prescribed, economic condition of the person does not allow him to continue treatment. Most patients who come to the clinic are people with limited resources. According to a report published by the AARP organization, pharmaceutical industries tend to increase the costs of their drugs the years before their patents expire. Cozaar and Vasotec are two of the most commonly used medicines to treat hypertension. Losartan and Enalapril is their respective generic. The cost for a monthly treatment with Cozaar is $50 to $115; while it's generic (Losartan) is $ 50 to $ 95. The cost of a monthly treatment with Vasotec is $90 to $280; while it's generic (Enalapril) $ 45 to $ 135. The cost of a monthly treatment based on *Crataegus oxyacantha* is between $25 to $150. The costs depend on the dose and how is presented this supplement (tincture or capsule). Though a natural treatment may be more economical than one allopathic the health insurances in Puerto Rico do not cover ND's consult and treatments.

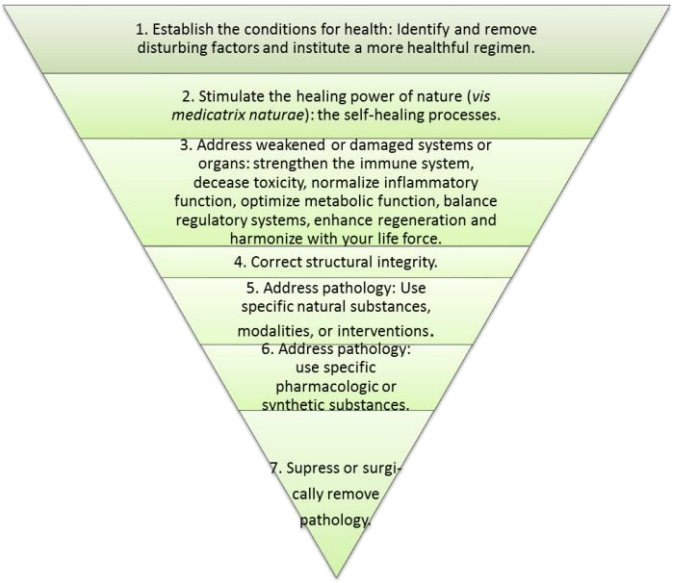

Fig. 5 Naturopathic Therapeutic Order. Adapted from Snyder Z.J., 2005.

Another reason that sustained the results is a fact. About 16% of patient reported taking five or more conventional medications for different conditions. Where people take such a diverse number of drugs it difficult for the Naturopathic physician include supplements in the treatment. In addition, some patients do not know or provide information and dosage of medications that they are taking, also do not inform supplements, vitamins or formulas that are consuming.

During the MMR we had some concerns. Missing information it was an inevitable problem with retrospective studies that can range from partial information in charts. If the MRR is to be conducted on a computerized data-based with a

spreadsheet format, all the information was more easy to be obtained.

V. CONCLUSION

In conclusion, most patients currently visiting the clinic used naturopathic medicine as a complement for traditional medicine. They want another approach for the complaints especially pain management because can't be controlled with allopathic medicine as the HTN. However although *Crataegus oxyacantha* is a safe botanical, other treatments prevail for hypertensive patients due to naturopathic approach and fundamentals. We should encourage research on medicinal plants in Puerto Rico and worldwide. In the case of *Crataegus oxyacantha* the benefits of this plant has been proven its effectiveness in different model organisms and clinical studies. But more clinical and molecular studies are needed to verify and understand better their benefits for cardiovascular health.

ACKNOWLEDGMENT

We gratefully acknowledge the financial support and the opportunity of the Puerto Rico Energy Center (PREC) and Massie Chair for Excellent Program Grant #DE-NA0000672 at the Universidad del Turabo at Gurabo, Puerto Rico. The scientific input to this research: Dr. Nydia Bou, Dean of School of Health Sciences; Dr. Nilda I. Boria, Associated Dean of School of Health Sciences, Dr. Diannie I. Rivera, Associated Dean of School of Health Sciences and Dr. Milva Vega, Clinical Professor. The laboratory support: Maritza Rodríguez, Carmen Bonilla and Francisco Rivera, sciences laboratory technicians.

REFERENCES

[1] Cardiovascular diseases (CVDs), World Health Organization. http://www.who.int

[2] Plan for Chronic Diseases, Health Department of Puerto Rico. http://www.salud.gov.pr

[3] High Blood Pressure, Texas Heath Institute. http://www.texasheart.org

[4] Naturopathic Medicine, AANP. http://www.naturopathic.org

[5] S. Marcinčák, L. Mesarčová1, P. Popelka1, M. Čertík, J. Šimková1, et al, "The influence of dietary supplementation with Melissa officinalis and combination of Achillea millefolium and Crataegus oxyacantha on oxidative stability of stored poultry meat," *Journal of Animal and Feed Sciences*, vol.20, pp. 236–245, 2011.

[6] D. Groposila, O. Popa, N. Babeanu, G. Margarit, A. Insuratelu, "Active Principles With Positive Effects On Lipid Metabolism" Scientific Bulletin. *Series F. Biotechnologies*, Vol. XVIII, 2014.

[7] D. Kostic, J. Velickovic, S. Mitic, M. Mitic and S. Randelovic, "Phenolic Content, and Antioxidant and Antimicrobial Activities of Crataegus Oxyacantha L (Rosaceae) Fruit Extract from Southeast Serbia" *Tropical Journal of Pharmaceutical Research*, vol.11 (1), pp. 117-124, February 2012.

[8] J.Graham,"Crataegus oxyacantha in Hypertension" *The British Medical Journal*, pp.951.November, 1939.

[9] R.Littleton, M. Miller and J. Hove, "Whole plant based treatment of hypercholesterolemia with Crataegus laevigata in a zebrafish model," *BMC Complementary and Alternative Medicine*,vol. 12, no.105, 2012.

[10] H. Alp, B. Cem, T. Baysal and A. Saide, "Protective effects of Hawthorn (Crataegus oxyacantha) extract against digoxin-induced arrhythmias in rats," 15(0): 000-000 DOI:10.5152/akd.2014.5869, 2015.

[11] Y. Benmaleka, O. Ait, A. Belkebira & M. Fardeaub"Anti-microbial and anti-oxidant activities of Illicium verum, Crataegus oxyacantha ssp monogyna and Allium cepa red and white varieties" Bioengineered, vol. 4:4, pp.244-248, 2011.

[12]CAND Naturopatic Guide to Botanical Medicines and Drug Interactions, pp. 1-4, January 2008

[13]N. A. "C*rataegus oxyacantha* (Hawthorn) Monograph, *Alternative Medicine Review*, vol. 15, no. 2, pp. 164-167.

[14]J. Wang, X. Xiong, and B. Feng, "Effect of Crataegus Usage in Cardiovascular Disease Prevention: An Evidence-Based Approach", *Evidence Bades Complementary and Alternative Medicine*, vol. 2013, 16 pages, http://dx.doi.org/10.1155/2013/149363

[15]H. Alp, B. C. Soner, T. Baysal, and A. S. Ş, "Protective effects of Hawthorn (Crataegus oxyacantha) extract against digoxin-induced arrhythmias in rats", *Anatol J Cardiol*, December 2014, DOI:10.5152/akd.2014.5869

[16]C. Cevik, and S.O. IŞeri, "The effect of acupuncture on high blood pressure of patients using antihypertensive drugs.", *Acupunct Electrother Res*.,2013.

[17]Zeff J, Snyder P. Course syllabus: NM51 71, Naturopathic clinical theory. Seattle: Bastyr University, 1997-2005

[18]Retrieved from: http://www.naturopathic.org/content.asp?contentid=59. Naturopathic Physicians: Natural Medicine. Real Solutions. House of Delegates Position Paper Amended 2011.

[19]Hu, M., Zeng, W., & Tomlinson, B. (2014). "Evaluation of a Crataegus-Based Multiherb Formula for Dyslipidemia: A Randomized, Double-Blind, Placebo-Controlled Clinical Trial." *Evidence Based Complementary and Alternative Medicine*, 2014.

[20]Chow, S., Dunn, S., Jackevicius, C., Lee, R., Trujillo, T., Vardeny, O., & Wiggins, B. "Key Articles Related to Complementary and Alternative Medicine in Cardiovascular Disease." *Pharmacotherapy*, *30*(1): 109., 2010.

Analysis of the Effect of the Changes on the Angle of Attack on the Lift and Drag of an Airfoil Using COMSOL Multyphysics Simulation

Harry Bonilla, Bachelor Degree Student Mechanical Engineering[1], Miguel A. Ramirez, Master Degree Student Mechanical Engineering[2], and Gerardo Carbajal, Associate Professor Mechanical Engineering Department[3]
[1]University of Turabo, Puerto Rico, hbonilla.hb@gmail.com*, gcarbajal1@suagm.edu
[2]University of Turabo, Puerto Rico, ramirez.mramirez.miguel1@gmail.com

***Abstract*– The objective of this paper was to study the effect of changes on the angle of attack on the lift and drag of an airfoil using COMSOL Multiphysiscs software. The S833 airfoil of NREL series and its family (S834, S835) were chosen due to their high efficiency for low power applications (around 1 to 3 KW). A mesh independent analysis for S833 determined that the best mesh for the simulation was the finer grid. The CL and CD for the three airfoils were calculated for various angles of attack, from 0° to 16°(increments of 2°). The best airfoil resulted to be the S833 because it has the highest lift and the lowest drag coefficients resulting in a very high CL/CD ratio at 4.25° angle of attack.**

Keywords—Lift, Drag, COMSOL, Simulation, Airfoil.

Nomenclature

CL	lift coefficient
CD	drag coefficient
F_L	lift force (N)
V	wind velocity (m/s)
C	wing cord (m)
F_D	drag force (N)
u	velocity field (m/s)
$\mathbf{u_0}$	velocity vector (m/s)
p	pressure (Pa)
p_0	relative pressure (Pa)
k	turbulent kinetic energy (m^2/s^2)
l	unitary vector
F	volume force (N/m^3)
C	turbulent model parameter
ep	turbulent dissipation rate (m^2/s^3)
n	boundary normal pointing out of the domain
P	turbulent model parameter
$\mathbf{u_{tang}}$	tangential velocity
K_V	turbulent model parameter
U	velocity magnitude
U_{ref}	reference velocity scale (
Alpha	angle of attack (deg)
Pi	*3.1416*

Subscripts

T	turbulence
c	correction factor
w	wall
x	x component
y	y component

Greek Symbols

ρ	density (kg/m^3)
∇	del operator
μ	dynamic viscosity (Pa*s)
ε	turbulent dissipation rate (m^2/s^3)
σ	turbulent model parameter

I. Introduction

The fossil fuel energy systems of the 20th Century are responsible for the green hose effect that is heating the planet. In order to reduce this effect non pollutant renewable energy systems must be used. Wind energy (wind turbine) is a source of renewable energy. The low cost of wind energy is competitive with more conventional sources of energy [1]. A wind turbine is an airfoil generator that converts the kinetic energy from the wind into electricity. Wind-driven electricity generation occurs when wind propels the blades of a wind turbine, turning a rotor. The rotor turns a generator that produces electricity [2]. There are two types of wind turbines: vertical axis (Figure 1b) and horizontal axis (Figure 1a).

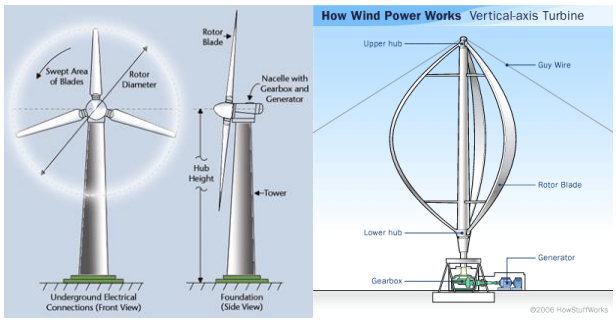

(a) (b)

Figure 1. Wind Turbine types: (a). horizontal axis; (b) vertical axis

Wind turbines can be used to power telecommunications antennas, electric fences, houses, street lighting, battery charging, communities (wind farms), etc.

When designing the rotor blades of a wind turbine it is important to consider the lift and drag forces, as shown in the sketch of Figure 2, because this forces affect the power produced by the turbine.

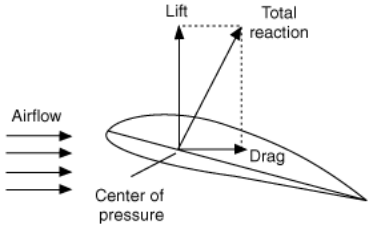

Figure 2 Sketch of airfoil, drag and lift forces

Lift is the aerodynamic force perpendicular to the air flow. The lift force is described by equation (1) as follows:

$$CL = \frac{F_L}{0.5 * V^2 * \rho * \mathbf{C}} \quad (1)$$

The lift coefficient, the most important parameter in equation (1), is proportional to the lift force and inversely proportional to the square velocity, the density of the fluid and the wing chord.

Drag is the aerodynamic force or air resistance that opposes the fluid motion. The drag is described by:

$$CD = \frac{F_D}{0.5 * V^2 * \rho * \mathbf{C}} \quad (2)$$

The drag coefficient is the most important parameter of equation (2). It is proportional to the drag force and inversely proportional to the square velocity, the density of the fluid and the wing chord.

Also, the airfoil shape (Figure 2) is very important in the design of a rotor blade. An airfoil is the shape of the cross sectional view of the wing. The airfoil type and shape will determine: its application (wind turbines, aircrafts, helicopter rotor blades, fans, propellers, compressors, etc.), the efficiency of the wind turbine and its power output, etc. For example, performance characteristics and thickness that are desirable for airplane airfoils are not necessarily good for wind turbine airfoils [3]. There are many types of airfoils: NACA series (National Advisory Committee for Aeronautics), NREL S series (National Renewable Energy Laboratory), DU family (Delft University), etc. The S833 airfoil of NREL series and its family (S834, S835) were chosen for this study due to their high efficiency for low power applications (around 1 to 3 KW). COMSOL Multiphysics software was used for the simulations of the airfoil in order to determine the lift and drag coefficients at different angles of attack. The CL/CD ratio was calculated.

The objective of this paper was to study the effect of changes on the angle of attack on the lift and drag of an airfoil using COMSOL Multiphysiscs software.

II. Mathematical Model

The simulations with COMSOL software were performed
using the K-ε turbulent flow model. This model is described by the following equations:

$$\rho(\mathbf{u}\cdot\nabla)\mathbf{u} = \nabla\cdot[-p\mathbf{I} + (\mu+\mu_T)\left((\nabla_\mathbf{u} + (\nabla_\mathbf{u})^T) - \tfrac{2}{3}\rho k\mathbf{I}\right] + \mathbf{F} \quad (3)$$

$$\rho\nabla\cdot(\mathbf{u}) = 0 \quad (4)$$

$$\rho(\mathbf{u}\cdot\nabla)k = \nabla\cdot\left[\left(\mu + \frac{\mu_T}{\sigma_k}\right)\nabla k\right] + P_k - \rho_\varepsilon \quad (5)$$

$$\rho(\mathbf{u}\cdot\nabla)k = \nabla\cdot\left[\left(\mu + \frac{\mu_T}{\sigma_c}\right)\nabla\varepsilon\right] + C_{c1}\frac{\varepsilon}{k}P_k - C_{c2}\rho\frac{\varepsilon^2}{k} \quad (6)$$

$$\varepsilon = ep \quad (7)$$

$$\mu_T = \rho C_\mu \frac{k^2}{\varepsilon} \quad (8)$$

$$P_k = \mu_T[\nabla_\mathbf{u}:(\nabla_\mathbf{u}+(\nabla_\mathbf{u})^T)] \quad (9)$$

The fluid properties of the air are given by equations:

$$\rho(\mathbf{u}\cdot\nabla)\mathbf{u} = \nabla\cdot\left[-p\mathbf{I} + (\mu+\mu_T)(\nabla_\mathbf{u}+(\nabla_\mathbf{u})^T) - \tfrac{2}{3}\rho k\mathbf{I}\right] + \mathbf{F} \quad (10)$$

$$\rho\nabla\cdot(\mathbf{u}) = 0 \quad (11)$$

$$\rho(\mathbf{u}\cdot\nabla)k = \nabla\cdot\left[\left(\mu + \frac{\mu_T}{\sigma_k}\right)\nabla k\right] + P_k - \rho_\varepsilon \quad (12)$$

$$\rho(\mathbf{u}\cdot\nabla)k = \nabla\cdot\left[\left(\mu + \frac{\mu_T}{\sigma_c}\right)\nabla\varepsilon\right] + C_{c1}\frac{\varepsilon}{k}P_k - C_{c2}\rho\frac{\varepsilon^2}{k} \quad (13)$$

$$\varepsilon = ep \quad (14)$$

For the K-ε turbulent flow model wall parameters (airfoil) are included and they are given by the following equations:

$$\mathbf{u}\cdot\mathbf{n} = \mathbf{0} \quad (15)$$

$$\left[(\mu+\mu_T)(\nabla_{\mathbf{u}}+(\nabla_{\mathbf{u}})^T)-\tfrac{2}{3}\rho k\mathbf{I}\right]\mathbf{n}=-\rho\frac{u_\tau}{\delta_w^+}\mathbf{u}_{tang}$$
(16)

$$\mathbf{u}_{tang}=\mathbf{u}-(\mathbf{u}\cdot\mathbf{n})\mathbf{n}$$
(17)

$$\nabla k\cdot\mathbf{n}=0$$
(18)

$$\varepsilon=\rho\frac{c_\mu k^2}{\kappa_v\delta_w^+\mu}$$
(19)

The inlet velocity is given by equations 20 and 21; and its stationary parameters are given by equations 22 - 25:

$$U_x=U*\cos(Alpha*\tfrac{pi}{180})$$
(20)

$$U_y=U*\sin(Alpha*\tfrac{pi}{180})$$
(21)

$$\mathbf{u}=\mathbf{u}_0$$
(22)

$$U_{ref}=\|\mathbf{u}_0\|$$
(23)

$$k=\tfrac{3}{2}(U_{ref}/T)^2$$
(24)

$$\varepsilon=C_\mu^{3/4}\frac{k^{3/2}}{L_T}$$
(25)

The outlet parameters are given by equations:

$$\left[-p\mathbf{I}+(\mu+\mu_T)(\nabla_{\mathbf{u}}+(\nabla_{\mathbf{u}})^T)-\tfrac{2}{3}\rho k\mathbf{I}\right]=-p^{\wedge}{}_0\mathbf{n}$$
(26)

$$\nabla k\cdot\mathbf{n}=0$$
(27)

$$\nabla\varepsilon\cdot\mathbf{n}=0$$
(28)

III. Set up

The airfoil was drawn in the COMSOL geometry section as shown in Figure 3

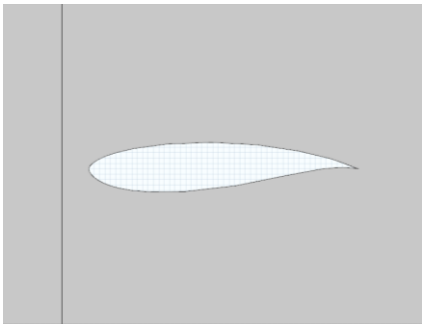

Figure 3 Drawing of airfoil on the COMSOL geometry section

The parameters established for the simulations analysis are shown on Table 1. In addition, stationary and steady state conditions and incompressible flow were assumed.

Table 1 Parameters established for the COMSOL software analysis:

Parameter Symbol	Parameter description	Value	Units
U	wind velocity	8	m/s
mu	wind viscocity	1.23	kg/m*s
rho	wind density	1.98E-05	kg/m^3
L	wind tunnel width	40	m/s
C	wing chord length	1	m/s
Alpha	Angle of attack	0	deg

Next, the inlet and outlet boundary conditions where set as shown in Figure 4. The flow was assumed to be turbulent over the entire airfoil.

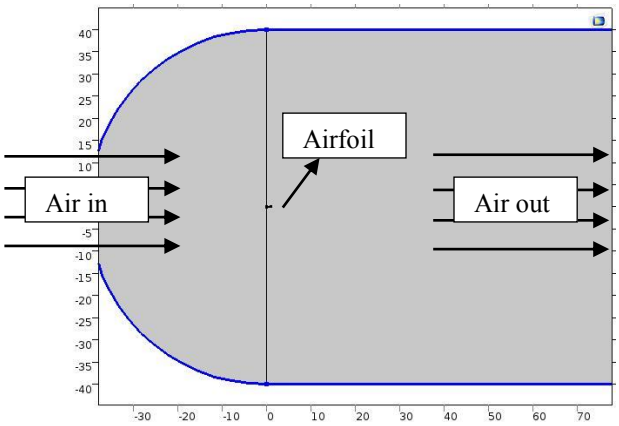

Figure 4. Boundary conditions

A meshing was applied to the airfoil for the analysis, as the one shown in Figure 5.

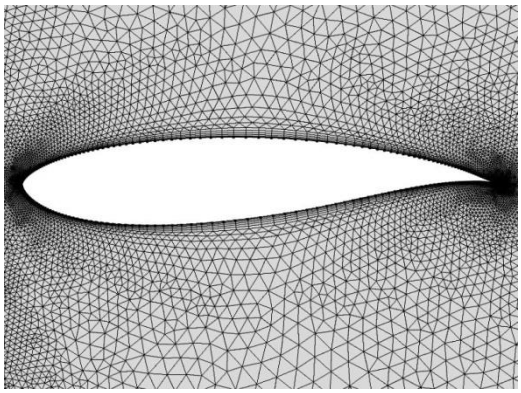

Figure 5. Airfoil with finer grid mesh

The lift and drag coefficients were calculated for various angles of attack, from 0° to 16°(increments of 2°), using linear integration and Equations 1 and 2 while keeping the air velocity constant and compared with a theoretical one [4].Then, the CL/CD ratio was determined for each airfoil.

IV. Results and Discussion

Figure 6 shows a mesh independence analysis performed with COMSOL software, where the lift coefficient is plotted against the angle of attack for the S833 airfoil. As the mesh grid gets finer the numerical curves start matching the theoretical curve. The finer and extra-fine grid curves match almost perfectly with the theoretical one. This means that these two grids produce very similar results. So, the finer grid was chosen for the analysis with a minimum numerical error of 0.97% and maximum numerical error of 28.96%, that are good, and it takes less time than the extra fine grid.

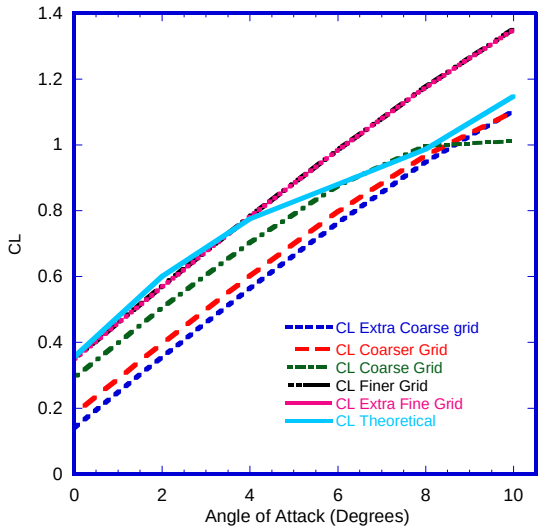

Figure 6. COMSOL mesh independence analysis of the Lift coefficient against angle of attack for the S833 airfoil.

Figure 7 shows the lift coefficient against the angle of attack for the S833, S834 and S835 airfoils. According to this graph, as the angle of attack increases the lift coefficient increases up to angle of 16 when it seems to begging to stall. The airfoil with the highest lift coefficient value was the S833 followed by the S834 and S835. This means that the S833 airfoil has a very good lift capacity when compare to the S834 and S835.

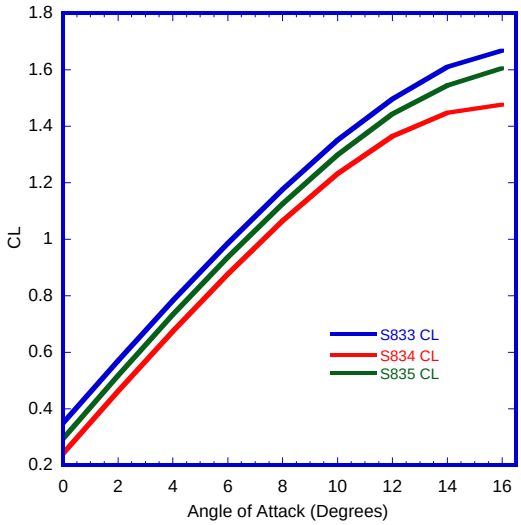

Figure 7.Lift coefficient against the angle of attack for the S833, S834 and S835 airfoils (COMSOL multiphysics simulation)

Figure 8 shows the drag coefficient against the angle of attack for the S833. The simulation curve resulted very different from the theoretical one. The error percent was very high (this behaviour was repeated for S834 and S835 airfoils). An explanation for this phenomena is that the simulation cannot account for the turbulence that occurs at the corners of the objects and other unexpected physics that might affect the actual experiments. Moreover, the estimated value might have significant difference with reference values probably due to error in area estimation or mesh allocation, etc. [5].The minimum error resulted to be 60% and the maximum resulted to be 652%.

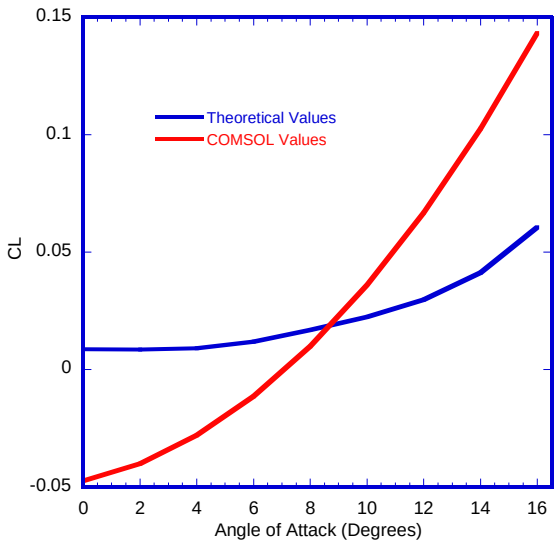

Figure 8. Drag coefficient against the angle of attack for the S833 (COMSOL multiphysics simulation).

Figure 9 shows the drag coefficient against the angle of attack for the S833, S834 and S835 airfoils using COMSOL multiphysics. It is noted that as the angle of attack increases the drag coefficient increases. The airfoil with the lowest drag coefficient value resulted to be the S833 followed by the S834 and S835. This means that the S833 airfoil has very low drag resistance when compared to the S834 and S835 (which is very good).

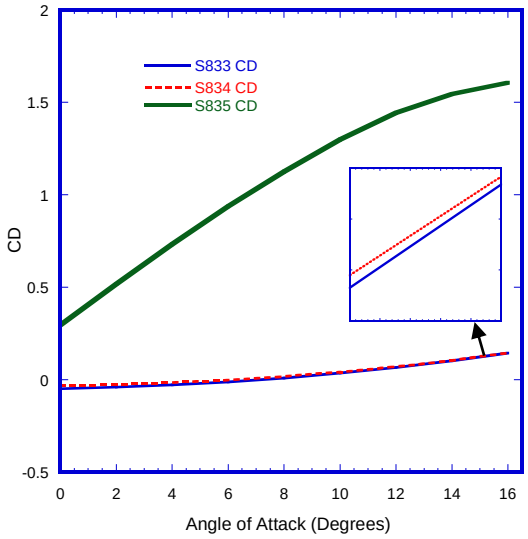

Figure 9. Drag coefficient against the angle of attack for the S833, S834 and S835 airfoils using COMSOL multiphysics.

Table 2 shows the maximum CL/CD ratio for each of the three airfoils and the correspondent angle of attack. The S833 resulted with the highest CL/CD ratio of 86.39 at 4.25° angle of attack. It was followed by the S834 and the S835 resulted with the lowest ratio. This finding suggest that the most efficient of the three airfoils is the S833 at an angle of attack of 4.25°.

Table 2. Maximum CL/CD ratio for the three airfoils and its correspondent angle of attack

Parameter	S833	S834	S835
Alpha (deg)	4.25	5.25	5.25
CL	0.7922	0.7131	0.8146
CD	0.00917	0.00878	0.01052
CL/CD	86.39	81.22	77.433

V. Conclusion

In conclusion, COMSOL multiphysics simulation is a very useful tool for the analysis of airfoils. The best airfoil resulted to be the S833 because it has the highest lift and the lowest drag coefficients resulting in a very high CL/CD ratio. This is very important when selecting the airfoil for a wind turbine rotor blades design because a high CL/CD ratio means high efficiency of the wind turbine.

VI. References

[1] Vendan1 S. P., Lovelin Aravind S., Manibharathi M., Rajkumar C.; "Analysis of a Wind Turbine Blade Profile for Tapping Wind Power at the Regions of Low Wind Speed"; International Journal of Mechanical Engineering; n.d. Retrieved from: http://vixra.org/pdf/1208.0187v1.pdf

[2] Pryor S., Shahinian M., Stout M.; "Offshore Wind Energy Development in the Great Lakes: A Preliminary Briefing Paper for the Michigan Renewable Energy Program"; April 2005; Retrieved from: http://www.erb.umich.edu/Research/Student-Research/Michigan_Offshore_ Wind.pdf

[3] Tangler J.L.; "The Evolution of Rotor and Blade Design"; National Renewable Energy Laboratory; n.d.; Retrieved from: http://www.nrel.gov/docs/fy00osti/28410.pdf

[4] NREL S series. Retrieved from http://airfoiltools.com

[5] Kwon H.J.; "USE OF COMSOL SIMULATION FOR UNDERGRADUATE FLUID DYNAMICS COURSE"; Andrews University; n.d.; Retrieved from: http://www.asee.org/public/conferences/8/papers/4407/view

[6] "Flow Around an Inclined NACA 0012 Airfoil," COMSOL Multiphysics 5.0, n.d. Retrieved from: http://www.comsol.com/model/flow-around-an-inclined-naca-0012-airfoil-14629

Considerations of the development of a Market research and Business Plan of a Wind Power System

Héctor Martínez Rosa[1], Pedro Rodríguez Ocasio[2], Ileana Nieves Ávila[3],
Jannette Pérez-Barbosa, MS, PE,
hectord45@hotmail.com[1], pedroj457@hotmail.com[2], ilenieves@gmail.com[3],
jperez222@suagm.edu
School of Engineering, Universidad del Turabo, Gurabo, PR, USA

Abstract- As part of a team developing an alternative energy system research is being performed in order to determine the appropriate market for the product. One attractive source of renewable energy is found in wind since it is competitive considering both overall costs and social aspects such as regulations. This study explores the market conditions needed to make a marketable and potential profitable alternative energy source in Puerto Rico. Some of the activities required to implement an eolic system on the island critical to any business plan are discussed. Expected limitations to develop an eolic system in the island include few areas of appropriate wind patterns and limited expertise in the business of wind turbines. Based on the research findings a portable "off grid" turbine to support potential applications to public sectors is recommended.

Keywords—turbines, market research, wind energy

I. INTRODUCTION

Wind power applications have achieved a large growth in the world market in recent years. The main purpose of the development of this and other alternative energy system is assisting business in leaving oil dependent technologies to reduce high energy costs.

A wind turbine is a device that converts kinetic energy of wind speed expressed in mechanical energy, which is transmitted to the generator to create electric power in turn. Blades should follow design considerations involving various parameters such as wind speed, speed, angle of attack, efficiency, etc. (Chiroque & Davila, 2008). Wind turbines are classified according to the orientation of the axis of the rotor as vertical and horizontal. The research objectives include describing basic models in wind turbines, existing applications and potential market. The analysis includes the advantages and disadvantages of each of the turbine design.

As part of the research and exploration of existing market for wind turbines in various markets, including Puerto Rico is performed. The initial stage in the research requires evaluating the application to be energized by the turbine. Depending on potential applications, the feasibility of this application in terms of market and design can be determined. Existing market researches in literature will be used as a baseline in the selection of a wind turbine application. Information on designs and applications based on market studies will then be utilized to develop design specifications for a physical design. As any design will include risks, these as well as areas of opportunity in existing turbines are discussed. A preliminary selection process for a recommended application and model of turbine is also discussed.

II. PROBLEM DEFINITION

There is a need to develop an alternative wind energy system considering market requirements that can potentially be used as a substitute to current energy sources. This system needs to generate sufficient energy for a selected application and be compliance with any regulations. To align with this deliverable current alternative energy systems available in the market are compared. Based in the attributes from these designs, functional characteristics will be used to develop design specifications.

III. LITERATURE REVIEW

The literature review will describe various types of wind turbines. Additionally, topics related to the advantages and disadvantages are compared to other sources of renewable energy. Considerations regarding the risks facing the implementation of this technology and its costs are mentioned. Finally any trends in the market of the technology are discussed. This section is organized in the following areas.

The United States Department of Energy (USDE, 2007) prefers wind power energy sources because wind power systems have some of the best relationships between costs and beneficial applications of renewable energy in homes. Depending on the wind availability, turbines can reduce the electricity bill between 50 and 90 percent. Additional advantages include the avoidance the high costs of extending supply networks to remote sites, prevent power outages and the use of clean energy.

Chiroque & Davila (2008), describe the operation of a wind turbine as a machine that uses the wind to drive an electric generator. The turbine absorbs the kinetic energy of the wind when it hits the blades connected to an electric generator and creates a rotational force. The produced airfoils transform the kinetic wind energy into mechanical energy. Then this energy is converted into electrical energy and, which can be interconnected to a power grid or used on site (Rivking & Randall, 2011).

There are generally, two (2) types of turbines. Gipe, (1995) classifies the turbines according to their axis of rotation. The most common wind turbine installed are the horizontal axis that have one, two or three blades, with 35% of efficiency in horizontal wind turbines vs. 30% of efficiency in vertical wind turbines installed in USA. If the blades are situated at an elevated height, the average speed of wind is increased and the turbulence intensity is less and this are an advantage in comparison with the other type of turbine (Carpman, 2011). The horizontal axis turbines can be classified according to the arrangement of the rotor: in front or behind the tower (Gipe, 1995 & Clarke, 1991). Micheloud & Vicini (2012) classify turbines is according to the position of the rotation axis with respect to the wind direction: horizontal axis (rotation axis parallel to the wind direction) and vertical axis (the rotation axis is perpendicular to the wind direction).

The risks in a wind power system are determined most by the topography and weather conditions (Huaiquan, 2015). If the wind velocity is constantly changing no one can know with exactitude how many risks a wind power system can bring in the future. Finally the technical risk in a wind turbine are unpredictable due the variability of wind in different places.

An important aspect to consider in an eolic system is related to costs. Small wind systems are generally more expensive than larger wind turbines relative to the amount of energy produced (Gipe, 2003). To cut costs and improve the reputation of expensive technology, Villarrubia (2004) describes improvement work in the fields of wind turbine with focus on the followings objectives: improvement of performance and endurance levels and safety, reduced mass of material of blades, decrease work and costs in maintenance of wind turbines, reduced noise levels, reduced disturbances on the electrical network, development of technical standards and third party certification processes. These concepts helps to identify new areas of opportunity in the design of a wind turbine. When designing a wind turbine considering these concepts is improved efficiency, lower costs and technology optimization is obtained.

buy energy from Independent Power Producers calls, through a power purchase agreement (PPA Power Purchasing Agreement). That is, all the energy produced by the park would be sold through this contract, in the case of Puerto Rico, would be the Electric Power Authority.

Another application of the wind turbines technology in the United Kingdom is the wind speed data base program ("Wind Power Program", 2015). This program can set the type of turbines with the velocity of wind needed to generate the optimal electrical energy. The program mentioned several leads for the development of the technology of wind turbines. One of the several leads that mentions the Wind Power Program is that specialists certified in the operation of turbines should de required when planning an installation technology wind turbines. Some of these potential clients are individual users interested in a small 'domestic' wind turbine who want to assess the performance and economics of a possible installation.

IV. Types of Turbines

Wind turbines are classified according to the orientation of the axis of the rotor, vertical and horizontal. The conventional and first historic wind turbines were classified horizontal wind turbines between 5 and 15 m and a width of the order of 20% of the blades length. Giordano (2015) mentions that the first turbines were called windmills and the main material uses to build the blades was wood. Another classic feature (Shemmeri, 2010) is its variable rotation speeds from 10 to 40 rpm, depending on the length of the blades, bigger blades make more slowly the rpm. The orientation of the paddle wheel to place it perpendicular to the wind incident was carried out by a swivel arm or via a small auxiliary wind acting as fin orientation or wing orientation. Another design (American Wind Energy Association, 2011) as a Slow Wind Turbine, is a generator with a large number of blades listed in wind turbines with horizontal axis. Generally in guidance systems by a rudder-vane the plane of the propeller is positioned always perpendicular to the wind direction. Some of its key features (Gipe, 2003) are the high number of blades, between 12 and 24, diameter from 3 to 10 m, limited by the heavy weight of the rotor. These adapt very well to low speed winds. Boot is produced from a wind speed of 2 to 3 m / s. The Slow Wind Turbines present a small powers generation, basically have two reasons to generated less power: they use low wind speeds (3 to 7 m / s) and are limited by the weight of the rotor due to the high number of blades. The application from this design is mainly extraction facilities and water pumping contracts (Meyers, 2013). The Slow Wind Turbines present a high coefficient of high torque for small values of specific speed.

The possible customers of Wind Turbines technology, can be individuals o

The best known and the most used today are rapid wind turbines. According with (Kid Wind Projects, ND), website focused in renewable energy's the type of wind turbine blade number is small, as also the previous horizontal axis. Currently being built wind rotor diameters reaching 90 m with a rated power of 3 MW, which gives an idea of the rotor swept area. The main and most popular

features is the small number of blades, between 1 and 4, although the most used are 3-blade. Lighter than slower wind, and therefore can be constructed larger machines. They require a wind speed for greater wind slow boot (between 4 and 5 m / s). Another characteristic, they reach their rated power for wind speeds between 12 and 15 m / s. From speeds of the order of 25 to 30 m / s rotor stop it occurs to avoid damage on the machine. These are used for power generation and may be in isolated or networked systems. The generators used in isolated systems are generally small (3-50 KW) than those who are connected to the mains (250 to 3000 kW). Among them there are several types of models just changing the number of blades or paddles in its design. Some of these examples as mono rotor blade two-bladed rotor blades these reduce material costs but are inefficient compared three turbine blades.

Wind Turbines with vertical axis of the rotor, are another type of wind generators, (Rommel, 2012). There have been numerous prototypes and experiences with different wind vertical axis, but for technical and economic reasons, its implementation in practice is very limited, so most wind generators are horizontal axis. There are two basic designs, the Savonius rotor is similar to a wind anemometer with cups or half cylinders for rotors. The Darrieus design uses a composite support surface and is generally more efficient. The rotor of vertical axis wind usually basically of the following types as rotor differential feed, with or without screen, this is called the Savonius design (Micheloud, 2012). Rotor cyclic variation called Darrieus incidence, is an example design of differential feed rotor is based on the different aerodynamic force exerted on airflow objects differently. If a rotor formed by a set of blades in the form of hemispherical cups or semi cylindrical placed in the manner indicated in the figure, the action causes wind different forces on the concave and convex of these cups, which gives conceived in a pair that rotates the rotor. Because the force that causes the pair is the difference between the blades or rotor blades, this type of machine is called differential feed (Rommel, 2012).

Wind turbines with vertical axis solve some of the problems associated with horizontal axes (Ragheb, 2015). These need not be oriented against the wind. The leaves are designed to use wind energy in any direction to rotate the turbine in one direction. Turning and take the wind back, the rotors are designed to offer less resistance reducing wear and tear on the machine. There are too many designs of wind turbine with vertical rotor shaft, but most of them their changes are more aesthetic and working under the same structure explained.

The most recent innovation is the Small Wind generators as it is known today, it is a smaller turbine, isolated without any grid connection, produces the electricity to turn its blades or blades after being hit by the wind (American Wind Energy Association, 2011). The small wind generators can be designed horizontal or vertical axis of rotor. The operation of small wind generators begins sending the energy to a battery where it is stored for later use. Between components a regulator, which regulates voltage, the machine and the proper functioning of the system is inserted. Such batteries will connect an inverter current (DC) stored in the batteries into alternating current (AC) at 230V which is what usually have everyone at home to run any traditional appliance. Currently in use of this technology it has increased favorably and that its low cost has been much more accessible to individual customers. There is a detailed classification of these conventional turbines (Cruz, 2012), but may be classified by its power generating and scanning areas is the area occupied by the blades. These can be classified into two categories of wind power technology and wind micro-mini. It is Micro Wind ranging from 20 watts to 7 kilowatts and an area of blades space are less than 40 square meters. Another classification of Small Wind turbines (Cruz, 2007) is that going 7 kilowatts to 100 kilowatts of power and an area less than 300 square meters, called mini wind generators.

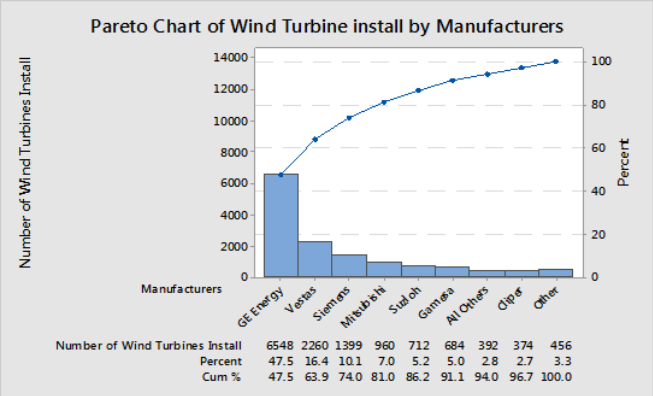

Figure 1. Pareto Chart of Wind Turbine install by Manufacturers

An interesting part of the research is determining what the current market for wind turbines is. The pareto chart in figure 1 will explain the total number of wind turbines installed from 2005 until 2011 in U.S by each manufacturer (Platzer, 2012). This allow to view what are the manufacturers that have been active the most in the area of wind turbines. The manufacturers that are presented in this Pareto chart are: GE Energy, Vestas, Siemens, Suzloh, Mitsubishi, Nordex, Clipper and Gamesa.

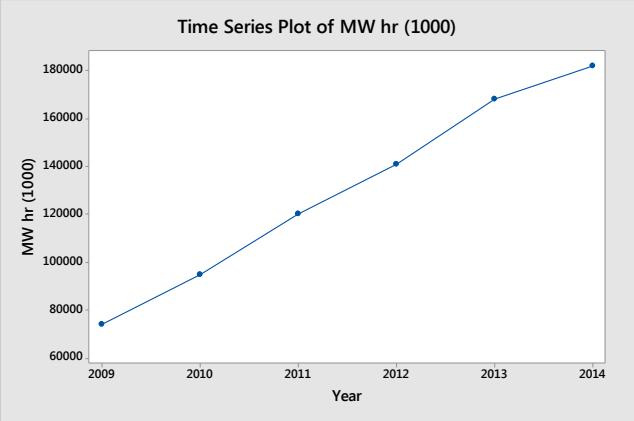

Figure 2. Net Generation Wind Energy (09-14)

Another aspect of the research is determine if there is a trend in the deployment of eolic energy. Figure 2 explains the year net generation wind energy through the years of 2009 and 2014. The results will represent the difference across the years in thousand megawatts hour. This time series a clear increment of the output of renewable source of wind (US Energy Information Administration, 2015).

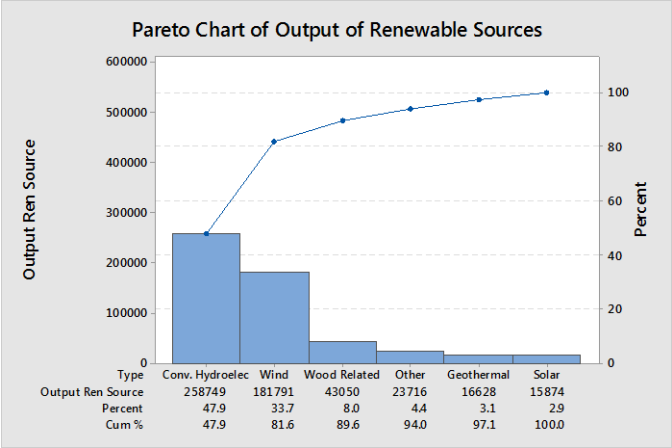

Figure 3. Pareto Chart of the different Renewable Sources and their outputs of energy.

The Pareto chart in figure 3 shows the yearly output of renewable sources that generate more energy in 2014 (U.S. Energy Information Administration, 2015). Data from each renewable sources based on the output in megawatts hour is evaluated to explain the renewable sources that are generating more or less power in 2014. The renewable sources considered are wind, solar photovoltaic, solar thermal, wood and wood derived fuels, landfill gas, and biogenic municipal solid waste, other waste biomass, geothermal and conventional hydroelectric. These renewable sources are the current generators of electricity that are used in U.S. and the U.S Energy Information Administration. The two major renewable sources are the conventional hydroelectric and wind.

V. Advantages and Disadvantages of Wind Turbines

To learn more about wind turbines some comparisons between the advantages and disadvantages of the turbines will be made. Some of the turbines to be considered are the horizontal axis which include the installed offshore wind turbines & vertical axis as well as the new model of small wind turbines that can be designed with horizontal or vertical axis rotor.

Research was performed to identify the advantages and disadvantages of horizontal axis turbines. The advantage as mentioned by Giordano (2015), easily converting the kinetic energy into electricity is less expensive than the solar energy source in comparison between. Some of the disadvantages, are the need of a yaw mechanism with the wind, high impact on the flora and fauna. Additionally, visual impact since many of the horizontal axis turbines are usually place high and have a large size. The maintenance becomes difficult due to the height of the turbine and the cost of the blades. Finally, the use of space is not optimal due to them covering too much space and the inability to place turbines close to each other, because the horizontal wind turbines have a bigger rotor diameter area occupying their blades in comparison with the vertical axis.

For horizontal axis turbines there is a type of offshore installation which is usually more efficient by having strong currents of wind in the sea (Rama, 2011). These turbines show great advantages in the sea since there are no obstacles which can reduce the wind speed and for this reason have more and continuous wind turbine generates more efficiently than on land. Another advantage is that the fewer environmental turbulence, which lowers the fatigue of a wind turbine, thus increasing its lifetime. In the sea it has vast spaces where to place wind turbines, which offers the opportunity to install large parks and generate electricity more efficiently so that more advantages installed on land. These also reduce the visual impact to be further away from urban centers. Finally, another of the advantages is that this distance also makes the noise is not a problem for manufacturers, because they can forget the expensive material to make a silence turbines. Therefore these can increase the speed of the turbine and reduced weight the structures being so cost savings and high efficiency is the better compared to the others models. But within so many advantages offered by this type of installation also has significant disadvantages. The wind resource assessment and study of the installation area is much more expensive than on land, there is no infrastructure to connect the areas with higher wind resources at sea with consumption centers. The transportation costs of electricity and the networks of these installations make the technology offshore too expensive. Another disadvantage is the difficulty to maintain because access to work on them is complicated. Its increase costs and hampered by the deepest and finally install the

machines require more space between them implying an increase in investment this is due to the low roughness of the sea makes the turmoil spread rapidly and the wake of the well influence other machines shorter life.

The second model is the vertical axis wind turbines. Giordano (2015), discusses advantages and disadvantages for vertical axis wind turbines: if you can put some more fences that others, do not need a yaw mechanism with the wind, maintenance becomes easier compared to the horizontal axis because are regularly closer to the ground, less affected flora and fauna, its visual impact is lower and finally, have an advantage that they can operate in places where wind currents is lower. This model shows some disadvantages, such as to not take advantage of wind currents in the highest, are of low efficiency and its cost is high because the materials are more expensive than the real savings generated by invoice.

The last model and one of the most innovative models mentioned and that caught a boom in recent years can be designed horizontal or vertical axis, is classified for the capacity and size of the turbine, is the model of domestic turbines or Small Wind turbines. The Kid Wind Projects website states, that the field of small wind turbine has not been impacted and there are still great opportunities for improvement within the designs. Within this model of small wind turbines they tend to be smaller and include any type of design either vertically or horizontally. This model shows great advantages (Probst, 2015) such that it can be effectively combined with other renewable energy sources such as solar panels. Another great advantage of the different models like horizontal axis or vertical axis of small wind turbines, is that these turbines are usually installed off grid and this means that there is no loss with endless kilometers of power lines because the energy is produced in the same place where most of the demand occurs. This technology is simple, and this is proven to be another advantage to expand their market. Other advantages is that dismantling non-marking, require little space for installation, are easily maintained and life is better compared to its cost. There are also some disadvantages (Probst, 2015), but the most significant but with great opportunity for improvement is that this technology is not considered to be a constant source of energy because they are mostly installed in places with little wind currents.

VI. Risk in Wind Turbines Related Business

A Cause and Effect Diagram was performed to define the occurrence of risks involved pursuing wind turbine related business. Beck & Martinot (2004) mention that a cause and effect diagram is performed to evaluate the effect of the risk in business pursuing a wind related business. The goal is to view what are the contributing factors and sub causes that can eventually will be a risk in the wind turbine business. The following contributing factors are taken in consideration: measurements, environment, methods, machines and personnel. Once the source of data was analyzed it was decided that these contributing factors are the most suitable for analyzed the effect (Hilario, 2011).

For this particular research the fishbone diagram helps to capture the effect, called here Risk in Business. This risk is defined as constraints of the wind related business. It can be seen in figure 4 many potential root causes are illustrated in the chart, these are detailed as:

- The measurements analyzed are costs that have an effect in the wind related business.
- In the environment factor the adverse impacts to the environment due to wind turbine related business are considered.
- There are certain methods that regulate the business of wind turbine (and potentially make the process more slow, consuming time and money).
- The contributing factor: machine includes the design of the wind turbine. This can be a significant factor to the success of the business.
- The last contributing factor is the human perception. Education can potentially play a large role in achieving solid business built with knowledge and motivation. Lack of visible installations can lead to the misconception that wind turbine are not a viable idea to improve the energetic problems. This can be perceive as negative and the interest in knowing the technology can be compromised.
- The human perception can be a risk due to behavioral manners that cannot be controlled Gipe, P. (2003). Every human perceives things differently and because of this the business needs to be actively improving the technology to appeal to the costumers.

There are 22 sub causes or risks divided in 5 causes to define the risks in the wind turbine related business. All causes are important to take into consideration in the wind related business. But the key ones are the environment and measurements because usually these are the starting point to start building the business. To evaluate the risks further research will be performed to understand the impact in the business. In the future more sub causes can be discovered, highlighting more potential risks to the business. These causes and sub causes are key part to the continuous improvement within the wind related business. Decreasing the occurrence of these risks can help businesses achieve better performance and growth.

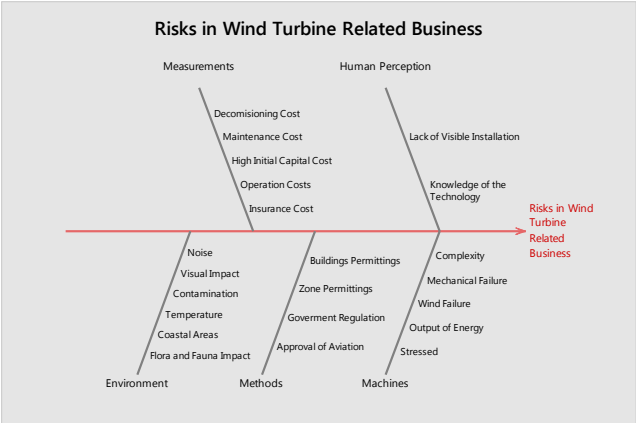

Figure 4. Cause and Effect Diagram of Risk in Wind Turbines Business (Fishbone)

VII. SELECTING A PRELIMINARY APPLICATION AND DESIGN

A decision matrix is an instrument used to choose an option between a numbers of possible options, typically more than two (Tague's, 2004). This tool is often used for planning activities to select a product, service, features or any option you want to evaluate different aspects and compared to others under the same headings.

For this research, the objective is selecting a type of turbine type of market. To reach this objective the team decided use two decision matrices, make a decision matrix to select apart the type of market and the type of wind turbine. Each decision matrices cataloged with its most significant aspects, and could not catalog the same aspects in different decision matrices, because not applied correctly or were not have the same significance. The decision matrix works by assigning scores on every aspect that option and end the option with the highest score is considered the best option under such conditions (Brooks, 2015). The decision matrix is evaluated considering rankings of 1-Poor, 3-Good and 5-Excelelent. The team decided to allocate these low scores so that the reader can understand the concept as easy as possible. Still we leave a space of two points between poor, good and excellent for the probability that two options remain outside less draws.

The Decision Matrix described in (table 1), shows an evaluation to select the better types of markets, these kinds of markets were selected based on international studies by WWEA (World Wind Energy Association) for its acronym in English. This World Wind Energy Association identified a number of potential customers in the wind power and these were adapted to the conditions of Puerto Rico into the evaluated options. These markets were evaluated under the most significant aspects to carry out the implementation of a wind turbine in any market. In addition (Rueter, 2011), state that the benefit of the small wind turbine is that can be deployed in so many places and can be attached to houses, schools, industrial facilities and boats. The small wind turbines have enjoyed their most success to date in developing countries.

Local Market is the local business, define it as small merchants, restaurants and distinctly Puerto Rican stores established in Puerto Rico. Companies and foreign food chains established in Puerto Rico are not considered Local Market. The option of Local Market as shown in (Table 1) was the highest scoring result compared to the other option so be the best choice under these conditions evaluated. To install a wind turbine necessary permits are much more stringent compared to other options that is why get a low score classified as poor by their difficulty to get and the number of permits.

TABLE 1
Decision matrix for market selection

TYPES OF MARKETS	PERMITS	EFFICIENCY	MAINTENANCE	INNOVATION	TOTAL
FARMING	5	5	1	1	12
RESIDENTIAL	3	1	5	1	10
LOCAL MARKET	1	3	5	5	14
GOVERNMENT AGENCIES	5	3	3	1	12
TOTAL	14	12	14	8	

The decision matrix described in (table 1), shows an evaluation to select a type of more efficient turbine taking into consideration the Puerto Rico conditions. The efficiency of a turbine wind in the Local Market always depends on the wind speed in any market and taking into consideration that there are many markets in Puerto Rico that are just within the city where the wind is low power. The residential market, to its location in the majority of Puerto Rico inside the city with too much interference to the wind, and for these obstacles will have a low score. Maintenance must be extremely easy to work, because it would be a small turbine and is built more closely to the ground. Finally in the local commerce it has great PR opportunity for the little use of water compared with the many projects that have other options together. In these two decision matrices it is considering all aspects that are evaluated options have the same weight when granting the score is and give decision.

Among the most significant aspects to assess different types of turbines, (table 2) shows that domestic turbine had

the highest score, making it the selected alternative. The small wind turbine off grid will have a lower cost compared to the offshore and large turbines. It's easier to get permission or sometimes do not need permits because they are disconnected from the network and do not applied the grid installation permits and costs. Its efficiency is not constant due to the variation of wind compared to other options. Their life expectancy is much longer by are exposed to lower levels of wind and its maintenance is easier and less expensive. Its visual impact is often lower because you do not reach large sizes and is given an intermediate score as those in offshore have less visual impact. The selected option would be one of the most innovative options due to the underdevelopment of this technology within the local trade.

TABLE 2
Decision Matrix for types of wind turbine

WIND TURBINE	COST	EFFICIENCY	PERMITS	USEFUL LIFE	FLORA AND FAUNA IMPACT	VISUAL	MAINTENANCE	TOTAL
OFF SHORE	1	5	3	1	3	5	1	19
SMALL WIND OFF GRID	5	1	5	5	5	3	5	29
BIG WIND TURBINE	3	3	3	3	1	1	1	15
TOTAL	9	9	11	9	9	9	7	

VIII. CONCLUSIONS

The global energy crisis, has driven a global interest in the development and use of alternative energy sources. Over the years there has been an increase in the renewable energies especially in the use of wind energy. It was possible to demonstrate the increase in electrical energy through wind turbines connected to the grid while additionally seeing an increase in domestic turbines that are not connected to the network (off grid). The research has observed a dynamic growth in the global market for wind turbines low power, having reached full capacity of 440 MW installed; the second renewable energy with most energy generated in the US. This is very good news for both environmental friendliness and the bottom line of consumers.

The research has applied technical engineering tools such as Decision Matrixes to analyze various important aspects in society and opportunities in the technology of wind turbines. After research the team decided to focus on evolving within the field of terrestrial domestic turbines in the local business market that is not connected to the network. The specific needs of the market with good local presence will allow to be very close to the customer and the present and future arising in the coming wind power deals and experience in operations and maintenance services represent a significant competitive advantage met.

IX. NEXT STEPS

This research is the first step to introduce a new energy model for Puerto Rico. Eolic technology has not significant growth yet in Puerto Rico. The paper helps readers gain an introductory information wind turbines and in turn understand the importance given in other countries to renewable energy. The next step, will be focused on applying the knowledge of this research completely in the Puerto Rico market. Market data from Puerto Rico will help to growth of this technology on the island.

A second study, focused entirely on the market of Puerto Rico, will feature gather information on the projects already completed, permits and upcoming projects on the island on this technology. This information will helps to promote eolic energy sources with knowledge and efficiency. A survey to collect the thinking of social opinion related to eolic energy will be developed, with the results obtained by the survey a part of future research. For this research technical data and market research conducted will be added with the social opinion on the technology of wind turbines. This will permit the research to find the right market and promote technology of wind turbines in Puerto Rico.

AUTHORIZATION AND DISCLAIMER

Authors authorize PREC to publish the paper in the conference proceedings. Neither PREC nor the editors are responsible either for the content or for the implications of what is expressed in the paper.

REFERENCES

2011 U.S. Small Wind Turbine Market Report. (2011). Retrieved July 18, 2015, from http://awea.files.cms-plus.com/2011_AWEA_Small_Wind_Turbine_Market_Report.pdf

Advantages and Challenges of Wind Energy. (n.d.). Retrieved June 8, 2015, from http://energy.gov/eere/wind/advantages-and-challenges-wind-energy

American wind power reaches major power generation milestones in 2013. (2014, March 5). Retrieved June 17, 2015, from

http://www.awea.org/MediaCenter/pressrelease.aspx?ItemNumber=6184
Babcock, D. (1991). Planning and Forecasting. In Managing engineering and technology: An introduction to management for engineers (4th ed., pp. 54-62). Upper Saddle River, New Jersey: Prentice Hall.
Beck, F., & Martinot, E. (2004). Renewable Energy Policies and Barriers. Enciclopedia of Energy, 365-382.
Brooks, C. (2015, June 26). What Is a Decision Matrix? Retrieved July 6, 2015, from http://www.businessnewsdaily.com/6146-decision-matrix.html
Bruno, L. (n.d.). Turbine - Types Of Turbines. Retrieved July 19, 2015, from http://science.jrank.org/pages/7031/Turbine-Types-turbines.html
Carpman, N. (2011). Turbulence Intensity in Complex Enviroments and its Influence on Small Wind Turbines. Retrieved July 8, 2015, from http://www.divaportal.org/smash/get/diva2:415655/FULLTEXT01.pdf
Chiroque, J., & Davila, C. (2008). Procesos de fabricacion de las turbinas eolicas. In Microaerogenerador IT-100-PE para electrificacion rural (1st ed., pp. 8-9). Lima, Peru: Forma e Imagen.
Energy Dept. Reports: U.S. Wind Energy Production and Manufacturing Reaches Record Highs. (2013, August 6). Retrieved June 9, 2015, from http://energy.gov/articles/energy-dept-reports-us-wind-energy-production-and-manufacturing-reaches-record-highs
Colon, A. (2010, August 1). Corriente Verde. Retrieved June 26, 2015, from http://www.corrienteverde.com/articulos/el viento.html
Freivalds, A., & Niebel, B. (2009). Problem Solving Tools. In Niebel's methods, standards, and work design (13th ed., pp. 22-24). New York: McGraw-Hill Higher Education.
Gipe, P. (2003). Economics - Does Wind Pay? In Wind power: Renewable energy for home, farm, and business (Rev. and expanded ed., pp. 71-81). White River Junction, Vt., Vermont: Chelsea Green Pub.
Hilario, C. (2011, August 1). Wind Turbien Inspection, a Strategic Service? Dewi Magazine No. 39, 56-64.
Manwell, J., & McGowan, J. (2002). Wind Energy Systems: Enviromental Aspects and Impacts. In Wind energy explained theory, design and application (2nd ed., pp. 547-585). Chichester, England: Wiley.
(n.d.). Retrieved June 3, 2015, from http://www.wind-power-program.com/turbine_characteristics.htm
Nelson, V. (2013). Measures of Performance. In Wind Energy: Renovable Energy and the Enviroment (2nd ed., pp. 167-188). Boca Raton, Florida: Taylor & Francis Group.
Platzer, M. (2012, December 18). U.S. Wind Turbine Manufacturing: Federal Support for an Emerging Industry. Retrieved June 18, 2015, from https://www.fas.org/sgp/crs/misc/R42023.pdf
Rivkim, D., Randall, M., & Silk, L. (2011). Wind Energy Generation and conversion. In Wind Power Generation and Distribution (p. 12). Burlington, Massachusets: Jone & Barlett Learning.
Rueter, G. (2011, May 13). Wind Industry Sees Big Potential for Little Turbines - Our World. Retrieved July 23, 2015, from http://ourworld.unu.edu/en/wind-industry-sees-big-potential-for-little-turbines
Tague, N. (2004). The Tools. In The Quality Toolbox (2nd ed., pp. 219-223). Milwaukee, Wisconsin: ASQC Quality Press.
The WindPower and UK Wind Speed Database programs. (n.d.). Retrieved June 30, 2015, from http://www.wind-power-program.com/
U.S. Energy Information Administration - EIA - Independent Statistics and Analysis. (n.d.). Retrieved June 30, 2015, from http://www.eia.gov/electricity/monthly/epm_table_grapher.cfm?t=epmt_1_01_a
Vicini, R., & Micheloud, O. (2012). Tipos de turbinas eolicas. In Smart grid: Fundamentos, tecnologías y aplicaciones (pp. 94-97). Monterrey, Mexico: Cengage Learning.
Villarrubia, M. (2004). Clasificacion de los aerogeneradores eolicos. In Energia Eolica (pp. 13-17). Barcelona, España: Ediciones Ceac.
Wind Energy Facts at a Glance. (n.d.). Retrieved June 8, 2015, from http://www.awea.org/Resources/Content.aspx?ItemNumber=5059

Synthesis and Characterization of Nanostructured Materials and its Application on Environmental Remediation Techniques†

Frankie O. Rolón Delgado, Keila M. Rivera Sánchez, Loraine Soto Vázquez and
Francisco Márquez Linares, Ph. D
frankieomar2@gmail.com, keilamir@hotmail.com, lorainesoto@gmail.com,
fmarquez@suagm.edu
School of Natural Sciences and Technology, Universidad del Turabo, P.R., USA

Abstract– Zinc oxide nanoparticles were synthesized using zinc acetate dihydrate as precursor. The product was successfully characterized by scanning electron microscopy, X-ray diffraction and energy dispersive spectroscopy. The photocatalytic activity of the synthesized zinc oxide nanoparticles was determined by measuring the photocatalytic degradation of benzophenone-4 in systems with different catalyst loadings. The photocatalytic activity was studied in the range of wavelength from 200 nm to 400 nm. A concentration of 1.0 g/L of ZnO nanoparticles was optimal since it promoted a higher photodegradation activity.

Keywords - Nanoparticles, photocatalysis, benzophenone 4, Zinc oxide

I. INTRODUCTION

Nowadays, photocatalysis is considered one of the most important chemical technologies because it is environmentally friendly [1]. Organic pollutants in water, such as benzene and its derivatives, can be decomposed using advance oxidation processes such as photocatalysis. These organic contaminants represent a significant potential hazard to human health and safety if they stay in the environment for long periods of time. The situation gets worse because some products for human care contain those chemicals as their active ingredient. Example of this, are the ultra violet (UV) filters. Since they are used during recreational activities, bathing or simply by littering, these pollutants enter the water sources easily by direct or indirect pathways [2]. Some of these substances have already been detected in rivers, lakes and coastal areas [3].

The photocatalytic oxidation process has been one of the best water treatments studied by establishing the superiority on the decomposition of pollutants. Zinc oxide is a commonly used photocatalyst that can be found in many products and materials including cosmetics, rubber, chemical sensors, piezoelectric transducers, solar cell and food [4]. Due to its versatility and attractive optoelectronic properties, it is a good candidate for a variety of device applications. Literature suggests that zinc oxide nanoparticles (ZnONPs) offer better performance than bulk size [4-6]. Other benefits of this catalyst are its high activity, low cost and high band-gap energy (3.37 eV), which is larger than other common catalysts, like TiO_2 (3.20 eV) [1]. During synthetic procedures the morphology of ZnONPs can be control by varying the basicity of the solution and the precursors employed [4].

The UV filters are mainly organic chemicals added to consumer sunscreen products that are able to absorb and dissipate the UV rays from sun radiation [7]. Several studies indicate that the active ingredient in many sunscreens can contaminate the environment. They constitute a potential risk to health since they are persistent in the environment and bio-accumulative [8]. Benzophenone-type UV filters, like benzophenone-4 (2-hydroxy-4-methoxybenzophenone-5 sulfonic acid), commonly called BP-4, are often used in sun blocks, cosmetics, plastics and packages because of their ability to highly absorb radiation without changing its composition [9]. The purpose of this investigation is to determine the photocatalytic activity of ZnONPs degrading BP-4 as an organic pollutant.

II. METHODOLOGY

A. Reagents and Materials

All reagents were used as received without any further purification or treatment. Sodium hydroxide pellets, Zinc acetate dihydrate and ethanol ≥ 97 % were bought from Fisher Scientific®. For all the experiments ultra pure water Milli-Q water, 18.2 Ωcm^{-1} at 25 ºC was used. During the photo-degradation procedure 0.45 µm syringe filters, Sigma-Aldrich BP-4 ≥ 97.0 % Fisher Scientific® hydrogen peroxide 50 %, the synthesized ZnONPs, a Shimadzu® 2401-PC Spectrophotometer and quartz cuvette cells with path lengths of 1 cm were used. A photo-reactor was built with light bulbs surrounding a magnetic stirrer. Mirrors around the system were used as reflectors to keep every angle lighted. A black blanket was placed over the photo-reactor to prevent external radiation from disturbing the system.

† This work is partially supported by DE-NA0000672.

B. Synthesis

A precursor solution was prepared by adding 4 g of zinc acetate dihydrate to 150 mL of water. Separately approximately 1.17 g of NaOH pellets were diluted in an alcohol solution of ethanol and water. After pellets were diluted, NaOH solution was poured over zinc solution and left to stir during 2 hours. Then, ZnONPs were centrifuged 7 x 10,000 rpm and dried in an oven at 60 ºC. Finally, the ZnONPs were calcined at 300 ºC for 15 minutes. The obtained product was then characterized.

C. Characterization

The ZnONPs were characterized by XRD with a Bruker D8 Advance X-Ray Diffractometer from 2Θ angle of 20 º to 80 º using a scan velocity of 2.0 º/min and scan step of 0.02 º. The tube voltage and current were 40 kV and 40 mA, respectively. A JEOL-JSM 6010A Scanning Electron Microscope (SEM) operating at 20 kV and coupled with an Energy Dispersive X-Ray (EDX) detector was used for morphology and elemental characterization.

D. Photodegradation experiments

Different catalyst loadings were varied from 0.4 g/L to 1.2 g/L and added to a BP-4 solution of 6 x 10^{-5} M. Then the pH was adjusted to 7 and the system was kept in dark for 30 minutes in constant stirring. Later, 5 mL of H_2O_2 and a constant air bubbling were added to the system at the time that the lights were turned on. Samples were taken every 30 minutes and analyzed by UV-Vis spectroscopy to determine the photocatalytic degradation of the as-synthesized ZnONPs.

III. Results

A. Characterization of synthesized ZnONPs

The SEM characterization confirmed the expected growth of ZnONPs when using zinc acetate as precursor. Images depict a sphere-like shape with homogeneous size and morphology. As shown in figure 1, ZnONPs were mostly a few hundreds of nanometers.

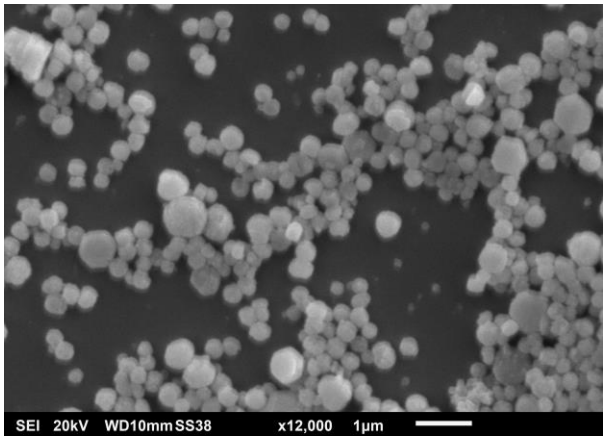

Fig.1 SEM image of ZnONPs.

As shown in figure 2, the elemental composition confirms the presence of zinc and oxygen in the as-synthesized ZnONPs. No foreign energy line of another element was detected; confirming the elemental composition of ZnO.

As represented in figure 3, the x-ray diffractogram showed peaks in the 2θ angles of 32.9 °, 35.5 °, 37.3 °, 48.6 °, 57.7 °, 64.0 °, 67.4 °, 69.0 °, 70.2 °, 73.6 ° and 78.0 °. Literature suggests that these results are characteristic of wutzite crystalline structure [10]. Peaks in XRD diffractogram were originated from reflections of crystal planes (100), (002), (101), (102), (110), (103), (200), (112) and (201). These correspond to hexagonal ZnO [10]. There are no foreign peaks detected which confirms pure wurtzite crystal structure.

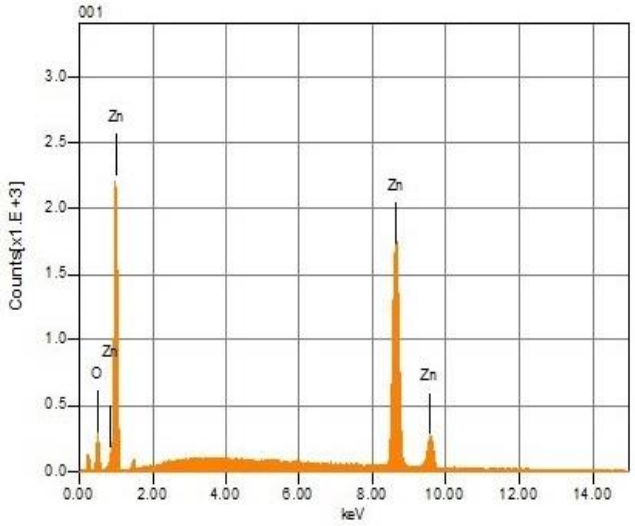

Fig 2. EDX results for synthesized ZnONPs.

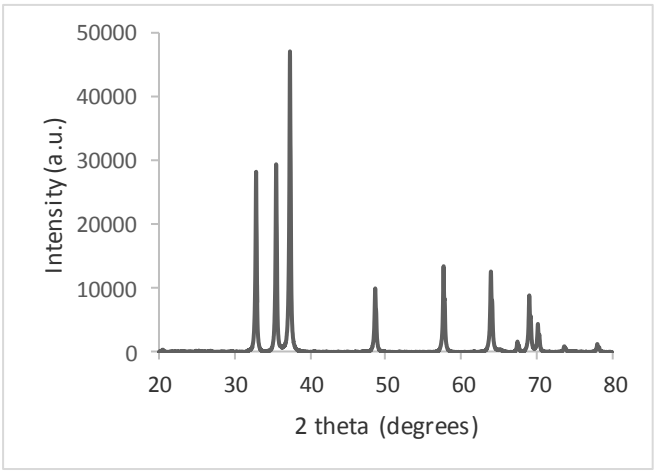

Fig. 3 XRD Diffractogram of ZnONPs.

B. Photocatalytic degradation experiments

The photocatalytic activity of the synthesized ZnONPs was studied by adding catalyst loadings from 0.4 g/L to 1.2 g/L into a BP-4 6 x 10^{-5} M solution. Figure 4 represents the degradation

of BP-4 under five different catalyst loadings of the synthesized ZnONPs. According to experimental results, a concentration of 1.0 g/L of ZnO was optimal, since it promoted a higher percentage of photodegradation. When the optimal concentration of catalyst is added to the system an adequate amount of it will interact with BP-4 and there will be a higher degradation of the pollutant. Furthermore, when the system has a higher concentration of catalyst there are more of these particles that promote a light screening effect. This stimulates less interaction between BP-4 with the as-synthesized ZnONPs. Since there are more particles of catalyst in solution, they interfere with the amount of light that enters the system and as a result, there is less photodegradation of the pollutant. The lowest percentage was obtained when 0.4 g/L of ZnONPs were added to the system. At this concentration there were not enough ZnONPs available to interact with the pollutant, hence less amount of it was degraded.

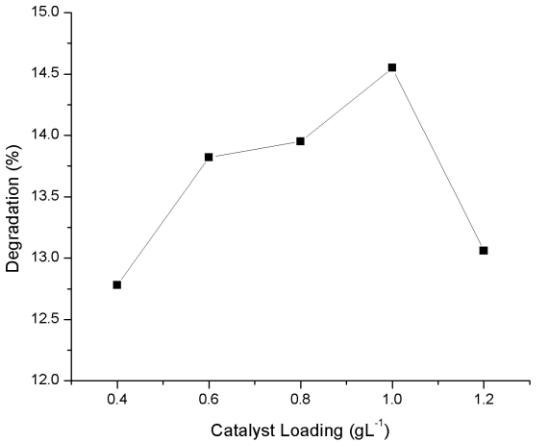

Fig. 4 Photocatalytic degradation of BP-4 under different catalyst loading of ZnONPs.

According to figure 5, a catalyst loading of 1.0 g/L will promote a higher degradation of BP-4 through time. This data concurs with the ones presented in figure 4. In general, on all five systems, BP-4 degradation increased through time being the system with 0.4 g/L catalyst loading the one with less degradation. The systems with catalyst loadings of 0.6 g/L and 0.8 g/L degraded almost the same amount of BP-4 at 180 minutes, even when results during 30 minute intervals were different. Similar photocatalytic activity was observed in systems with a catalyst loading of 0.4 g/L and 1.2 g/L at 180 minutes. With a low catalyst loading there is not enough amount of it to interact with the contaminant, hence photodegradation is minimal. At higher catalyst concentrations the photodegradation decreases due to the light screening effect [10]. This pattern can be observed in the results. When compared to other systems, at 60 minutes, the system with a catalyst loading of 1.0 g/L degraded a significant amount of BP-4. At the same time, the system with a catalyst loading of 0.6 g/L showed very little photocatalytic activity.

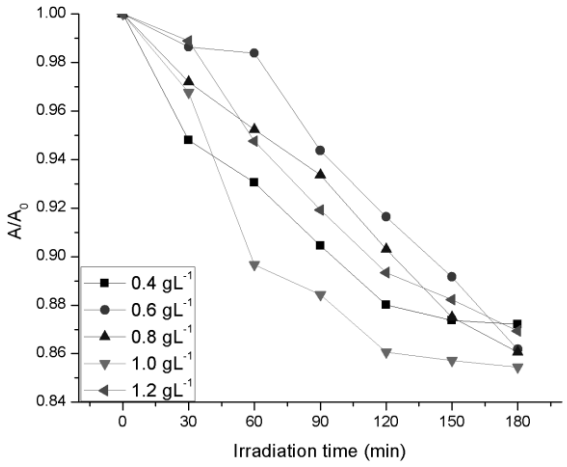

Fig. 5 Study of the photocatalytic degradation of BP-4 under different catalyst loadings of ZnONPs through time.

IV. Conclusion

ZnONPs were successfully synthesized and characterized by precipitation using zinc acetate dihydrate, NaOH and ethanol as precursors. The morphology, elemental composition and diffraction pattern was confirmed which suggest a pure ZnONPs with wurtzite crystal structure. The ZnONPs, employed as catalyst, proved to be effective in photodegrading BP-4 present in the system at pH 7. Experimental results demonstrate that 1.0 g/L was the optimal concentration of catalyst needed. In future works the effect of BP-4 initial concentration using the optimal catalyst loading conditions will be studied.

ACKNOWLEDGMENT

Authors would like to thank Abniel Machín and the Puerto Rico Energy Center (PREC) and Massie Chair for Excellence Program Grant #DE-NA000672 located at the Turabo University for their continual support during this investigation.

References

C.W. Tang. "Study of photocatalytic degradation of methyl orange on different morphologies of ZnO catalysts." *SciRes*. No. 2, pp.19-24, April 2013.

Q. Liu, Z. Chen, D. Wei, Y. Du. "Acute toxicity formation potential of benzophenone-type UV filters in chlorination disinfection process" *J. Environ. Sci*. No. 26, pp. 440-447, May 2013.

K. Fent, P. Kunz, A. Zenker, M. Rapp. "A tentative environmental risk assessment of the UV-filters 3-(4-methylbenzylidene-camphor),2-ethyl-hexyl-4-trimethoxycinnamate, benzophenone-3, benzophenone-4 and 3-benzylidene camphor" *Mar. Environ. Res.* Vol. 69, supplement 1, pp S4–S6, 2010.

R. M. Alwan, Q. A. Kadhim, S. K. M. Sahan, R. A. Ali, R. J. Mahdi, N. A. Kassin, A. N. Jassim. "Synthesis of Zinc Oxide Nanoparticles via Sol-Gel Route and Their Characterization", *Nanosci. Nanotechnol*. Vol. 5, No.1, pp. 1-6, February 2015.

D. Sridevi, and K. V. Rajendra, "Synthesis and Optical Characteristics of ZnO Nanocrystals" *Bull. Mater. Sci*. Vol. 32, No. 2, pp. 165-168, April 2009

S. S. Kumar, P. Venkateswarlu, V. R. Rao, G. N. Rao. "Synthesis, characterization and optical properties of zinc oxide nanoparticles" *Int. Nano Lett.* 3:30, May 2013.

P. Gago-Ferrero, K. Demeestere, S. Díaz-Cruz, D. Barceló. "Ozonation and peroxone oxidation of benzophenone-3 in water: Effect of operational parameters and identification of intermediate products." *Sci. Total Environ.* 443, pp. 209-217, November 2012.

S. Zucchi, N. Blüthgen, A. Ieronimo, K. Fent. "The UV-absorber benzophenone-4 alters transcripts of genes involved in hormonal pathways in zebrafish (Danio rerio) eleuthero-embryos and adult males." *Toxicol. Appl. Pharmacol.* Vol. 250, No. 2, pp.137-146, 15 January 2011.

E. De Laurentiis. M. Minella, M. Sarakha, A. Marrese, C. Minero, G. Mailhot, M. Brigante, D. Vione. "Photochemical processes involving the UV absorber benzophenone-4 (2-hydroxy-4-methoxybenzophenone-5-sulphonic acid) in aqueous solution: reaction pathways and implications for surface waters." *Water Res.* 47, pp. 5943-5953. July 2013.

D. Sridevi, K.V. Rajendran. "Synthesis and optical characteristics of ZnO nanocrystals" *Bull. Mater. Sci*., Vol.32, No. 2, pp. 165-168, April 2009.

Lift and Drag Indicator Using LabVIEW

Marizabeth Serrano, Undergraduate B.S. Mechanical Engineering[1] and Raymond Rodriguez, Undergraduate B.S. Mechanical Engineering[2]
[1]Universidad del Turabo, Gurabo, P.R., smarizabeth@yahoo.com, rodriguez.rg29@gmail.com

***Abstract*– The main objective in this project to design and build a low-cost lift and drag measuring system to be used in a wind tunnel. It is key part is to understand the effects of lift and drag forces do in airfoils or other structures. This was performed by a custom-designed lift and drag measuring system. Experimental data was compared to theoretical data to evaluate the effectivity of this design.**

Keywords-- Lift, drag, airfoil, load cell, aerodynamic.

I. Introduction

On 1901 the Wright brothers were frustrated because their aircraft was not behaving as well as they predicted according to the Lilienthal data. Otto Lilienthal was a civil engineer that in 1886 published an aerodynamic data book, in which he included experimental lift data results collected from 16 different glider types that he crafted and tested. The book called "Bird Flight as the Basis for Aviation" emphasized that birds wing shape was the secret to lift, he dedicated his life to calculate and evaluate this. The data was later used by the Wright brothers to fabricate their aircrafts [1, 2]. However, the Wright brothers had trouble with the results found using the book, so they decided to evaluate and run their own test. They built a wind tunnel (Fig. 1) in which they were able to make a scale for lift and drag balance analysis. A wind tunnel it's a small sealed tunnel with a rotor like a fan that generates wind under controlled conditions. The brothers were then capable to create close to two hundred different models running multiple tests in their wind tunnel evaluating lift and drag forces to solve the inconsistencies with the Lilienthal work, creating the aircraft with the chosen wing model on 1903 [3].

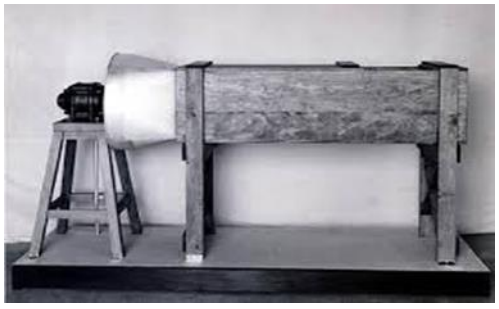

Fig. 1 Wright Brothers wind tunnel.

A. *Lift and Drag*

When an object is moving through a fluid there are four forces acting over its body: weight, lift, drag and thrust (Fig. 2). The first one is due by gravity. Lift is the aerodynamic force that opposes to gravity and makes a wing to go upward [4]. Drag is what is called the skin friction or aerodynamic friction because is the friction produced between a solid surface and a fluid moving around it [5]. Finally, thrust comes in the opposite direction of the drag force, normally this is generated by a motor. These forces are easy to be observed on an aircraft but how about a wind turbine?

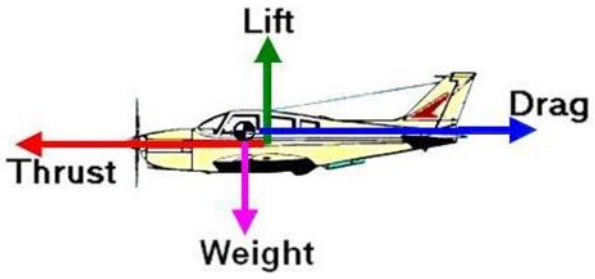

Fig. 2 Aerodynamic forces example in an airplane

B. *Wind Turbines*

On aircrafts most of the forces that keep them in the air are on the wings. In the case of the wind turbines, these forces make the blades rotate. The most known wind turbine designs are vertical axis (Fig 3) and horizontal axis (Fig 4). Horizontal wind turbines are the most common found, these ones works in a similar way than an airfoil does. When the air flows through the blades the fluid creates a differential in pressure in where there is a low pressure over the airfoil and a high pressure under, giving that everything goes from higher pressure to lower pressure the blade moves upwards making the wind turbine turn. An airfoil is the base of the design of an airplane wings and wind turbines blades. Each airfoil has different lift and drag parameters. Therefore the reaction of each one under the effect of a fluid flow will be different and that is why depending on the task required a different airfoil shape can be selected. For example if there is a horizontal wind turbine is

most likely to have a higher lift but if there is a vertical wind turbine it may better to have higher drag coefficient. This is because most vertical wind turbine designs are well known as drag turbines. Giving that these forces are pretty important to measure according to the application it is necessary to use some method or instrumentation to find these forces experimentally [6].

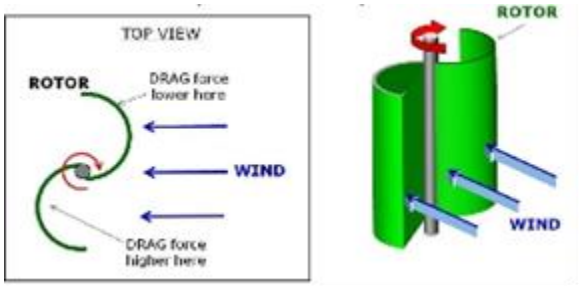

Fig. 3 Drag wind turbine diagram.

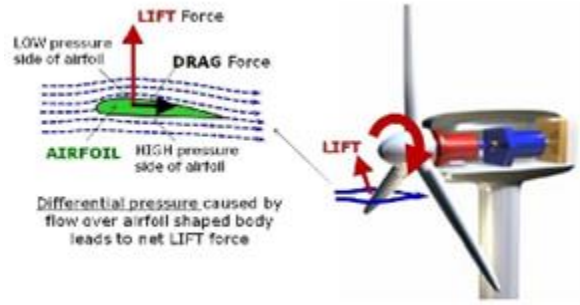

Fig. 4 Horizontal wind turbine diagram.

C. Strain Gages

Load cell (Fig 5) are strain gage based sensors that convert an applied force into an electrical output to be measured through specialized equipment. These sensors can be used in many areas in engineering. They are commonly used in equipment to measure weight such as laboratory balances or weight scales (from home use to industrial applications). When used with specialized software, such as LabVIEW, they can be used in multifunctional test machines applications.

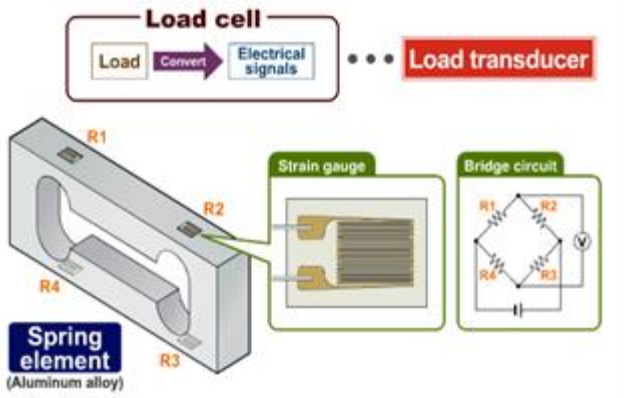

Fig. 5 Diagram of a load cell.

II. Objectives

The main objective for the research project is to create a new low-cost lift and drag measuring system to be used in the Hampden H-6910 Wind tunnel available in the facilities of the Mechanical Engineering Department. In order to achieve the objective, it was needed to redesign the measuring system with new components to replace the damaged system already in the wind tunnel. To complete this project, it is helpful to understand the main principals of wind tunnel testing, to calculate lift and drag forces in models using aerodynamics and fluid mechanics concepts from class and to test experimentally these theoretical models.

III. Project Scope

The project focuses on the construction and calibration on the lift and drag measuring system to be placed in the wind tunnel. Theoretical calculations and experimental evaluations are needed to determine the values on lift and drag forces using the new measuring system.

The scope study is presented below:

1. Construction an assembly of the load cell system
2. Calibration of load cell for lift and drag readings using LabVIEW
3. Performing experiments to gather data to compare againts theoretical values.

IV. EQUATIONS

Lift force (F_L) and drag force (F_D) are calculated using the lift coefficient (C_L), the drag coefficient (C_D), air velocity (V), air density (ρ), and cross sectional area (A), as shown below. The Reynold's number (Re) is also calculated using the characteristic length (L) and the dynamic viscosity (μ).

- Lift Force: $F_L = \frac{C_L}{\left(\frac{1}{2}V^2\rho A\right)}$
- Drag Force: $F_D = \frac{C_D}{\left(\frac{1}{2}V^2\rho A\right)}$
- Reynold's Number: $\mathrm{Re} = \frac{(\rho V L)}{\mu}$

V. LIFT AND DRAG SYSTEM

During the lift and drag system design, the first step to start was to try to fix and understand the inner workings of the Hampden H-6910 wind tunnel drag and lift system. The original measuring system showed in the Fig. 6 was designed as a balance separating the drag sensor from the lift sensor. The sensors employed were pressure load cells (Fig. 7). The plates in where the load cells are placed had linear bearings to help minimizing the friction of the balance. As shown in Fig. 6, the sensor pointing upwards measured lift force and the other placed horizontally read drag force. Unfortunately, the whole system including the drag and lift load cells, display unit and the power supply were in unknown conditions.

Fig. 6 Original lift and drag measuring system.

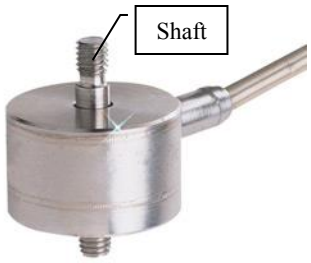

Fig. 7 Example model of the load cell used in the original system.

The lift and drag system was not properly calibrated since 1997. The testing took longer than expected since the display only showed one sensor reading at a time with a selecting switch to choose lift or drag. Both sensors used the same calibration, but when one sensor was calibrated the other displayed a different reading. The display unit was not reliable after calibration. Therefore, a National Instrument NI 9211 card was used with LabVIEW to calibrate, measure and evaluate more clearly the behavior of the two load cells. During this process, the original load cells were found not reliable to be reused.

Since the drag and lift sensors were no longer in working conditions it was decided to create a new lift and drag system with the load cells available in the laboratory. Different designs were made in order to have two sensors with the same size one of them to read drag and the other for lift. The decision criteria to choose the design was the ease of manufacturing, compact size and that one sensor do not affect the other sensors reading. The selected design is showed in the Fig. 8 and Fig. 9. Both sensors were connected to LabVIEW with an input voltage of 5.4 volts (the original power supplied was salvaged) and calibrated separately using weights (Fig. 10) creating a linear calibration equation in Excel. The load cells where exposed to almost 4 newtons of force in positive and negative direction of the load cell with the whole system installed to check if one sensor affects the other.

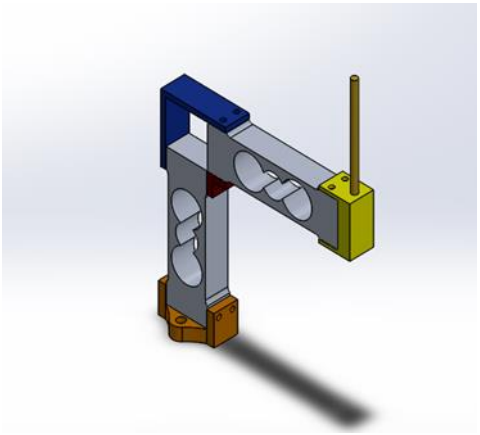

Fig. 8 New lift and drag measuring system on isometric view in SolidWorks.

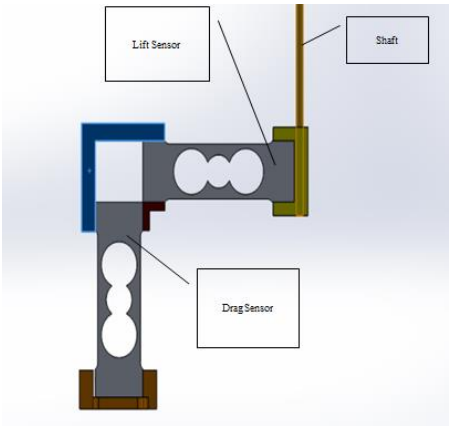

Fig. 9 New lift and drag system diagram.

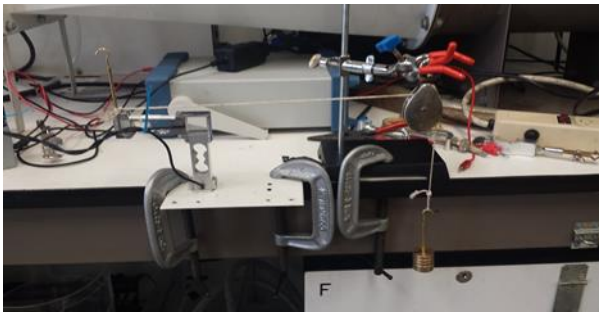

Fig. 10 Calibration of drag sensor using weights.

Initially, the two sensors installed had different ranges (2 kg and 600 g) therefore the calibration equation slope was different. The 600 grams sensor had some sort of deformation that was affecting the data and it was replaced with another 2 kilograms load cell which even shows to have a similar slope and be in a better condition.

The main purpose of the wind tunnel with a drag and lift system is to evaluate the aerodynamic behavior of an object under several wind speeds. Therefore since the wind tunnel does not have any wind velocity sensor it was necessary to find a way to determinate the wind velocity inside the wind tunnel. A pitot-tube was considered but the one available in the lab was bended thus the velocity data would be affected too. The hot wire available in the lab was found as a better fit for that application. One of the advantages of the hot wire was that this one was small and unobtrusive, which means that it won't affect the fluid flow. Other advantage was the ease of use with LabVIEW, meaning that the program can display lift, drag and the hot wire measures on the computer (comparing theoretical calculations with experimental ones). Fortunately the hot wire available in lab was the omega FMA905A and the calibration procedure for this model was similar as the load cells. Using a flow meter several data points were taken to create the necessary linear equation to transform the hot wire voltage output to the wind velocity.

To make sure that the systems was working well and was reliable, several lifts and drag tests were made. During the process it was also noticed that the wind tunnel fan knob has some unusual behavior. The gauge was sensitive, with a slight knob tap it showed a change in velocity and it was even easy to hear how the power of the motor changed. When taking data below 50% or over 100% of the motor power the wind velocity varied too much, so the authors recommend to use this equipment between 50% to 100% even when this one has a 0% to 125% range but it starts creating wind flow at around 15% .

The first test was made with a toy ball to evaluate a sphere shape and compare the results with the experimental data from textbooks. But this toy ball was not smooth at all and had a sticky surface which affected the data results. Next a mouse ball was used since it was small and smooth. The results showed in Fig. 11 were on the acceptable range according to the textbooks, so the drag sensor was working correctly.

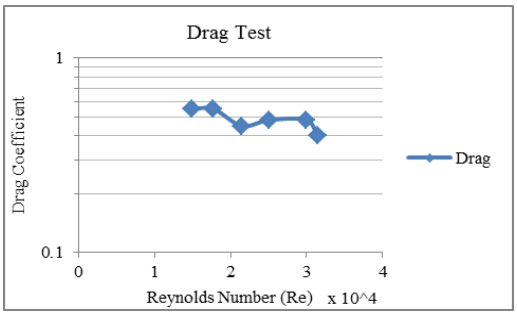

Fig. 11 Experimental drag coefficient plot.

After that it was necessary to test the lift sensor. For that a 3D printed model of an S833 Airfoil at 7 degrees (Fig. 12) was used and compared with the results given by the program Q-blade (Fig. 13). This programs is capable to create an analysis of an airfoil design manipulating Reynolds number, roughness, design and airfoil angle of attack.

Fig. 12 Testing S833 airfoil.

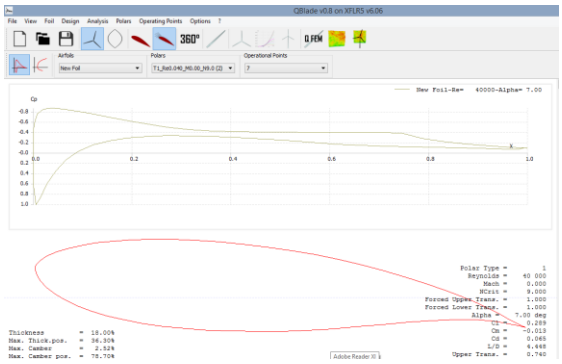

Fig. 13 Data from the Q-blade software using S833 airfoil.

Thanks to the software the Lift/Drag coefficient was found to be within a 2% of error for the ratio. As shown in Table I, the difference between lift and drag coefficient is visible but the lift/drag coefficient ratio is not different at all with the one that is provided by the program in Fig. 13. Thanks to that it was acceptable to conclude that the lift sensor was also working correctly. However to arrive to this results it was needed to cover the 3d printed airfoil model with aluminum paper in order to have a smooth surface.

TABLE I
S833 DATA COMPARISON

	Q-blade	Tested
C_D	0.065	0.035
C_L	0.289	0.160
L/D	4.448	4.571
	L/D % error	2.7%

VI. CONCLUSION

The drag and lift system designs is functional to be used during aerodynamic testing in the H-6910 wind tunnel available in the Fluids Mechanics Laboratory. However people who use this system have to have certain details to consider. For example, every time this system it going to be used, users have to make sure that everything it's correctly connected. To collect the data there is a LabVIEW program named "Drag & Lift STM" this one contains the digital display correctly calibrated with the two forces and the wind velocity. Users have to consider that even when the sensors are calibrated the zero may change during use. Therefore it is highly recommended to zero the initial data: the first value after the system get stabilized in the lift and drag display and on each measure taken, this number has to be added or extracted from the display total value. The authors have established future plans to eliminate this problem adding a feature in where the program does this automatically. Other consideration during the use of this equipment is that the wind tunnel works more uniformly between 50% to 100% of the rated power. every model that it's going to be tested in the wind tunnel has to be adapted to the mounting shaft which is the piece that connects the model to the sensors. The test box has dimensions for a maximum cross sectional area of 8 x 8 inches and it is recommended that in order to have a better reading the origin or center of the model to be tested must be on the center of this cross sectional area. Finally, an important point to consider in every aerodynamic analysis it is that every object have roughness, those who have very low roughness are considered smooth. Most of the aerodynamic calculations assumed that the material has a smooth surface, therefore it is recommended to use or make model as smooth as possible.

VII. FUTURE PLANS

One milestone for the project was to have the system fully functional for the wind turbine team testing the model to be used through the wind turbine competition in New Orleans in May 2016. Because the prototype is going to have 45 cm^3 in

size, for the testing of it has to be outside or in a bigger wind tunnel. Future plans are to make a manual for users that are going to employ the system. Next step is design a test system

1) The system has to be portable.

2) The system has to function with Arduino board and software.

3) Can withstand any weather conditions on the wind tunnel perform.

ACKNOWLEDGMENT

We are fully grateful to Puerto Rico Energy Center and Massie Chair for Excellence Program Grant #DE-NA000672 at the Universidad del Turabo for this opportunity and for the funding provided for this project. Our mentor Prof. Edwar Romero who has giving us advice, suggestion and guidance through the whole process making the project a success. As well to Prof. Hector Rodriguez & Gerardo Carbajal who give their knowledge to use in a critical moment on the project.

REFERENCES

Otto Lilienthal - Germany. (2009, November 22). Retrieved July 10, 2015, from http://aviation-history.com/early/lilienthal.htm

Jakab, P. (1997). Otto Lilienthal - 'The Greatest of the Precursors' AIAA Journal, 601-607. Retrieved June 15, 2015, from http://arc.aiaa.org/doi/abs/10.2514/2.154?journalCode=aiaaj&

Wright 1901 Wind Tunnel Tests. (n.d.). Retrieved June 22, 2015, from http://wright.nasa.gov/airplane/test1901.html

What is Lift? (n.d.). Retrieved June 22, 2015.from https://www.grc.nasa.gov/www/k-12/airplane/lift1.html

What is Drag? (n.d.). Retrieved June 22, 2015, from https://www.grc.nasa.gov/www/K-12/airplane/drag1.html

Design Principles of Wind Turbine Blades. (n.d.). Retrieved June 22, 2015, from http://wenku.baidu.com/view/42c5cedb50e2524de5187ed9.html

Coherent Application Threads (CATS). (n.d.). Retrieved July 11, 2015, from http://people.bu.edu/dew11/liftanddrag.html

Load cell. (2011). Retrieved July 17, 2015, from http://www.ishida.com/technologies/loadcell/html.html

Carbajal G. (2013). ENGI 305, Introduction to Fluid Mechanics. Class Manual, 319. Retrieved June 15, 2015.

PbSe Base Solar Cell Development (DIY Sensitize Solar Cell)

Angel L. Mangual Rotger, Mechanical Engineering Student, Edie A. Adorno Resto, Electrical Engineering Student,
Amaury Malave, Associate Professor Mechanical Engineering Department
angelm5512@Outlook.com, edieabdieri1@gmail.com; ajmalave@suagm.edu

Abstract– A novel Solar cell was prepared via chemical bath deposition method. A ZnO window layer (1in²) was deposited on a conductive glass. A lead selenide (PbSe) absorber layer (1in²), to fabricate a (Zno/PbSe) junction. The effects of changing molar concentration of the absorber layer on structural and optical properties of the corresponding PbSe thin films and solar cells were investigated. The optical band gap of the film decrease as the molarity increase. The photovoltaic properties (short circuit current, fill factor, open circuit voltage, and the efficiency) of the ZnO/PbSe cell were examined under LUX cooper light 120v, 4.2A 60Hz T-3 lamp. 500 watts max. Changing molar concentration improved the photovoltaic cell performances, the cell exhibited its highest efficiency of 39.40%

Keywords: PbSe, ZnO, Solar Cell, hexane, ethanol.

I. Introduction

Solar energy harvesting developments are getting more efficient each day, it is expected to be one of the top clean energy producers since "more energy from sunlight hits planet Earth in one hour (4.3 x 1020 J) than all the energy consumed by humans in a year (4.1 x 1020 J)" [1]. Recently great advances have been made in the solar cells world like: multi junction solar cell with 43.8% efficiency made by the National Renewable Energy Laboratory (NREL), organic solar cell that can be manufactured in a printer and new semiconductors that are being studied because these are much cheaper than normal Si solar cells for example PbSe solar cells. Now changing to solar energy is even more interesting since CEO of Tesla Energy, Tesla Motors and Space X, Elon Musk announced the release of the Powerwall. Powerwall is a battery that has a 7kW for daily usage and 10kW for backup storage, this battery is designed due to the problem that solar light peak hours are around 12pm and maximum power usage in houses is at evening hours [2]. When the user of solar panels does not have a battery the power generated at solar light peak hours is sold to the power supplier at a low price and bought again at a high price in the evening. New technologies in batteries are making the solar cells an alternative more interesting for consumers and thus the research in new solar cells cheaper than silicon is rising at an exponential rate.

Two main types of solar cells are: the conventional solar cell for example the silicon p-n junction cell and the exciton solar cell (XSC). An exciton is created when an electron is excited with energy, commonly a photon, the electron leaves the valence band and moves to the conduction band consequently leaving a hole in the atom, this a creates a bound of an electron-hole or better known as an exciton[3]. The main difference between p-n junction cell and the XSC solar cell is that the XSC absorbs light in the process of creating an exciton and in the p-n junction cell photons create free electron-hole pairs. The exciton solar cell mechanism is represented by greatly by two main pillars: the organic solar cells (OSC) and the colloidal semiconductors nanocrystals (NC). OSC are solar cells which uses conductive organic polymers to create the photovoltaic effect and generate a voltage. These are used commonly in applications that does not need a long life span because they degrade with time and applications which does not need great efficiencies. The highest efficiencies achieved with OSC is around the 10%, but this is compensated with easy manufacturing, flexibility and cost per unit. Since OSC could not develop as good as silicon solar cells, researchers are trying to find new ways of doing cheap and efficient solar cells with NC. NCs have become in vogue in view of the fact that their properties can be handled by changing its shape, size and composition [4]. By reducing the size of NC the excitons will have less space to move resulting in higher kinetic energy magnitudes. Increasing the kinetic energy of excitons will create more current seeing that the flux of electrons will be higher.

II. EXPERIMENTAL PROCEDURE

In the experiment solar cells were fabricated with NC PbSe as the active layer that creates excitons donating an electron to NC ZnO and leaving a hole in PbSe. PbSe is used as the active layer due to the fact that the diameter of the NC can be varied from 2 to 10mm enabling the NC to have an energy gap from 1.4 to 0.4 eV [5]. Not all solar cells have the ability to convert infrared radiation into light, a bigger range of absorptivity of the light wavelengths will produce more electricity. PbSe have been proved to absorb infrared light and it has been used even as an infrared detector [6].

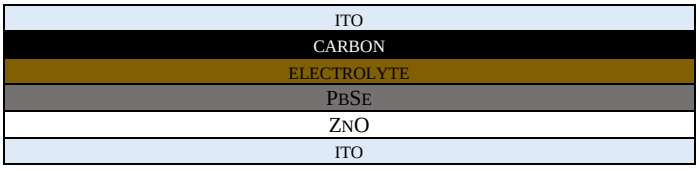

Figure 1: Model of the Experimental setup

1. ITO (conductive glass)
2. Carbon
3. Electrolyte 1-1/3 solution (p6-2100-14)
4. PbSe
5. ZnO
6. ITO (conductive glass)

First of all the solution of ZnO and ethanol was made. 1g of ZnO and mixed with 2ml of distilled water, then it is homogenized in the ultrasonic bath for 10 minutes this is done to have a homogeneous solution and to increase the surface area due to the fact that ultrasonication breaks the chains of molecules. Once the desired consistency has placed in the ITO with an area of 1 square inch. On the other crystal a coal layer was created to replace the copper layer as coal turned out to be better conductive. When the ZnO surface is cracked the electrons do not cross efficiently through the ZnO film resulting in a reduction in the current and the voltage generated by the solar cell. ZnO solution was deposited in the ITO by putting 3 drops and heating it until the water was evaporated and repeating the process until having the desired amount. PbSe was suspended in hexane and deposited in top of the ZnO carefully to not crack the ZnO, then heat for about 20 minute at 200°C until all the hexane was evaporated. Finally the transparent conductor was clamped with the rest of the setup and irradiated with sun light to measure the Voc that it created. After making this procedure it was evident that the solar cell was not achieving the results expected because water was not a good solvent for ZnO, as a result the solution was not totally homogenous and in consequence reducing the efficiency of the solar cell. The procedure was performed in the same way but replacing the solvent of ZnO to ethanol to outcome this problem. The use of ethanol also increases the manufacturability of the cell since the ethanol dryers faster than water, allowing to avoid crack by rapid solidification of the solution ZnO/Ethanol. A comparison of the the results can be seen in tables 1 and 2.

To determine the current the equation was used (Ohm's Law)

$$V = I * R \qquad (1)$$

To determine the power of the cell this equation was used.

$$P = V * I \qquad (2)$$

To determine the efficiency of the cell this equation was used.

$$\frac{output - work}{input - work}(100) = efficiency \qquad (3)$$

III. RESULTS

While the investigation was carried out it was observed that the solar cell PbSe exposed for a period of time of approximately 15 minutes to a 500 watt bulb that no quantitative results were obtained. It was observed that the panel had relatively high temperatures therefore higher electrical resistance and less energy available for PV generation. An artificial mean for heat extraction was added by using a small personal computer fan (the model AD0912UX-A7BGL 12 volts and 0.5 amps). Heat dissipation was incresed and the results obtained are shown in the table 3, below. From the results we observed that the highest power generation resulted in around 3 W/m^2 which is still lower the commercial PV cells but improvements in the manufacture and adding a heat dissipation mechanism can improve energy generation considerably. Future improvements will include a heat extraction mechanism either fins or otherwise.

TABLE 1
Measurements of the process with distilled water

ZnO (g)	Destilled H_2O (mL)	Drops of ZnO solution (1 drop = 0.05mL)	Drops of PbSe (1 drop = 0.05mL)	Minutes in the ultrasonic bath	Voltage measured in the solar cell (V)	Current measured in the solar cell (A)	Power measured in the solar cell (W)	Watts of the bulb (W)
1.0307	100	16	8	10	0	0	0	500 w

TABLE 2
Measurements of the process with ethanol

ZnO (g)	Ethanol (mL)	Drops of ZnO solution (1 drop = 0.05mL)	Drops of PbSe (1 drop = 0.05mL)	Minutes in the ultrasonic bath	Voltage measured in the solar cell (mV)	Current measured in the solar cell (mA)	Power measured in the solar cell (mW)	Watts of the bulb (W)
1.0043	5	3	3	10	280	703.52	196.98	500

TABLE 3
Measurements including heat dissipation mechanism

	Celda Solar Fecha 06/13/2015					
Voltage (mV)	Resistance (mΩ)	Currents (A)	Area (m²)	Watts (mW)	mW/m²	
136.6	0.432	316.2037037	0.0645	43.19342593	669.6655182	
170	0.545	311.9266055	0.0645	53.02752294	822.1321385	
173	0.568	304.5774648	0.0645	52.69190141	816.928704	
280	0.398	703.5175879	0.0645	196.9849246	3054.029839	
147.6	0.493	299.3914807	0.0645	44.19018256	685.1191094	

CONCLUSION

In conclusion the solar cell was made successfully made and measured with a 500 W bulb and a multimeter. On the first try ZnO was tried to be diluted with water, which did not worked because the solution was not homogenous enough and the film of ZnO had many cracks due to slow solidification of the solution ZnO/water when heated. On the second try was treated with another method. It had the purpose of creating a more consistent solution to better cover the surface of the conductive crystal. Adding 2 mL of ethanol instead of 100mL of water was found to be more suitable because ethanol is better solvent of ZnO than distilled water. High temperatures were reducing the efficiency of the cell and a dissipation mechanism was added to increase the power output. A maximum power output of 3 W/m2 was found and it is expected to be improved by optimizing the manufacture process and the heat dissipation in the cells.

REFERENCES

[1] Semiconductor Nanocrystals as Light Harvesters in SolarCells

[2] Musk, E. (n.d.). Powerwall. Retrieved May 9, 2015.

[3] Gregg, B. (n.d.). Excitonic Solar Cells. The Journal of Physical Chemistry B, 4688-4698.

[4] El-Sayed, M. (n.d.). Small Is Different: Shape-, Size-, and Composition-Dependent Properties of Some Colloidal Semiconductor Nanocrystals. Accounts of Chemical Research, 326-333.

[5] Choi, J., Lim, Y., Santiago-Berrios, M., Oh, M., Hyun, B., Sun, L., Hanrath, T. (2009). PbSe Nanocrystal Excitonic Solar Cells. Nano Letters, 3749-3755.

[6] Rogalski, A. (2003). Infrared detectors: Status and trends. Tarrytown, N.Y.: Elsevier Science.

[7] Niobio - Nb. (n.d.). Retrieved May 12, 2015, from http://www.lenntech.es/periodica/elementos/nb.htm

Structural Dynamic Evaluation for Building-Mounted Wind Turbines

Ronaldo J. Robles[1], Anthony Rivera[2], Héctor M. Rodríguez and Rolando García
[1]Universidad Del Turabo, Puerto Rico, *rrobles14@email.suagm.edu*,
[2]Universidad del Turabo, Puerto Rico, arivera746@email.suagm.edu

Abstract – ***The purpose of this research is to better understand how wind turbines induced vibration affects typical structures found in the built environment. The study considers the dynamic response in a building structure when it is coupled with a wind turbine. In particular, the study compares the effect in the change in the natural frequencies and forced response due to unbalance as a wind turbine when either a horizontal-axis wind turbine or a vertical-axis wind turbine is coupled with a typical building structure. From the simulations it is found that the horizontal axis wind turbine is more suitable for structures in the built environment while the vertical axis wind turbine in some cases was found not suitable because its vibration would cause discomfort to individual inside the structure.***

Keywords—Wind Turbines, Built Environment, Frequency Response, Ansys Workbench, Unbalanced Response, Building Vibrations.

I. INTRODUCTION

The idea of installing wind turbine on roof tops seems reasonable when you look into ways of taking advantage of wind resources. However, this idea has been implemented before but it has not been explored scientifically how it should. When you bring the wind turbine technology to an urban area there are more variables which need to be taken into consideration as they can affect the performance of the turbine. The fact that you are installing something on a structure which never took such installation into consideration when it was designed and constructed makes it a subject to study well to ensure a safe and effective implementation.

The National Renewable Energy Laboratory (NREL) published a report where they established key factors needed to be studied in order to eliminate barriers and improve the understanding of wind turbines on built-environments [1]. For instance, when looking at building-turbine integration very little is known about resulting or changes on their natural frequencies. Additionally, guidelines to keep designs with compliance to building codes and safety standards are needed to further improve the implementation of this technology.

When working with a device containing a rotating mass we have to take into consideration the dynamic effects. As any other system, the wind turbine and any given structure have natural frequencies which can suffer a change during the integration of technologies. The vibration induced to the structure from the turbine may or may not have an effect on its natural frequencies [1]. Also, the structures vibrations can induce some effect in the functionality of the wind turbine. This study looks to find the vibration effects of integrating small wind turbines (SWT) in the built environment and verify that they will not cause a problem if they were to be installed.

The present research is focused on the vibration characteristics of the wind turbine and the installation structure. The natural frequencies of each system by itself, as well as when integrated, were evaluated to understand their interactions. Simulations were done using typical small wind turbine parameters including a vertical axis and a horizontal axis wind turbine. The structures used vary in height and materials in order to evaluate different typical structures where this technology could be implemented.

II. PROBLEM STATEMENT

The application of wind technologies on built environments is a field which much is still needed to be study in order to advance these technologies in this direction. Integrating wind turbines to large structures, like buildings, brings up a series of challenges which require research in order to have a more knowledgeable approach into implementing such ideas [1].

We are studying the mechanical vibration effects in the interaction between wind turbines buildings structures because we want to determine if this technology is a viable option to implement without compromising the structures and the working environment within the structure in order to help improve the understanding and usage of wind technology on a built environment.

III. Purpose and Scope of Work

The purpose of this research is to analyze and understand how will a SWT would mechanically affect the building in which is being installed. This can later lead to have a better understanding of the mechanical interactions between the SWT and the building so they can be safely implemented through the built environment effectively.

IV. Introduction to Wind Turbines

A wind turbine is a machine that converts the power from the wind to electricity. The most common wind turbine design is the horizontal wind turbine (HAWT) as shown in Figure 1. That is that the axis of rotation is parallel to that of the ground. But there is also another design of wind turbines that is being used which is the vertical axis wind turbine (VAWT). The rotational axis of this type of wind turbine design is perpendicular to the ground. Wind turbines consist of a rotor, drive train, generator, nacelle, yaw system (only applies to HAWT's), tower, and a foundation each of these are important components of a wind turbine [2].

The rotor is the most important part of the wind turbine in consideration of cost and performance since it contains the hub and the blades. Most wind turbines today have upwind rotors with three blades but there are some downwind rotors with two blades. The rotor of an upwind rotor turbine is positioned similarly to a propeller drive airplane and this is to keep the turbine facing the direction of the wind and a yaw and tail system is required for orientation. But the downwind turbine has the rotor on the back of the turbine and the nacelle is typically designed to seek the wind thus eliminating the need of a yaw mechanism. Some manufacture use pitch control systems but some intermediate wind turbines use fixed-blade pitch and a stall control. The materials used on the blades are commonly composites primarily fiberglass or carbon fiber reinforced plastics [2]. The drivetrain consists of the other rotating components, thus not including the rotor; it thus consists of the shafts, gearbox, coupling, a mechanical brake and the generator [2].

Most of the wind turbines use either induction or synchronous generators. For this design it is important to have a constant or nearly constant rotational speed when the generator is directly connected to the utility network. Otherwise if the generator is used to power electronic converters the turbine can operate at variable speed [2].

The nacelle cover protects the machine bed plate or main frame from the weather since the main frame provides for the mounting and proper alignment of the drive train components [2]. The tower is design most commonly to be free standing and its height is designed to be from 1 to 1.5 times that of the rotor. The tower is supported by its foundation [2].

V. Built Environment Wind Turbines

Built Environment Wind Turbine (BWT) is defined as wind turbines located in an urban or suburban environment. BWT's are mostly categorized as SWT which are wind turbines that can generate 100 kilowatts or less. To date there is limited understanding of the unique challenges that come with BWT's since most of the SWT's are designed for the rural environment and not necessarily for the built environment. The built environment contains low average wind speed and higher turbulence and frequent air flow direction changes. Not completely being sure of how this factors may affect and also poorly locating the wind turbine may cause turbine failure, which could cause injury, property damage and these are potential liabilities. These unknown risks that could affect can also cause a negative perception on BWT and possibly to wind technology [1]. For the purpose of this paper it is important to understand how the induced vibrations of SWT may affect the different structures typical structures found in the built environment.

VI. Methodology

For wind turbine technology to be able to advance towards the build environment effectively the interaction between wind turbines and building must be carefully study. This will help to set certain parameters for wind turbines in the built environment.

When wind turbines are coupled with buildings they introduce vibrations on to the buildings. In particular, the typical operation of SWT is in the range of 1-10 Hz. Therefore, a practical approach might be to avoid natural frequencies within this range. The potential resonant interaction between the turbine operation and the structural natural frequencies of the turbine-building system can be observed using a Campbell diagram. Furthermore, even without a resonant condition, the vibration transmission into the building structure can be a source of discomfort. Table 1 shows typical vibration acceleration limits for discomfort depending on the application of the building [3].

The approach in this study will be to model and compare the dynamic response between a HAWT and a VAWT as they coupled with typical building structures. The dynamic response will be evaluated in terms of the natural frequencies

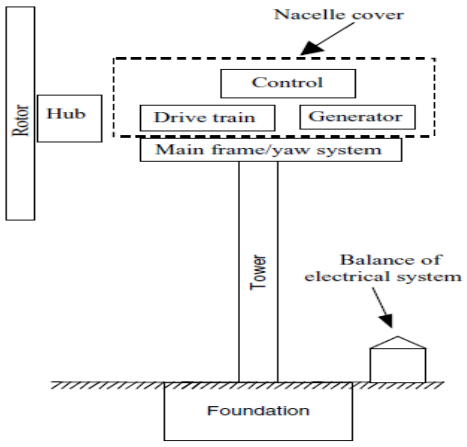

Fig. 1. HAWT and its components [2].

and forced response due to unbalance. The natural frequencies will be compared to potential rotor frequencies in a Campbell diagram. The forced response due to unbalance will be used to compare the acceleration response to the recommended limits in Table 1 for residential and office applications.

VII. Results and Discussion

The structural dynamic interaction between wind turbines and building structures is investigated in this study for two 3kW wind turbines, a HAWT and a VAWT. Both turbines are modelled under unbalanced conditions to see the force reactions generated on the roof of the structures and see how the vibrations of the structure changes when the wind turbine is applied.

The parameters to model the wind turbines are drawn from typical small wind turbines. In both cases, the turbine is modeled as a cantilevered steel tower (i.e., using beam elements) and the rotor/nacelle is considered as a concentrated (i.e., point) mass. The unbalance rotational forces are applied on the concentrated mass. Both turbine models assume an 8 m tall hollow tower. This is typically the minimum height to avoid the turbulent layer of the air [4]. Both towers have an external diameter of 25.4 cm and a thickness of 3.17 mm. The HAWT model, shown in Figure 2, considered a total top mass of 220 kg, a rotor mass of 11.1 kg, and a rotor diameter of 3 m. In this case the total mass is concentrated at the top of the 8 m tower. The VAWT model, shown in Figure 3, considers a rotor mass of 45 kg with a total top mass of 106 kg located at 6.5 m from the wind turbine support.

TABLE 1.
Acceptable Building Vibration [3].

Application	Time	Continuous Acceleration ($\frac{m}{s^2}$)
Critical Working Areas (Hospital operating rooms)	Any	0.0036
Residences	Day Night	0.0072 0.0050
Offices	Any	0.0140
Workshops	Any	0.0280

The wind turbine models for the HAWT and VAWT are shown in Figures 1 and 2, respectively. The fundamental natural frequency of the HAWT and VAWT were determined by a modal analysis and it yielded 1.92 Hz and 2.91 Hz, respectively.

The building structures in the study considered typical buildings found in Puerto Rico (P.R.). The first building is a typical single story concrete (SSC) of a typical residential building in P.R. [5]. The second structure is a typical three-story concrete (3SC) building in P.R. [6]. The third building is a three-story steel (3SS) structure. Finally, the fourth structure represents a typical eight-story steel (8SS) structure found in P.R. The models for these structures are shown in Figures 4 to 7. Table 2 shows the fundamental natural frequencies for the four buildings. As shown in the results, the fundamental natural frequencies are lower as the height (i.e., number of stories) increases. The results also show that for the case of the three story building, the concrete structure has a higher fundamental frequency when compared to the three-story steel building.

TABLE 2
Fundamental Frequencies of each Structure

Building Type	f_n (Hz)
SSC	7.43
3SC	2.83
3SS	1.10
8SS	0.45

Natural Frequencies Analysis

The analysis of the building-mounted wind turbines considers the two turbines (i.e., HAWT and VAWT) mounted on top of the four types of buildings (i.e., SSC, 3SC, 3SS, and 8SS) at two different locations (i.e., corner and center) for a

total of 16 different cases. Table 3 shows the fundamental natural frequencies of the 16 cases.

TABLE 3
Fundamental Frequencies of Each Case

Case	Building	Turbine	Loc.	f_n (Hz)
1	SSC	HAWT	Corner	1.42
2	SSC	VAWT	Corner	2.32
3	SSC	HAWT	Center	1.89
4	SSC	VAWT	Center	2.79
5	3SC	HAWT	Corner	1.45
6	3SC	VAWT	Corner	2.10
7	3SC	HAWT	Center	1.85
8	3SC	VAWT	Center	2.76
9	3SS	HAWT	Corner	1.80
10	3SS	VAWT	Corner	2.60
11	3SS	HAWT	Center	1.91
12	3SS	VAWT	Center	2.67
13	8SS	HAWT	Corner	1.85
14	8SS	VAWT	Corner	2.77
15	8SS	HAWT	Center	1.79
16	8SS	VAWT	Center	4.22

The interaction between turbine operations and natural frequencies is better observed in a Campbell diagram. The Campbell diagram is used to identify any possible points of conflict between the natural frequencies of the system and the frequency at which the wind turbine is at any given rotational velocity. This is a crucial in order to have safe operation and to avoid failure of the product so it last as it is designed. Figures 8 through 11 show the Campbell diagrams for all the turbine configurations. Each figure has the HAWT and VAWT turbines at the two locations of the four buildings. Figure 8 shows the case of a HAWT located at the center of the considered buildings. The results indicate that HAWT operation could become resonant between 36 rpm to 39 rpm. The wind turbine should stay away from operating at this range of speeds in order to avoid the excitation of the natural frequencies. Similarly, Figure 9 shows the case of a HAWT located at the corner locations. In this case the turbine should operate outside the 35 rpm to 65 rpm range. Figure 10 shows the case of a VAWT located at the center of the considered buildings. The results indicate that VAWT operation could become resonant between 28 rpm to 38 rpm. Finally, Figure 11 shows the case of a VAWT located at the corner locations. In this case the turbine should operate outside the 45 rpm to 85 rpm range.

FORCED RESPONSE ANALYSIS

The forced response analysis considers the vibration acceleration amplitude due to the unbalanced loading in the turbines. The unbalanced condition is modeled assuming that two of the three blades have a $\pm$5% weight difference from the nominal expected weight. This method has been used before to model unbalance wind turbines [6]. The unbalance force for each model is calculated as

$$F = F_0 (2\pi f)^2, \quad (1)$$

where f is the rotating speed in Hz, and the unbalance is

$$F_0 = M_T \times r_{cg} \ . \quad (2)$$

M_T and r_{cg} in equation (2) are the rotor mass and radial location of the center of mass of the rotor, respectively.

The nominal weight for a single blade in the HAWT is 3.71 kg. Since the wind turbine has three blades, one blade weighs -5% less the nominal mass and the other +5% the nominal mass. This causes the turbine to be unbalanced and generates an unbalance of F_0=0.31 kg-m. The blades of the VAWT weight is assumed to be 15 kg and using the previous procedure the unbalance is F_0=1.95 kg-m.

Similar to the case of the natural frequencies analysis, the forced response analysis considers the two turbines (i.e., HAWT and VAWT) mounted on top of the four types of buildings (i.e., SSC, 3SC, 3SS, and 8SS) at two different locations (i.e., corner and center) for a total of 16 different cases. For each case, the forced response is calculated using Ansys Workbench assuming a wind turbine operation in the 0-10 Hz (i.e., 0-600 rpm). For example, Figure 13 shows the case of HAWT installed in the corner of a 3 story steel building. The response of vibrations in the z-axis is shown in Figure 14. As shown in the figure, the acceptable operation range is between 0-105 rpm and from 135 to 375 rpm when it's in a residential building. For the case of a building used as offices the range of acceptable operation is from 0 to above the 600 rpm. The same procedure was followed to with each case studied and the summarized results are in Table 4.

Table 4 shows a summary of the acceptable operation ranges for each case. An acceptable operation range considers acceleration responses below the ones in Table 1 (i.e., 0.005 m/s^2 for residential applications and 0.014 m/s^2 for office applications).

TABLE 4
Acceptable Rotational Speed Rage for Wind Turbines in Different Cases

Case	Building	Turbine	Loc.	Acceptable Range (rpm)
1	SSC	HAWT	Corner	<375, 500-550
2	SSC	VAWT	Corner	<124, 175-220
3	SSC	HAWT	Center	<350
4	SSC	VAWT	Center	<135
5	3SC	HAWT	Corner	<540 (R), < 580 (O)
6	3SC	VAWT	Corner	<109, 200-249 (R) <130, 200–349 (O)
7	3SC	HAWT	Center	<600 (R) <600(O)
8	3SC	VAWT	Center	<129, 276-324 (R) <130 , 225-425 (O)
9	3SS	HAWT	Corner	<100, 150-520 (R) <540 (O)
10	3SS	VAWT	Corner	<70 (R) <125 (O)
11	3SS	HAWT	Center	<100, 150-250 (R) <350 (O)
12	3SS	VAWT	Center	<100 (R) <110 (O)
13	8SS	HAWT	Corner	<100, 135-375
14	8SS	VAWT	Corner	<110
15	8SS	HAWT	Center	<100, 135-315
16	8SS	VAWT	Center	<600

Table 4 show the results of each case of the wind turbines located at the center and at the corner of each structure, these results show the acceptable rotational speed of each wind turbine in order to not cause discomfort people inside the structures. Cases 1 – 4 are the single story structure which was analyzed using the limit of vibrations for residential buildings. Cases 5 – 12 each building was evaluated using both residential and office buildings acceptable vibrations (i.e., R for residential, and O for offices). Cases 13 – 16 are evaluated using only office building vibration limit. As shown in the table in case 1 the acceptable speed its read from 0 – 375 rpm and from 500 – 550 rpm are the acceptable rotational speed ranges, each case is read in the same manner.

VIII. CONCLUSION

When comparing all the scenarios together it is shown that for the vibrations induce to the structures by the HAWT that in average they cross the threshold around 450 rpm. We can conclude that the most adequate structure was the intermediate concrete with the WT in center, which reached the 600 rpm without exceeding the limit of vibration for both residential and office purposes. This would be an acceptable integration of BWT for our representative turbine because its average speed was 400rpm. For the VAWT the rotational speed of operation established on our parameters was 320 rpm. The structure with less vibrational effect was the tall steel structure with the WT in center, which did not exceed the threshold limit for offices purpose; making this the best candidate for our representative VAWT. To avoid the excitation of the natural frequencies of the system we can conclude that the operational speed of the wind turbine should be over 39 rpm for HAWT and over 85 rpm for VAWT. In General the average operating speed of small wind turbines goes over 100 rpm meaning that if the system has low natural frequencies the turbine should not excite these frequencies

REFERENCES

[1] J. Smith, T. Forsyth, T. Sinclair and F. Oteri, "Built-Environment Wind Turbine Roadmap," National Renewable Energy Laboratory, 2012.

[2] J. F. Manwell, J. G. McGowan and A. L. Rogers, Wind Energy Explained, John Wiley & Sons, 2009.

[3] A. Piersol and T. Paez, "Human Response to Shock and Vibration," in *Harri's Shock and Vibration Handbook*, 2010, p. 41.30.

[4] M. Ragheb, "Wind Turbines in the Built Environment".

[5] E. Velez, "Experimental Cyclic Behavior of Reinforced Concrete Wall Houses Located in Their Weak Direction," University of Puerto Rico, Mayaguez, 2007.

[6] L. Mieses Hernandez, "Seismic Perofrmance and Fragility Curves for Reinforced Concrete Frame and Shear Wall Residential Buildings in Puerto Rico," University of Puerto Rico, Mayaguez, 2007.

[7] H. J. T. Kooijman, C. Lindenburg and D. Winkelaar, "DOWEC 6 MW Pre-Design: Aero-elastic modeling of the DOWEC 6 MW pre-design in PHATAS," Energy Research Center of the Netherlands, 2003.

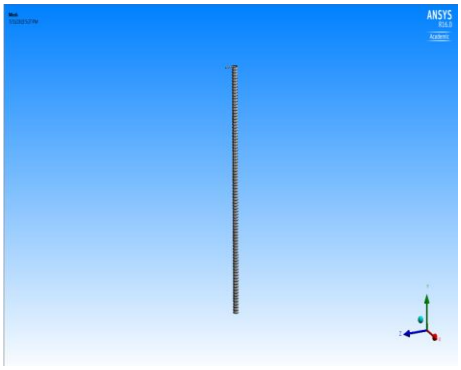

Fig 2. HAWT Ansys Workbench Model

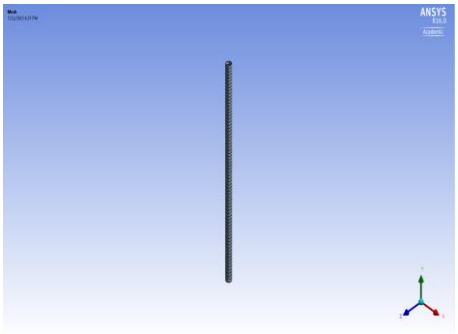

Fig 3. VAWT Ansys Workbench Model

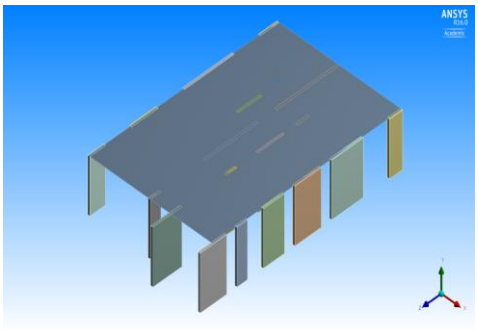

Fig 4. Small Structure Ansys Workbench Model

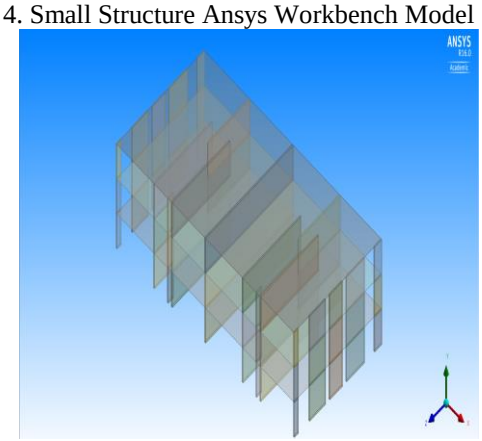

Fig 5. Intermediate Concrete Structure Ansys Workbench Model

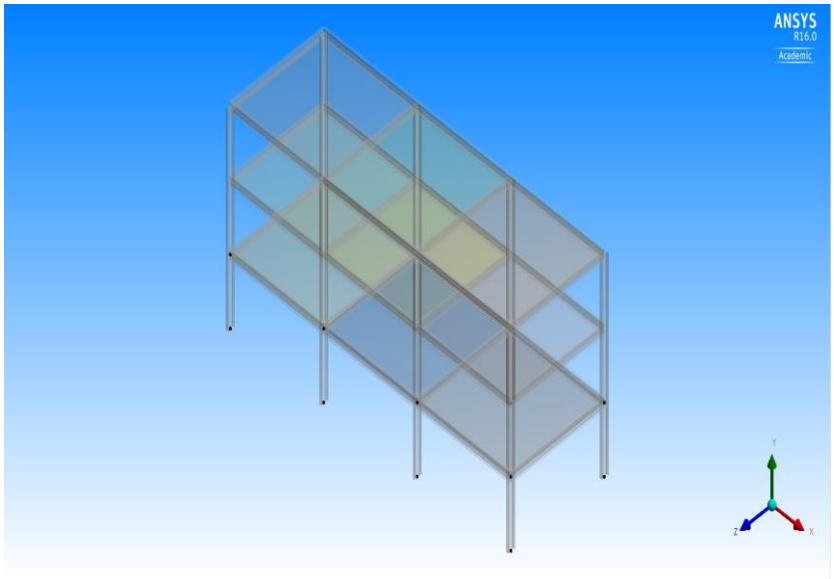

Fig 6. Intermediate Steel Structure Ansys Workbench Model

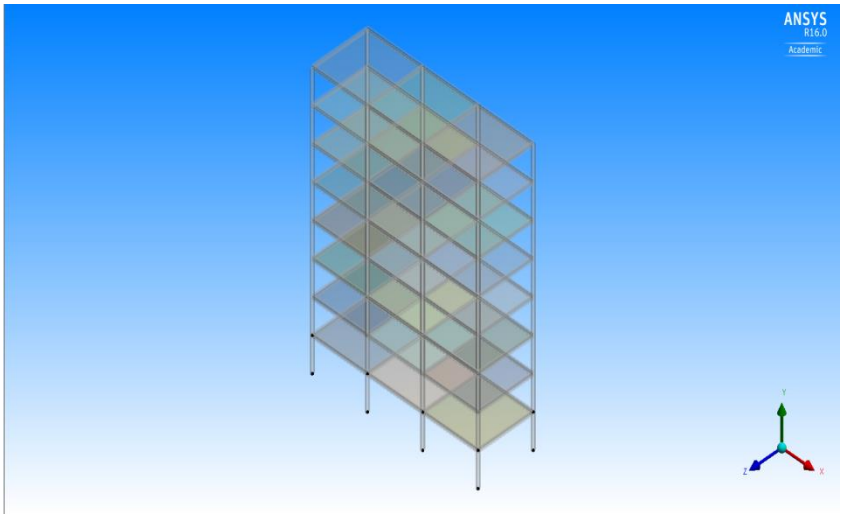

Fig 7. Tall Structure Ansys Workbench Model

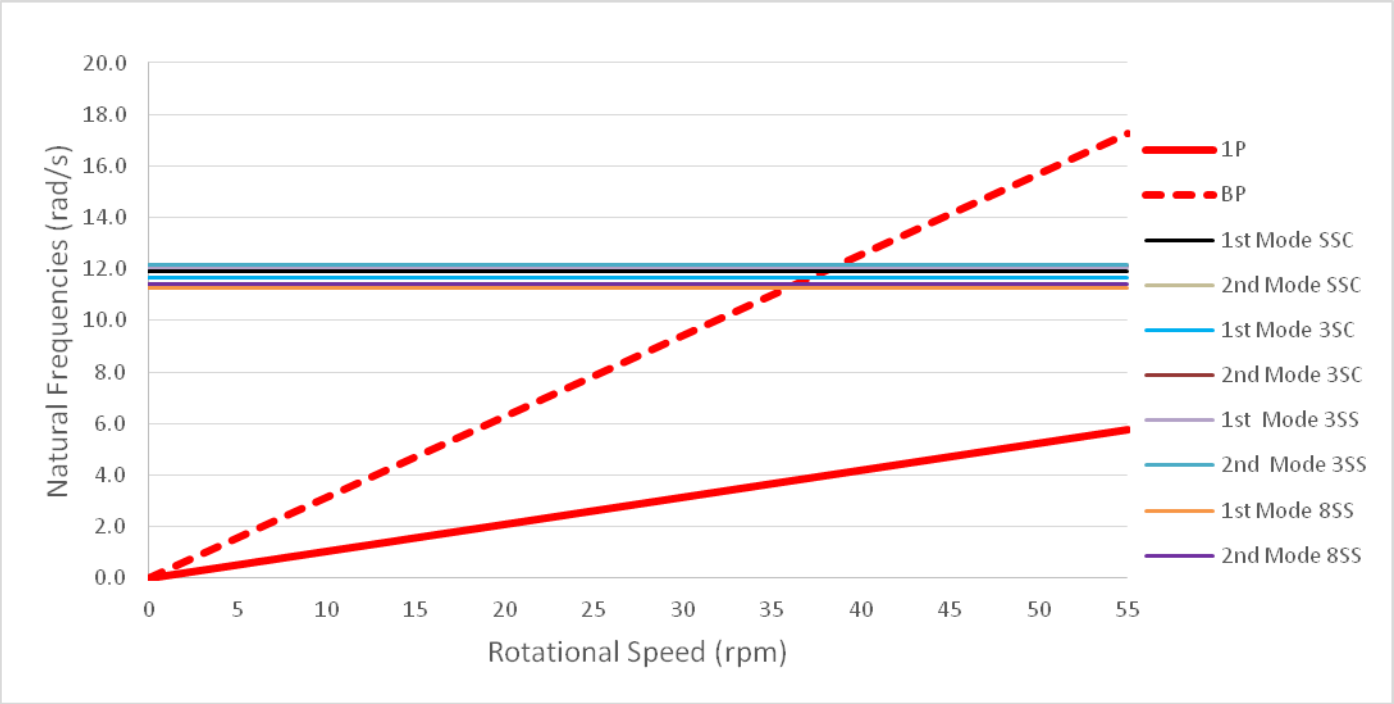

Fig. 8. Campbell Diagram HAWT Center

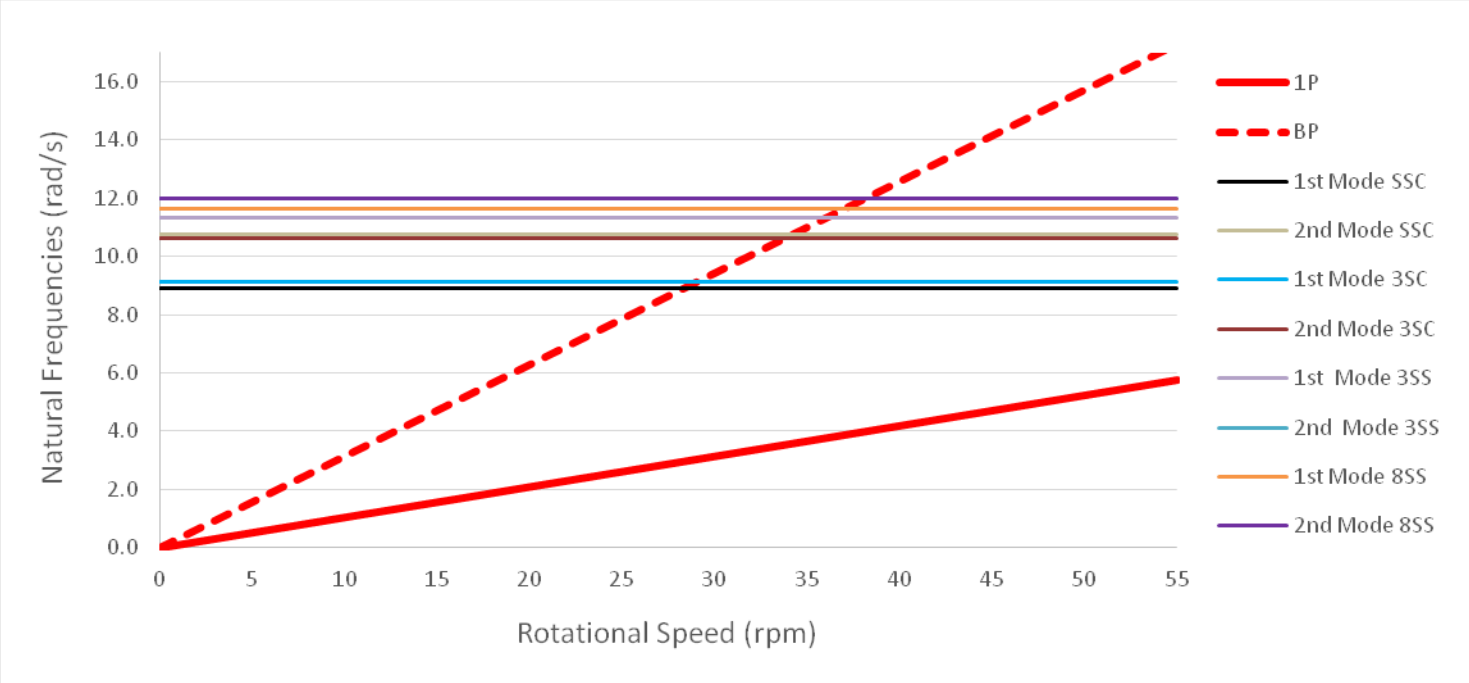

Fig. 9. Campbell Diagram HAWT Corner

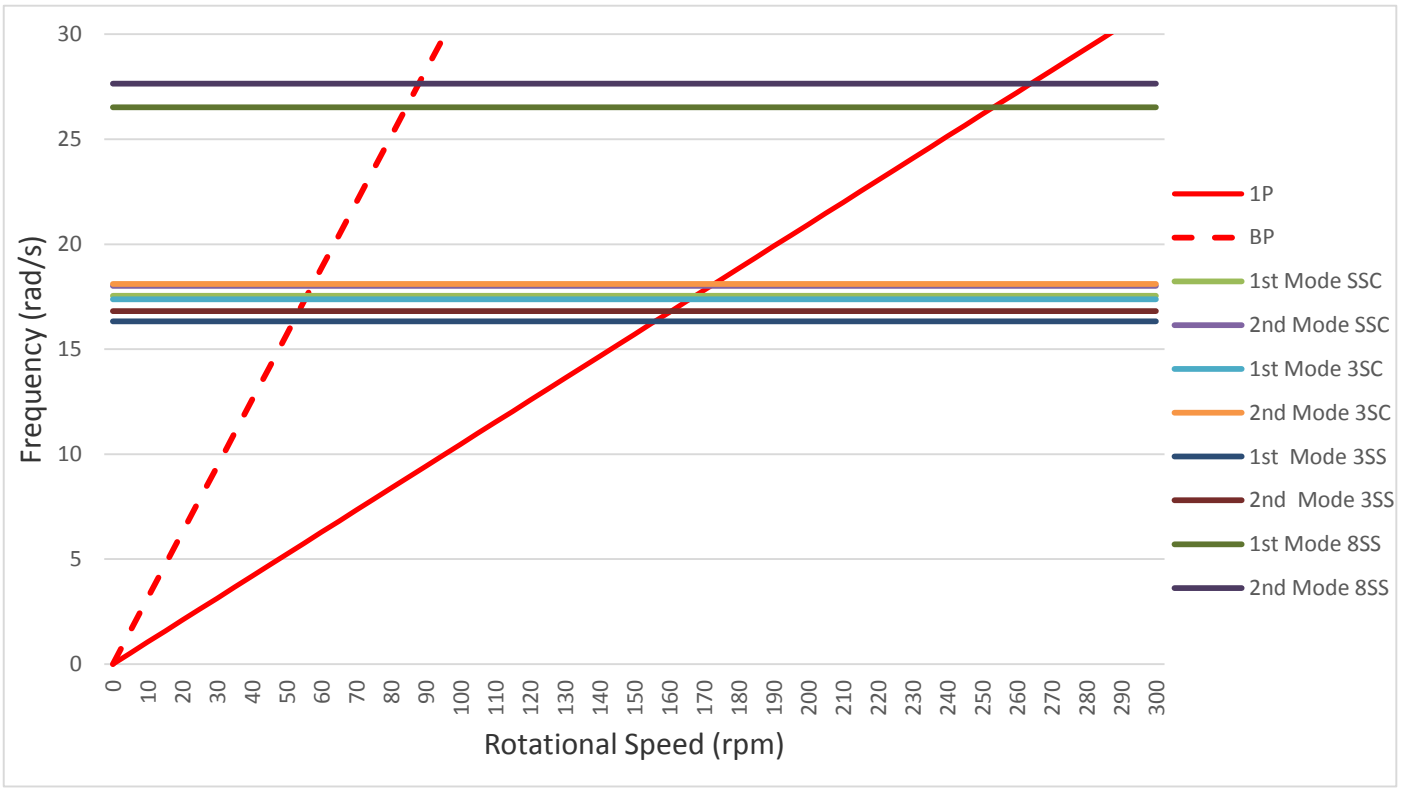

Fig. 10. Campbell Diagram VAWT at the Center of Buildings

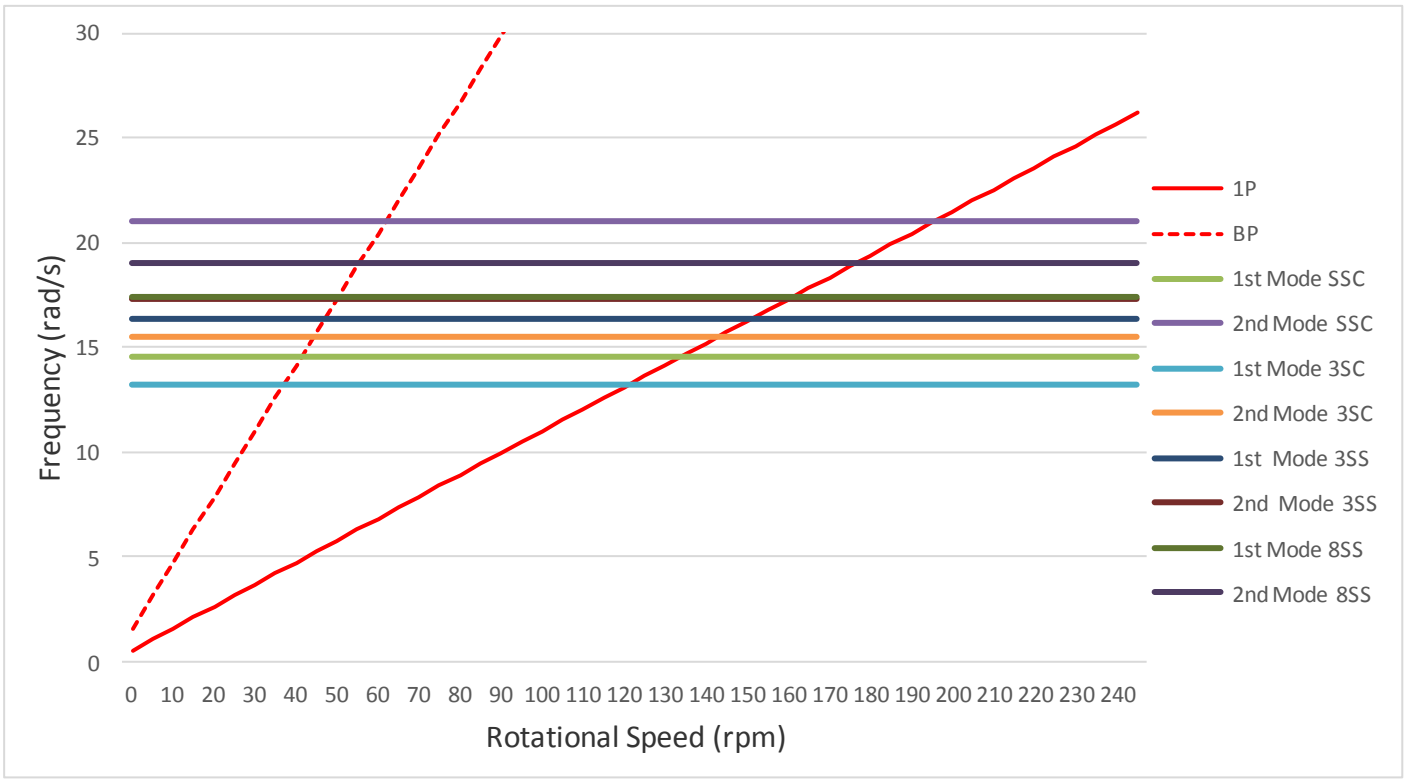

Fig. 11.Campbell Diagram for VAWT on Building Corners

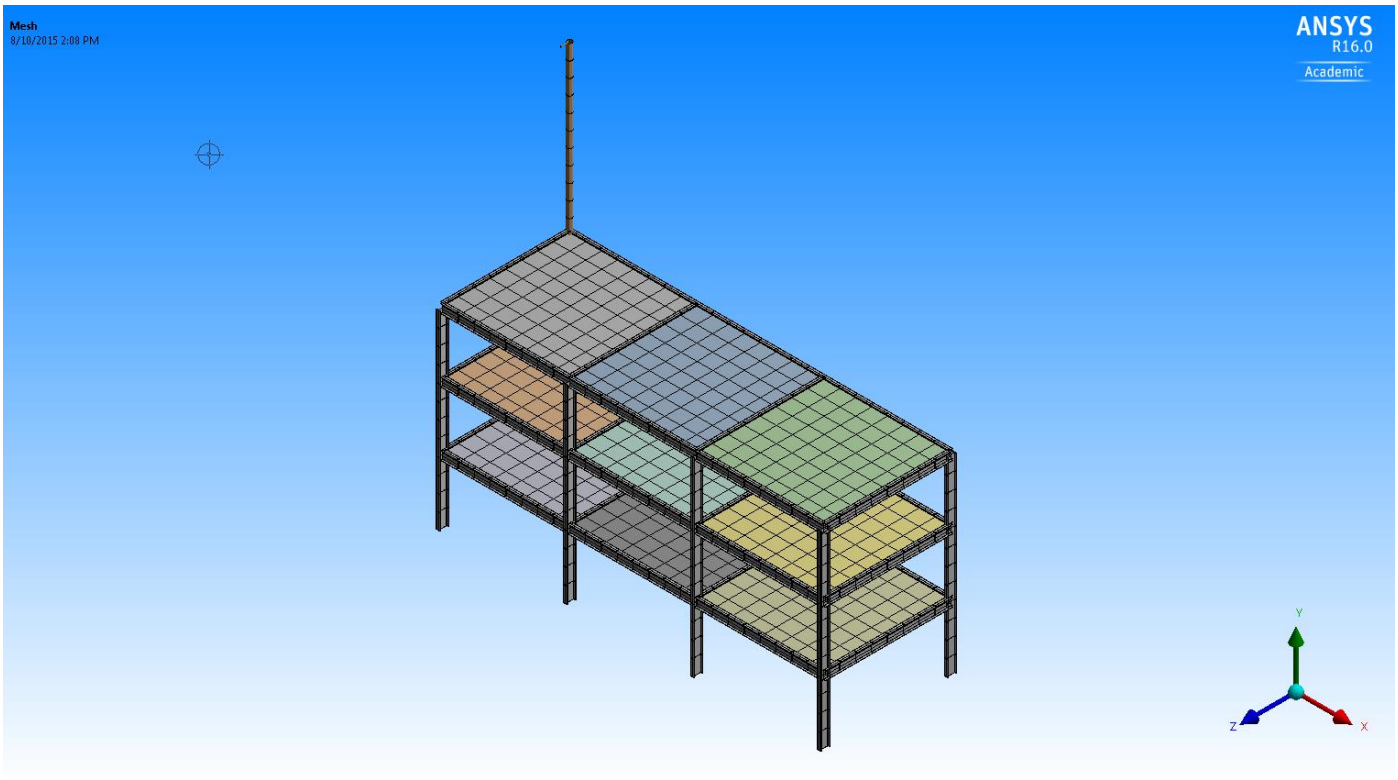

Fig 12. HAWT located at the Corner of 3SS

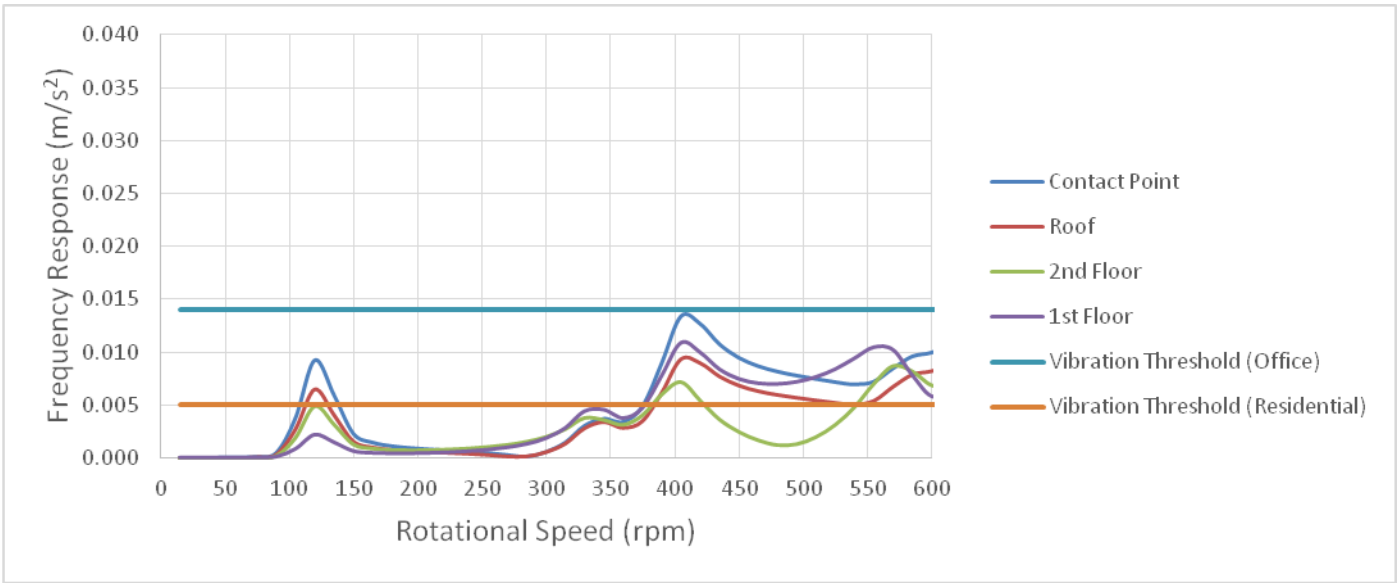

Fig. 13. Frequency Response 3 Story Steel Structure with HAWT Located at the Corner in the Z-axis

Aqueous Synthesis of (Ag,Cu, Au) Nanoparticle Embedded Polymer Nanofibers and Their Antibacterial Activity

Yariann Cardona[1], Dalia Huguet[1], and Ileana González-González[1]
[1]Chemistry and Physics Department,
School of Natural Sciences and Technology, Universidad del Turabo, Gurabo, PR

Abstract– Inspired by natural surfaces, such as plant leaves, fish scale, and spider silk, numerous hydrophobic surfaces have been extensively developed over the past decade. By combining the hydrophobic properties of a polymer fiber and the antibacterial properties of known metallic species we create a novel antibacterial material that is useful for a wide variety of applications. To achieve this we have organized this research project in two main objectives: the synthesis of antibacterial (Ag, Cu, Au)/PTBAM nanofibers and to test its antibacterial activity against two microorganisms (E. coli and S. aureus). The diameters of inhibition from the modified Kirby Bauer test range from 7mm to 12mm.

Keywords—Antibacterial, Nanoparticle, cationic polymer.

I. Introduction

Inspired by natural surfaces, such as plant leaves, fish scale, and spider silk, numerous hydrophobic surfaces have been extensively developed over the past decade. By combining the hydrophobic properties of a polymer fiber and the antibacterial properties of known metallic species we create a novel antibacterial material that is useful for a wide variety of applications. The extensive use of synthetic polymeric materials in health and biomedical, food, textile, packaging, and personal hygiene industries thus demands incorporation of biocidal compounds.[1] This paper reports the one-step fabrication of copper, silver, silver-copper mixtures and gold nanoparticles embedded into poly[2-(tert-butylaminoethyl) methacrylate] (Ag/PTBAM) nanofibers by radical-mediated dispersion polymerization.[2] It has been reported that poly[2-(tert-butylaminoethyl) methacrylate] (PTBAM) has high antibacterial activity and low toxicity to human cells.[3-4] The pendant bulky secondary amine of PTBAM causes phase separation of lipid layers inside bacteria, resulting in cell death.[2] Moreover, in contrast to other amine containing polycationic substances, PTBAM exhibits bactericidal activity without additional quaternization.[5-7] To confirm this assumption, the authors studied antibacterial properties of the synthesized metal (Ag, Au, Cu) nanoparticles embedded into PTBAM nanofibers. Our results revealed zones of inhibition (ZOI) against Gram-negative *Escherichia coli* (*E. coli*) and Gram-positive *Staphylococcus aureus* (*S. aureus*).

Materials. The monomer 2-(tert-butylaminoethyl) methacrylate were purchased from Sigma Aldrich. TBAM was used without further purification. Poly(vinylalcohol) (PVA), silver nitrate ($AgNO_3$), $Cu(CO_3)_2$, $HAuCl_4*H_2O$ and the initiator 2,2-azobis-(isobutyronitrile) (AIBN) were also obtained from Sigma Aldrich. All reactions were carried out under atmospheric pressure. Nanopure water was used at all times to reduce metal residues.

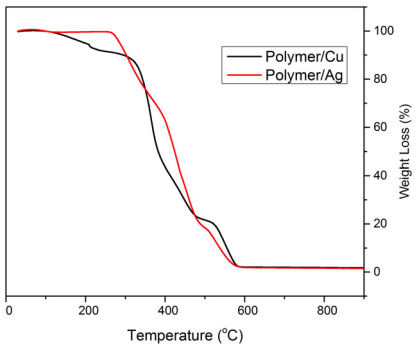

Figure 1. Weight loss as a function of time of polymers of Ag and Cu.

Methodology

Synthesis and characterization of antibacterial (Ag, Cu, Au)/PTBAM nanofibers

PVA was dissolved in deionized water, after the metallic precursor was added to the PVA solution and stirred for 1hr with a magnetic stirring bar. Next, a methylene chloride solution containing AIBN was injected into the PVA solution, followed by the addition of the TBAM monomer. The polymerization of TBAM and the reduction of metallic ions proceed under vigorous stirring at 60°C for 24hrs. The resulting material was then centrifuged and washed with methanol to remove residual reagents.

The morphology and chemical compositions of the as-fabricated surfaces were characterized by X-ray diffraction and thermogravimetric analysis will give us information of the metallic properties of the material and the organic/metal content ratio. The XRD difractogram was obtained by Bruker D8 Advance. TGA graph was obtained with a Perkin Elmer STA 6000.

B. Antimicrobial activity characterization of (Ag, Cu, Au)/PTBAM nanofibers

Modified Kirby-Bauer test, (Ag, Cu, Au)/PTBAM nanofibers were pressed into a disk shape with a diameter of 3-5 mm using a hydraulic press. Then, each prepared sample disk was gently placed on the center of the bacteria growth on LB agar plates and incubated for 12hrs at 37°C. Bacterial colony growth was observed, and the zone of inhibition was measured to evaluate the antibacterial performance.

b.) For the kinetic test, E. coli and S. aureus was prepared. The culture medium of each bacterium was inoculated with bacteria and incubated overnight at 37 °C. Bacterial growth rates were measured by monitoring the optical density at 600 nm (OD600) using a spectrophotometer measuring every 20 minutes for 4 hours.

III. Results

As part of the material characterization, X-ray diffraction analysis was performed to the metallic embedded nanofibers. No significant peak was found in the difractogram. This could be indicative of that no crystalline structure is present in the polymer or due to the small amount of metal in the embedded polymer. As shown on Figure 1, thermogavimetric analysis was performed to determine organic/metallic ratio. It was found that the embedded polymer had a 2 wt % of metal.

A modified Kirby Bauer test was done to study the antibacterial performance of the (Au,Cu,Ag)/PTBAM nanofibers. The (Au,Cu,Ag)/PTBAM were pressed into discs with diameters of 5 mm-7 mm. The discs were then placed in the center of LB agar plates with the respective bacteria *S. auerues* and *E. coli*. The antibacterial performance was measured by measuring the zone of inhibition around the disk after 18 hrs and 24 hrs after incubation at 37˚C. In Table 1 we can observe the different zones of inhibition. The range of diameter fluctuates from 7mm to 12mm. Whereas the highest results were obtained with the mixture of metals Ag and Cu at a ratio of 50% Cu and 50% Ag nanofibers in *S. aureus*. The diameter of inhibition was of approximately 12mm. In figure 2 we can observe diameters of inhibition.

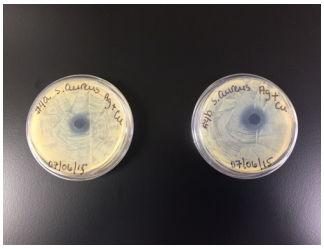

Figure 2. Modified Kirby Bauer Test of (Cu, Ag)/PTBAM with S. aureus

Bacteria		Diameter of Inhibition (mm)										
		Ag/PTBAM		Cu/PTBAM		Ag(0.25)Cu(0.75)/PTBAM		Ag(0.50)Cu(0.50)/PTBAM		Ag(0.75)Cu(0.25)/PTBAM		Au/PTBAM
		18 hrs	24 hrs	18 hrs	24 hrs	18 hrs	24 hrs	18 hrs	24 hrs	18 hrs	24 hrs	NA
E. coli	Batch 1	-	-	-	-	9.72	10.14	9.35	9.69	8.54	8.92	NA
	Batch 2	9.43	NA	-	NA	9.65	NA	9.73	NA	10.17	NA	8.93
S. aureus	Batch 1	7.96	9.65	8.16	8.16	10.46	11.23	12.34	12.70	10.17	10.47	NA
	Batch 2	7.61	NA	10.01	NA	10.29	NA	11.35	NA	8.625	NA	-

Table 1. Results of Modified Kirby Bauer Test

A bacterial growth curve was used to study the growth kinetics of *E. coli* and *S. aureus*. The optical density at 600 nm (OD_{600}) was measured to monitor the bacterial growth. In Figure 3 we can observe the graph obtained for both bacteria. The determination of bacterial numbers was also done. E. coli presented 46 x 10^7 CFU/mL and S. aureus presented 250 x 10^6 CFU/mL.

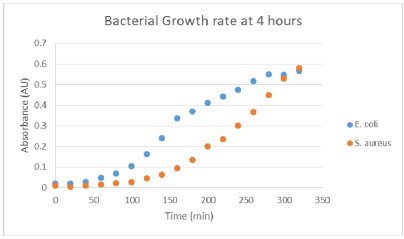

Figure 3 Bacterial growth rate of E. coli and S. aureus at 4 hours.

The nanofibers were synthesized by radical-mediated dispersion polymerization. The metallic ions were added to an aqueous solution of PVA and were coordinated to hydroxyl groups on the PVA[2]. AIBN was then added to the metallic-PVA solution acting as a reducing agent for the metallic ions and as a radical initiator for the TBAM monomer[2]. The metallic nanoparticle-PVA complexes were linearly and tightly assembled due to both the high shear conditions and dipole-dipole interactions between metallic nanoparticles[2]. In order to confirm the proposed chemical interactions further chemical characterization needs to be done to the synthesized nanofiber, including XPS, ICP-OES, and FT-IR.

In conclusion, (Au, Cu, Ag)/PTBAM exhibited antibacterial activity against both Gram-negative E. coli and Gram-positive S. aureus based on the microbial properties of the metals embedded in the PTBAM substrate. The best results were obtained with disks containing mixture of metals (Ag and Cu). Nanofibers Cu/PTBAM and Ag/PTBAM against *E. coli* did not show significant results, further investigation is required. These results suggest that (Au, Cu, Ag)/PTBAM nanofibers have potential for use in hygienic applications. Further investigation is required to optimize the process of (Au, Cu, Ag)/PTBAM nanofiber fabrication.

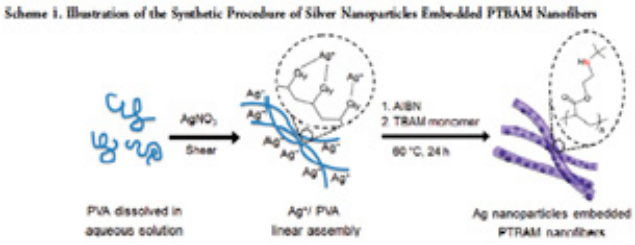

Acknowledgment

The authors want to acknowledge the Molecular Science and Research Center for the usage of Thermogramivemtric

Analysis. This work was supported in part by UT-DOE Massie Chair of Excellence Grant #XXXXX. Yariann Cardona and Ileana González-González gratefully acknowledge support from PREC and UT Massie Chair of Excellence Summer Internship. The authors also acknowledge the support from Francisco J. Rivera Figueroa from the biology department for all the support and training on the microbiology experiments.

REFERENCES

[1] Sambhy, V.; MacBride, M. M.; Peterson, B. R.; Sen, A. J. Am. Chem. Soc. **2006**, 128, 9798−9808.
[2] Song, J.; Kang, H.; Lee, C.; Hwang, S. H.; Janj, J.; *ACS Appl. Mater*. *Interfaces* **2012**, 4, 460−465
[3] Seyfriedsberger, G.; Rametsteiner, K.; Kern, W. Eur. Polym. J. **2006**, 42, 3383−3389.
[4] Voccia, S.; Ignatova, M.; Jeróˆme, R.; Jeróˆme, C. Langmuir **2006**, 22, 8607−8613
[5] Harney, M. B.; Pant, R. R.; Fulmer, P. A.; Wynne, J. H. *ACS Appl. Mater. Interfaces* **2009**, 1, 39−41
[6] Bouloussa, O.; Rondelez, F.; Semetey, V. Chem. Commun. **2008**, 951−953.
[7] Lenoir, S.; Pagnoulle, C.; Galleni, M.; Compere, P.; Je`roˆme, R.; Detrembleur, C. Biomacromolecules **2006**, 7, 2291−2296.

2015 Summer Internship

Clean Technologies Research

Students

Ángel Mangual
Universidad del Turabo, Gurabo, PR, USA

Anthony A. Rivera
Universidad del Turabo, Gurabo, PR, USA

Carolis A. Meléndez
Universidad del Turabo, Gurabo, PR, USA

Cassandra Santiago
Universidad del Turabo, Gurabo, PR, USA

Eddie Adorno
Universidad del Turabo, Gurabo, PR, USA

Frankie O. Rolón Delgado
Universidad del Turabo, Gurabo, PR, USA

Hector Martínez Rosa
Universidad del Turabo, Gurabo, PR , USA

Jonathan J. López Carrasquillo
Universidad del Turabo, Gurabo, PR, USA

Jorge I. Valentín
Universidad del Turabo, Gurabo, PR, USA

Juan C. Arango Lozano
Universidad del Turabo, Gurabo, PR, USA

Keila M. Rivera Sanchez
Universidad del Turabo, Gurabo , PR, USA

Luis G. Gonzalez
Universidad del Turabo, Gurabo, PR, USA

Marizabeth Serrano
Universidad del Turabo, Gurabo, PR, USA

Miguel A. Ramirez
Universidad del Turabo, Gurabo, PR, USA

Mentors

Abniel Machín De Jesús, Candidate MS
Universidad del Turabo, Gurabo, PR, USA

Amaury Malave, PhD
Universidad del Turabo, Gurabo, PR, USA

Bruyanelis Ramos Aponte, Candidate PhD
Universidad del Turabo, Gurabo, PR, USA

Dayna M. Ortiz Rodríguez, Candidate MS
Universidad del Turabo, Gurabo, PR, USA

Edwar Romero, PhD
Universidad del Turabo, Gurabo, PR, USA

Francisco Marquez Linares, PhD
Universidad del Turabo, Gurabo, PR, USA

Frank J. Valentín Silva, MD
Universidad del Turabo, Gurabo, PR, USA

Gerardo Carbajal, PhD
Universidad del Turabo, Gurabo, PR, USA

Hector Rodríguez, PhD
Universidad del Turabo, Gurabo, PR, USA

Ileana González González, PhD
Universidad del Turabo, Gurabo, PR, USA

Ileana Nieves Avila, Candidate MS
Universidad del Turabo, Gurabo, PR, USA

Janette Perez Barbosa, MS, PE
Universidad del Turabo, Gurabo, PR, USA

Jose R. Perez Jimenez, PhD
Universidad del Turabo, Gurabo, PR, USA

Karin J. Millán Díaz, Candidate PhD
Universidad del Turabo, Gurabo, PR, USA

Authors

August 21, 2015

2015 Summer Internship

Clean Technologies Research

Students

Pedro Rodríguez Ocasio
Universidad del Turabo, Gurabo, PR, USA

Raymond Rodríguez
Universidad del Turabo, Gurabo, PR, USA

Ronaldo J. Robles
Universidad del Turabo, Gurabo, PR, USA

Yariann M. Cardona
Universidad del Turabo, Gurabo, PR, USA

Yavier I. Rodríguez Ortíz
Universidad del Turabo, Gurabo, PR, USA

Mentors

Loraine Soto Vázquez, Candidate PhD
Universidad del Turabo, Gurabo, PR, USA

Luis G. González, Candidate PhD
Universidad del Turabo, Gurabo, PR, USA

Miguel Ramirez, Candidate MS
Universidad del Turabo, Gurabo, PR, USA

Maria D. Cotto Maldonado, PhD
Universidad del Turabo, Gurabo, PR, USA

Authors

August 21, 2015

2015 Summer Internship

Clean Technologies Research

Collaborators

Armando Soto

Darlene Muñoz Villafañe

Genesis Castellanos Rojas

Ián Gutierrez Molina

Jannette Pérez

Josefina Melgar

Phillip Murray

Sandra R. Pedraza Torres

Suheilie Rodríguez González

Sandra Mendez Pagán